NCSX Engineering Design Document

Design Description
Stellarator Core Systems (WBS 1)

NCSX CDR

May 21-23, 2002

Lead Author: Brad Nelson

Table of Contents

Table of Figures

Tables

1   DESIGN OVERVIEW

The stellarator core is an assembly of four magnet systems that surround a highly shaped plasma and vacuum chamber. The coils provide the magnetic field required for plasma shaping and position control, inductive current drive, and error field correction. The vacuum vessel and plasma facing components are designed to produce a high vacuum plasma environment with access for heating, pumping, diagnostics, and maintenance. All of the NCSX coil sets are cryo-resistive and operate at liquid nitrogen temperatures, so the entire system is surrounded by a cryostat. Figure 1 shows a cutaway view of the stellarator core assembly.

Figure 1 Cut-Away View of the Stellarator Core Assembly
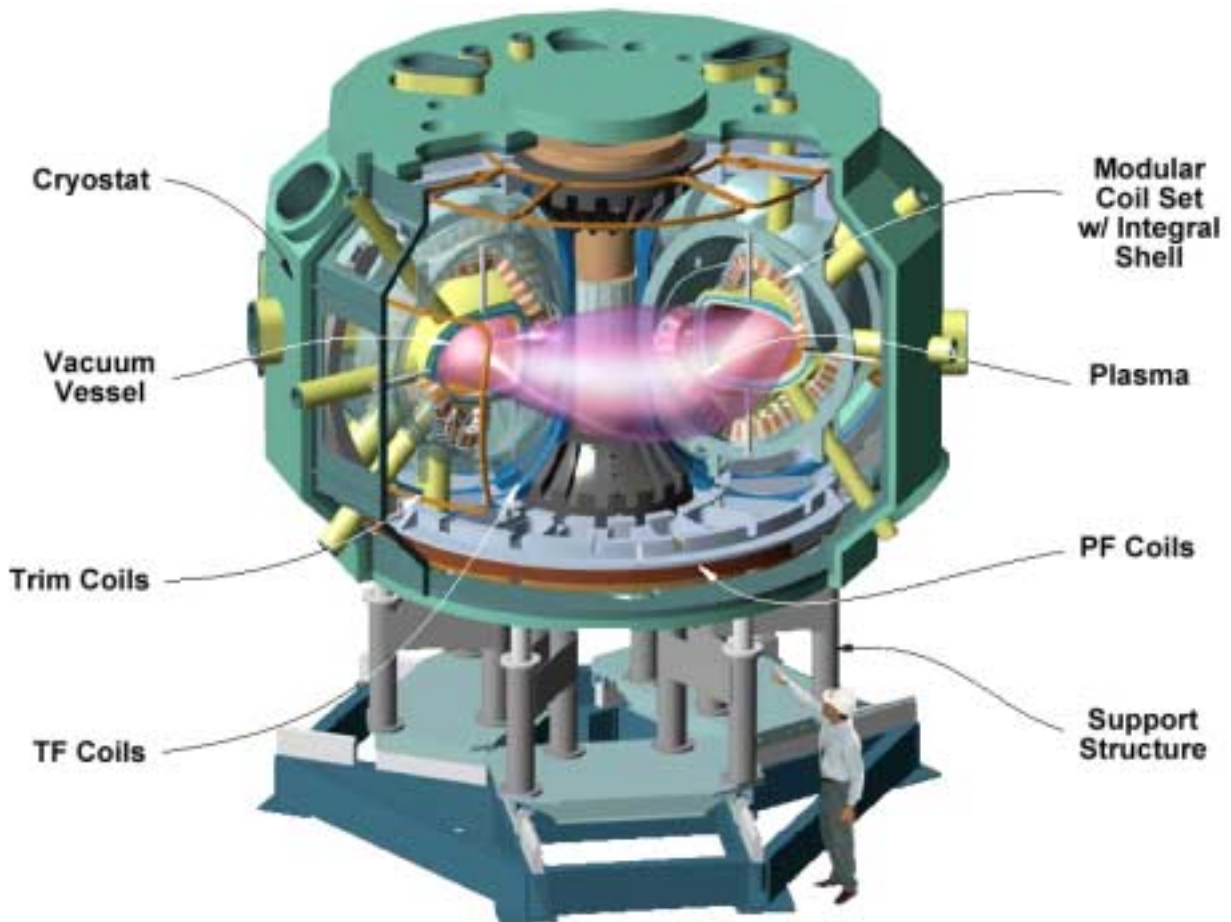
Table 1 NCSX Parameters

Parameter	Value
Major radius	1.4 m
Minor radius	.33 m
B_{max}	2 T
Plasma current	Up to 350 kA
TF coil configuration	+/- 0.5 T, 1/R (18 coils)
Plasma heating methods	3 MW NBI
	6 MW NBI (future upgrade)
	6 MW ICH (future upgrade)

The overall parameters of NCSX are listed in Table 1. The principal feature of NCSX is the set of modular coils that surround and shape the plasma. There are three field periods with 6 coils per period, for a total of 18 coils. Due to stellarator symmetry, only three different coil shapes are needed to make up the complete coil set. The coils are connected electrically in 3 circuits (with all like coils are in series), which are independently powered to provide maximum flexibility. The maximum toroidal field at 1.4 m produced by the modular coils with a toroidal field flattop of ~ 0.2s is 2 T. The toroidal field on axis can be raised above 2 T by energizing the TF coils, which can add ±0.5 T to the field generated by the modular coils.

The windings are wound on and supported by the tee-shaped structural member, which is an integral part of the coil winding form. The winding forms are bolted together to form a structural shell that both locates the windings within the +/- 1.5 mm accuracy requirement and supports them against the electromagnetic loads.

A set of toroidal field (TF) coils is included to provide flexibility in the magnetic configuration. Adding or subtracting toroidal field is an ideal "knob" for lowering and raising iota. There are 18 identical, equally spaced coils providing a 1/R field at the plasma.

A set of poloidal field coils is provided for inductive current drive and plasma shape and position control. The coil set consists of two inner solenoid pairs (PF 1 and PF 2), and 4 pairs of ring coils. Coil pairs are symmetric about the horizontal midplane and each coil pair is connected in an independent circuit.

External trim coils are provided on the top, bottom and outside perimeter of the coil support structure primarily to reduce n/m=1/2 and 2/3 resonant errors that may result from manufacturing or assembly errors in the modular coil geometry.

Nestled inside the coil set is a highly shaped, three-period vacuum vessel, which means the geometry repeats every 120º. Stellarator symmetry also causes the geometry to also be mirrored every 60º so that the top and bottom sections of the first (0º to 60º) segment can be flipped over and serve as the corresponding sections of the adjacent (60º to 120º) segment. The vessel will be constructed in full field periods and joined together at bolted joints. Numerous ports are provided for heating, diagnostics, and maintenance access. Several port sizes and shapes are used to best utilize the limited access between modular coils.

The PFCs inside the vessel will be introduced in stages. The first phase will include a simple set of limiter tiles at the three $v=1/2$ symmetry planes which correspond to the vessel field joints. Later upgrades will provide a contoured liner, constructed of molded carbon fiber composite (CFC) panels mounted on a frame of poloidal rings.

One of the challenges for the design is the allocation of space among the components. Specially developed computer codes have been used to optimize the winding path trajectory to satisfy stringent physics requirements while not violating engineering constraints on bending radii, coil-to-coil spacing, coil-to-plasma spacing, and access for neutral beam injection. The coil cross section is further limited by the space requirements for the PFCs, support ribs, vacuum vessel, thermal insulation, and coil clamping features. The space allocations are shown in Figure 2.

Figure 2 - Space Allocations Between Plasma and Modular Coils
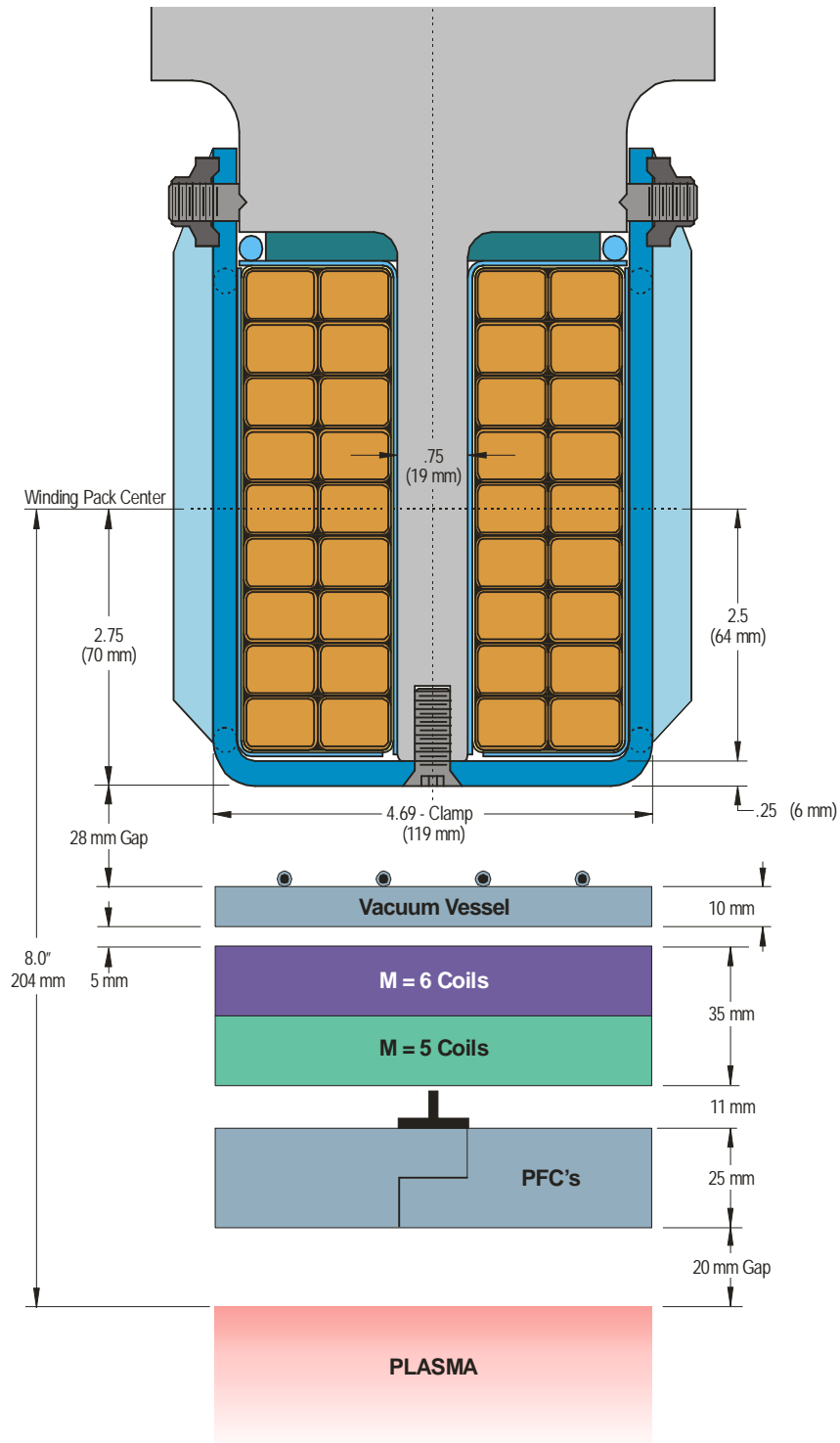
The NCSX stellarator core will be assembled from three individual field period assemblies that are bolted together atop the support stand in the test cell. Each of the three field periods are pre-assembled in a separate area at PPPL, and consist of one third of the vacuum vessel, TF and modular coils, trim coils and in-vessel diagnostics. The modular coils in each half field period will be completely pre-assembled at the factory for fit-up, inspection, and testing prior to shipping. The vacuum vessel will be delivered in three sections plus the port extensions.

The modular coils will first be assembled over the vacuum vessel (VV) segment. The vacuum vessel will then be supported (hung) from the modular coil structure. The TF coils will be installed and the port extensions will be welded into place. The vacuum vessel segment will be baked out to 150ºC and a vacuum leak check will be performed. The completed field period sub-assembly will be transported to the test cell and placed in a temporary position on the test stand. When all three subassemblies are in place, they are moved radially into final position. All three subassemblies are moved simultaneously to avoid interference with the interlocking modular coil boundaries, which extend past the shell and vessel connecting flanges.

The NCSX device is presently completing the conceptual design phase. The general configuration has been selected and baseline concepts exist for all of the primary design features. Scoping analyses have permitted sizing and performance evaluation of the key components. Manufacturing studies have been carried out for the two most critical elements of the design, the modular coils and vacuum vessel. Some analyses, such as the TF and PF structural analyses, have not been completed, but these components are based on conventional concepts and there is high confidence that a successful design solution has been proposed.

Following the conceptual design review, in the balance of FY 2002, concept refinement will be carried out for all components, and design suggestions from the conceptual design review panel will be evaluated and incorporated. Specifications will be developed for prototype components of the vacuum vessel and modular coils. Highlights in future years include:

FY03   Preliminary design starts in FY03. R&D will begin in earnest for the modular coils and vessel. Full-scale prototype winding forms will be procured from two different vendors. Multiple winding, vacuum impregnation, and mechanical and electrical tests will be performed of prototype modular coil conductor pack sections. Tooling will be designed and fabricated to wind and vacuum impregnate full-scale modular coils at PPPL. Additional contracts will be let for full-scale partial prototypes of key vacuum vessel regions, up to and including a half field period segment.

FY04   Production winding forms will be ordered. The prototype winding forms and tooling produced in FY03 will be used to produce a complete prototype modular coil. The vacuum vessel contract will also be awarded.

FY05   The production modular coil winding will begin. The first and second vacuum vessel field period segments will be completed.

FY06   All the modular coils will be completed. The vacuum vessel field period segments will be shipped to PPPL and assembly of all the field periods will be completed. The final assembly in the test cell will begin.

FY07   Assembly in the test cell will be completed and by March 2007 first plasma will be initiated.

2   VACUUM VESSEL AND IN-VESSEL COMPONENTS

2.1   Design Requirements and Constraints

The vacuum vessel and in-vessel components are required to provide ultra-high vacuum conditions and power handling capability for high performance plasma operation. The basic requirements are listed in Table 2. These requirements flow from the **General Requirements Document**, provided as part of the Conceptual Design Report.

Table 2 Requirements for the Vacuum Vessel and In-Vessel Components

Vacuum vessel requirements	
General /geometry	The vessel will fill as much of the coil-bore volume as possible consistent with assembly of the coils over the vessel and necessary insulation space.
	The inner surface of the vacuum vessel shall be electro-polished (or treated to produce an equivalent, cleanable surface.)
	Access ports shall be provided for diagnostics, heating, and maintenance / reconfiguration of in-vessel components.
	Space shall be provided on the inboard side, at the v=1/2 symmetry plane, for the installation of ICRH launchers as a future upgrade
	The design shall be capable of accommodating internal trim coils for high-poloidal mode number helical field perturbations
Plasma facing components (PFCs) requirements	
General	PFCs are required to support power and particle-handling research, protect the vacuum vessel and in-vessel components from the plasma and from neutral beam shine-through., and limit sputtering of high Z impurities.
	The design will provide an initial system of PFCs sufficient for ohmic operation
	The design is able to accommodate the installation of a more extensive system through future upgrades, as required by the research program.
	Areas which are expected to come in contact with the plasma shall be armored with carbon-based, i.e. graphite or carbon fiber composite (CFC) components, which shall be bakeable in situ to 350C
Baseline configuration (included in project cost)	An array of poloidal limiters will be provided for initial ohmic operations.
Upgrade configurations (to be implemented during operations)	Future upgrades shall be accommodated by designing a flexible system that can be implemented in stages. It shall provide the potential to implement a slot divertor with active pumping in a sealed plenum, up to 100% wall coverage, capability to electrically bias regions of the plasma boundary relative to each other and the vacuum vessel..
Power handling	The baseline configuration shall be designed to handle ohmic heat loads, (0.3 MW for 0.3 seconds)
	The upgrade configuration shall be capable of accommodating heat loads associated with up to 12MW of plasma heating power for 1.2s (including 6MW of neutral beam injection)

Vacuum Vessel and In-vessel Component Requirements

Disruption requirements	The device shall be designed to withstand electromagnetic forces due to major disruptions characterized by the disappearance of the plasma at the maximum plasma current (350 kA).
Field errors	The toroidal flux in island regions due to fabrication errors, magnetic materials, or eddy currents shall not exceed 10% of the total toroidal flux in the plasma.
	The relative magnetic permeability of the vacuum vessel and in-vessel components shall be less than 1.02 except in welded regions, where the relative magnetic permeability shall be less than 1.05.
Electrical (eddy current) requirements	Eddy currents in conducting structures surrounding the plasma shall not give rise to unacceptable field errors.
	The vessel and in-vessel structures shall be designed with stellarator symmetry to minimize field errors from unsymmetrical eddy currents.
External kink mode stabilization	The time constant of the vacuum vessel and in-vessel structures must be less than 10 ms.

Temperature requirements

Bakeout temperature	The vacuum vessel shall be bakeable at 150C.
	The vacuum vessel shall be compatible with the capability to bake carbon plasma facing components at 350C (as a future upgrade).
Pre-shot operating temperature	The pre-shot operating temperature of the vacuum vessel shall be capable of being maintained in the range of 20C-100C without ratcheting.
	The pre-shot operating temperature of the plasma facing components will be such that the peak temperature during a shot will not exceed 1200C to avoid carbon blooms

2.2   Design Description and Performance

2.2.1   Vacuum Vessel

The vacuum vessel is a highly shaped, three-period structure, i.e. a geometry that repeats every 120º toroidally. The geometry also has stellarator symmetry, i.e. it is mirrored every 60º so that the top and bottom sections of the first (0º to 60º) segment can be flipped over and serve as the corresponding sections of the adjacent (60º to 120º) segment. Table 3 lists the main vacuum vessel parameters.

Figure 3 and Figure 4 illustrate the basic vessel geometry.

The vessel will be baked to 150ºC and operate with a nominal operating temperature of 25ºC. The vessel is maintained at temperature by helium gas circulated through tracing lines attached to the vessel exterior. The vessel is insulated on its exterior surface to provide thermal isolation from the modular coils, which operate at cryogenic temperature (80K). Inconel 625 is the material chosen for the vessel shell. It was selected over stainless steel primarily because of its low permeability (both in the parent and weld material) and high electrical resistivity. The electrical resistivity of Inconel 625 is 70% higher than for austenitic stainless steel. Higher resistivity results in a shorter vessel time constant, which is beneficial for the fast field penetration required for plasma current profile control.

Using Inconel also avoids the permeability issues associated with stainless steel. Stainless steel is prone to have elevated permeability when subject to severe cold working or when welded. Furthermore, the regions of elevated permeability are not necessarily uniform from one period to the next. Non-uniform regions of elevated permeability are a concern because they are a potential source of field errors.

Table 3 Vacuum Vessel Parameters

Physical parameters	
Material	Inconel 625
Thickness	0.95 cm (3/8 in)
Time constant	5.3 ms (calculated)
Inside surface area (without ports)	27.6 m^2
Inside surface area (with ports)	57.6
Enclosed volume (without ports)	10 m^3
Enclosed volume (with ports)	13 m^3
Weight with ports (without pfc's)	5375 kg
Operating parameters	
PFC bakeout temperature	350ºC
Vessel bakeout temperature	150ºC
Vessel nominal operating temperature	25ºC
Maximum plasma heat load	12 MW
Heating pulse duration (max)	1.2 seconds
Cool down time between shots	15 minutes

Figure 3 Vacuum Vessel Assembly Showing Thermal Insulation
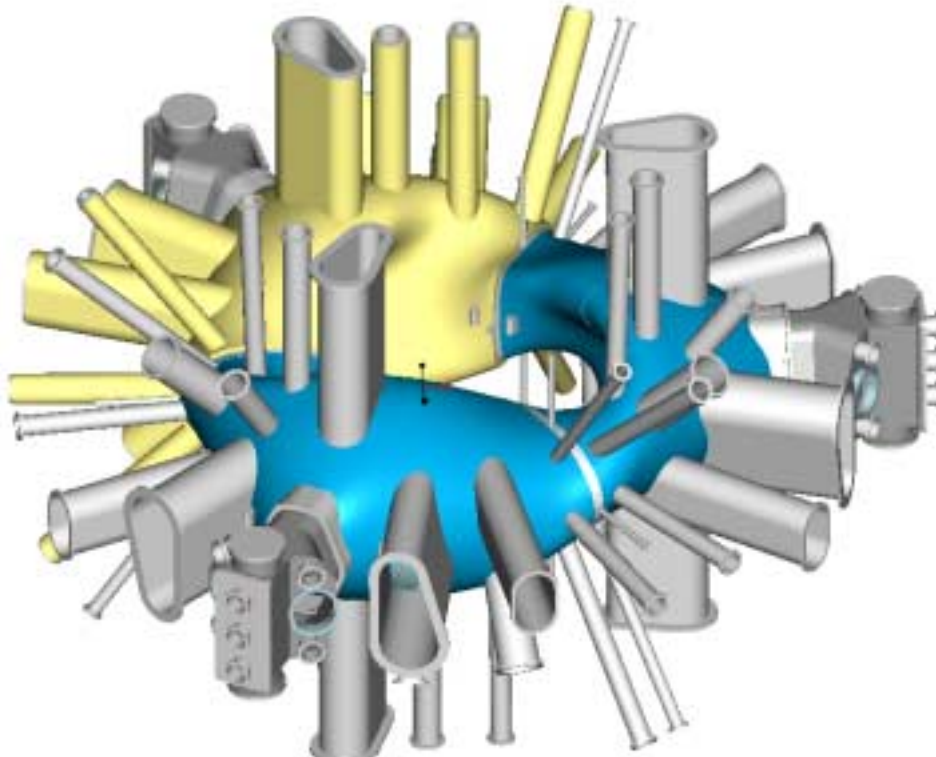
Figure 4 Vacuum Vessel Dimensions
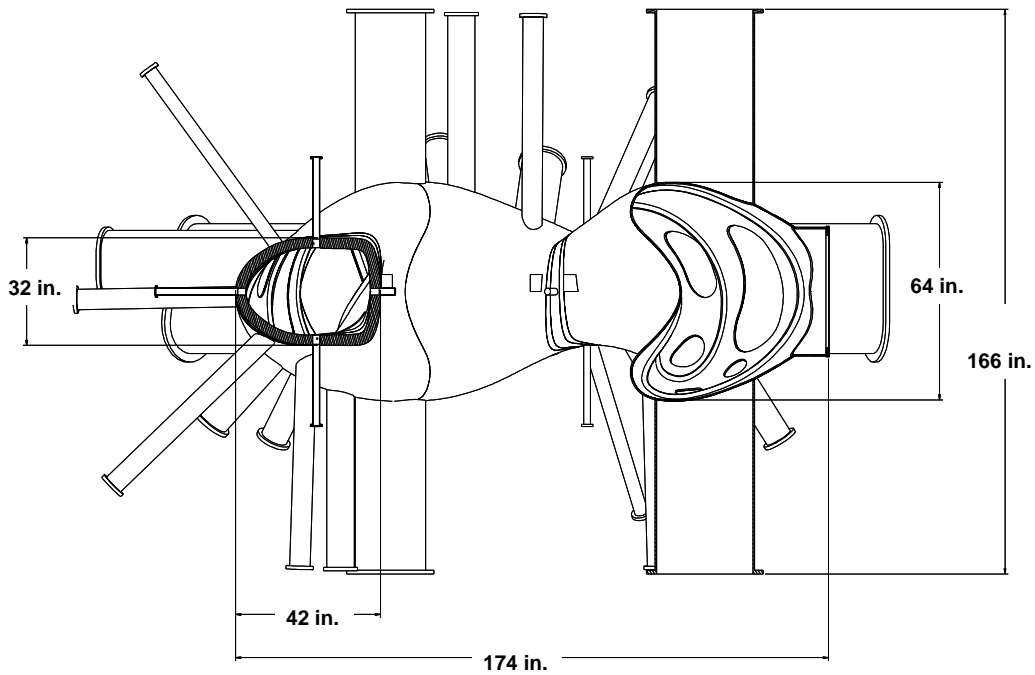
The port configuration is illustrated in Figure 5. Several sizes of radial and vertical ports, tabulated in Table 4, are used to best utilize the limited access between modular coils. The arrangement is designed to meet access requirements for the diagnostics, including future upgrades. The large neutral beam ports and the ports immediately adjacent to the NBI ports are designed to permit personnel access into the vacuum vessel interior for final assembly of the three vessel sub-assemblies and maintenance of diagnostics and in-vessel components. The ports will be welded onto the vessel body during pre-assembly, after installation of the modular and TF coils onto the vessel segments, prior to final assembly. Port stubs are provided on the vessel to permit the modular coils to slip on first, followed by welding of the port extensions from the outside using an automatic pipe welder inserted down into the port extensions

The vessel will be supported from the modular coil structure via vertical and lateral support hangers for ease of adjustment and to minimize heat transfer between the two structures. Significant relative thermal growth must be accommodated when the modular coils are cooled to cryogenic temperatures or when the vacuum vessel is heated for bakeout. The vertical hangers are located in four positions per field period, while the lateral supports are located at each neutral beam duct. The hangar geometry is illustrated in Figure 6.

Figure 5 VV Port Arrangement
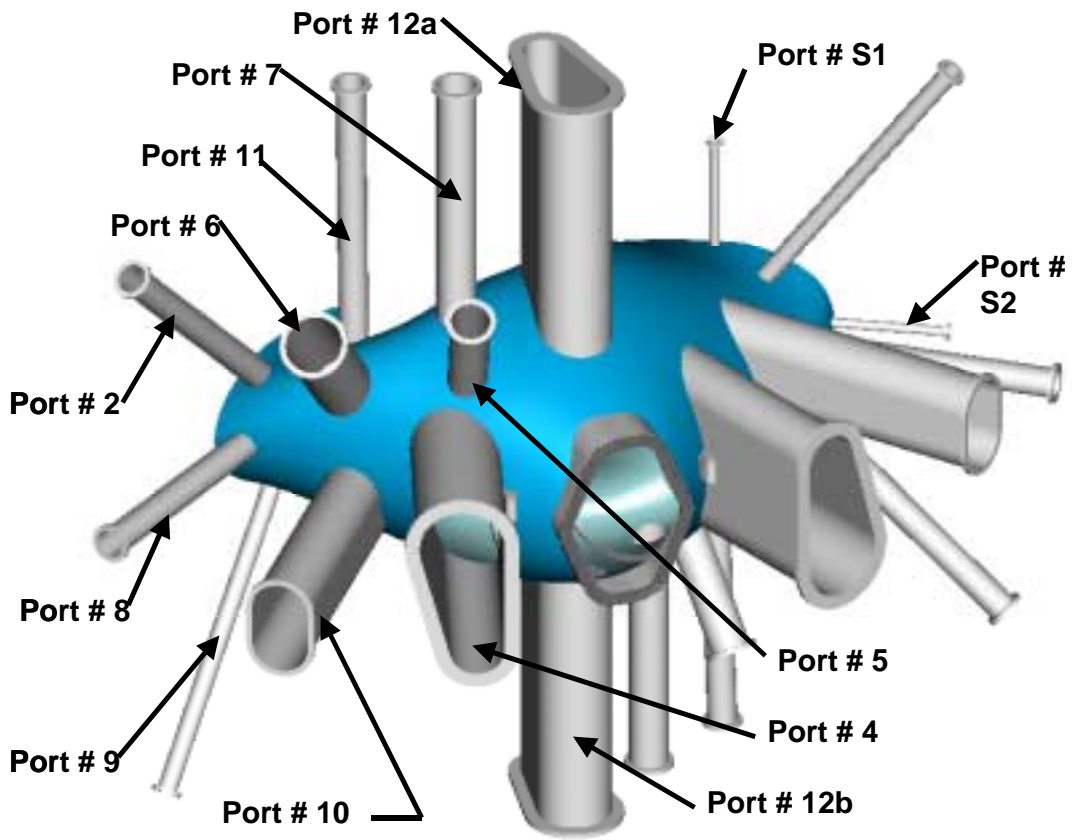
Table 4 Vacuum Vessel Port Dimensions

Port ID	No. per period	O.D. (inches)	total	Port ID	No. per period	O.D. (inches)	total
2	2	4 .	6	10	2	6 x 6 x 8	6
4	2	12 x 18 x 23.25	6	11	2	6	6
5	2	8	6	12	2	9 x 15 x 17.25	6
6	2	12	6	Neutral Beam	1	33 x 23	3
7	2	8	6	S1	2	2	6
8	2	6	6	S2	1	2	3
9	2	6	6	Total number of ports			72

Figure 6 Vacuum Vessel Support Hanger Geometry

Fabrication is a significant challenge, since the vessel has a contour closely conforming to the plasma on the inboard side. The vessel shell may be formed by pressing, explosive forming, or possibly casting sections of the vessel and welding them together to form the finished shape. Embossments can be incorporated to locally strengthen the wall thus permitting thinner gauge material and fewer piece parts and seams. Segmentation of the vessel is driven by assembly requirements and inherent fabrication limitations. Fabrication by pressing requires the panel sections to be removable from the tooling dies. This requirement must mesh with the desire for half-period segments. The result is that the number and geometry of poloidal segments is dictated by the die contour. A first cut at the segmentation indicates that the half period can be formed with four poloidal sections, as shown in Figure 7. For practicality, die size limitations may require more sections than this.

Figure 7 Typical Vacuum Vessel Shell Segmentation
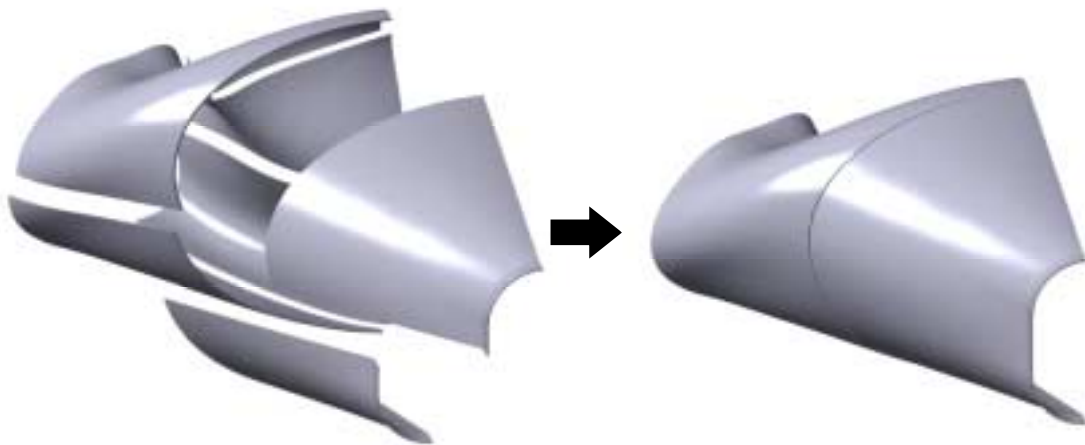
The form tolerance of the vessel must be very accurate in the inboard region, with a tolerance of +/- 0.15 inches to provide adequate clearance to both the coils and the plasma. On the outboard side the tolerance can be relaxed significantly to about +/- 0.5 inches. These tolerances must be held after the vessel is completely welded and assembled, so intermediate heat treatments during fabrication may be necessary.

Port stubs are included in the present design to reinforce the port openings and to provide a better interface for attaching the port extensions. Several concepts for these stubs are under consideration, and one of these is illustrated in Figure 8. The port opening is machined and a blank stub is welded in place. Leak checking of the torus is performed, followed by machining of the stub to provide the opening and a proper fit for the port extension. Elimination of the reinforcement was recommended during the manufacturing studies as a possible way of reducing costs, but this will require evaluation of the welding geometry, welding distortion, and stress levels that would be present without the reinforcement.

Figure 8 Port Stub Concept

After each field period of the shell is constructed and port stubs welded in place, coolant tracing is installed on the outside surface. To minimize distortion of the vessel, these lines are not skip welded or brazed, but are attached by clips and compression gaskets, spot-welded to the vessel, on approximately 15 cm centers. Heat transfer may be enhanced with special putty made for this purpose. The helium will be supplied to the torus bottom in a 3 inch (OD) header. Three, 2 inch (OD), distribution lines will feed to the large vertical port flanges, one at the bottom of each period, where a 1.5 inch (OD) "C" shaped header will feed the 13, 3/8 inch feeder lines (26 total) on each side of the port. A return header configuration identical to the supply header is located at the top of the torus. Each of the feeder lines will wrap around a port standpipe and traverse the liner wall up to the return header. An effort will be made to keep spaces approximately the same throughout.

The final assembly requires precise fit. To accomplish this, spacers are provided between the mating flanges of the vessel periods. Any misalignment that is encountered can be compensated by machining the spacers to fit. The seal interfaces are also machined into the spacer. A double seal is planned, with a metal seal on the plasma side and a viton seal on the air side. Interstitial pumping will be provided for reliability and to allow leak checking of the seals without pumping out the vessel. In addition to the assembly advantages, the spacer provides small ports on the v=1/2 symmetry plane for diagnostics such as Thomson scattering. Figure 9 illustrates the spacer and seal arrangement.

Figure 9 Spacer and Seal Arrangement
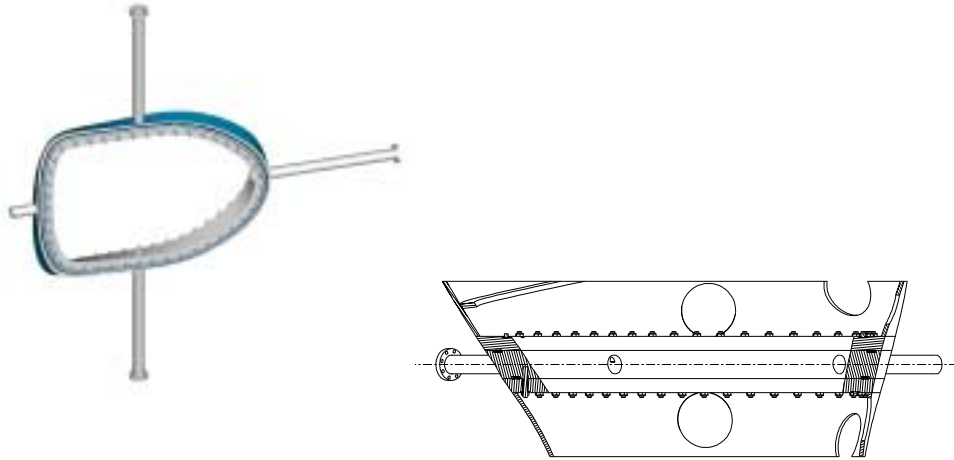
As noted previously, the installation of the port extensions will occur during final machine assembly. This requires that the vacuum vessel be placed inside the modular coils, by sliding the coils over each end of the vessel subassembly. The port extensions are then slipped into the port stubs and welded on from inside. The three sub-assemblies (periods), complete with coils, are bolted internally into a final torus at the oblate (wide) sections. The torus sections are provided with internal, machined end flanges that provide a double o-ring, bolted assembly. The alternative, welding the period sections together, would be very difficult and has therefore been rejected. There is also no access from the outside to reach an external weld joint. Achieving quality welds by welding on the inside would be very difficult due to the tight space constraints and contorted geometry inside the vessel. A bolted joint facilitates pre-installation of in-vessel components and assembly of the vacuum vessel. Figure 10illustrates three segments being brought together to complete assembly of the vacuum vessel. The bolted joint feature also makes disassembly possible for major modifications of the device in the future.

Figure 10 Final Assembly of the 3 Field Periods
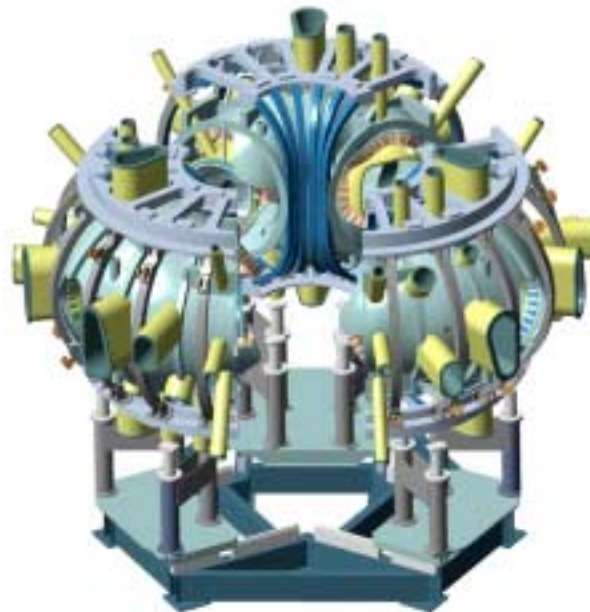
Access Features

Diagnostic access

Port locations were defined based on available space between modular coils, trim coils, PF and TF coils, and structure. The ports are located between these obstructions and aimed in radial planes directly at the magnetic axis. As discussed above, the sizes and numbers of ports appear well matched to our needs for diagnostic access.

Access for plasma heating

The requirement for neutral beam access is to accommodate two of the PBX-M neutral beams in the initial configuration. These beams must be oriented for tangential injection with one co-injected beam and one counter-injected beam. In addition, the device must accommodate the two remaining PBX-M neutral beams as a future upgrade. One of these beams must be oriented for tangential co-injection. The other beam must be capable of being oriented in either the co- or counter directions.

The neutral beams will be injected through a port centered on the v=0 (bean-shaped) cross-section. Figure 11shows the device configured for two co- and two counter-injected neutral beams. If the fourth beamline was configured for co-injection, it would be located at the remaining v=0 plane.

Figure 11 Neutral Beam Injection Into Plasma
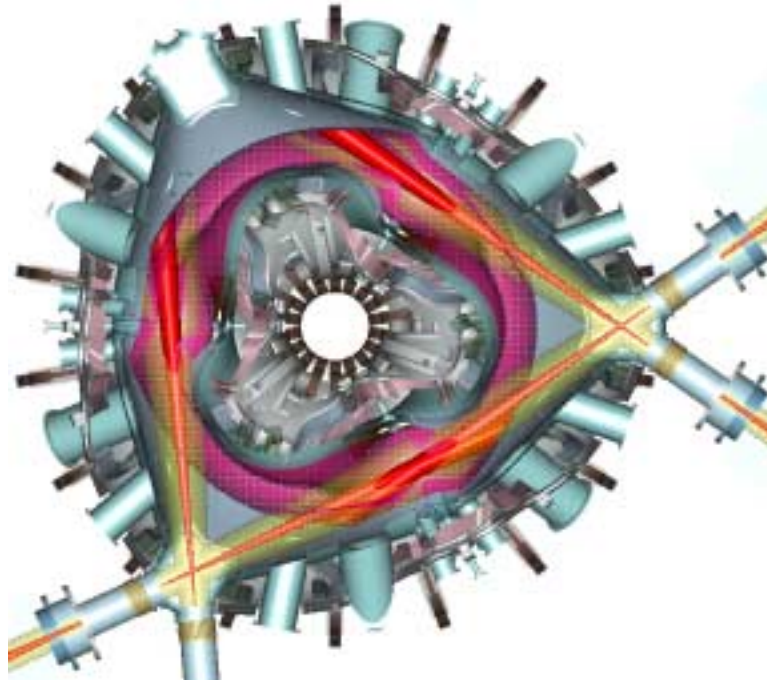
NCSX is being designed to accommodate 6 MW of ion cyclotron resonant frequency (ICRF) heating in addition to neutral beams. The leading candidate for ICRF heating is a 20-30 MHz system that employs a 6-strap design inboard of the plasma at the v=0.5 (the oblate or bullet-shaped cross-section). The envelope required for each strap with Faraday shield is approximately 10 cm deep x 10 cm wide x 50 cm tall. This option is attractive because of the physics advantages derived and because it makes use of existing RF sources at PPPL. Design studies indicate that system illustrated in Figure 12 is feasible.

Figure 12 Inboard RF Launcher Concept
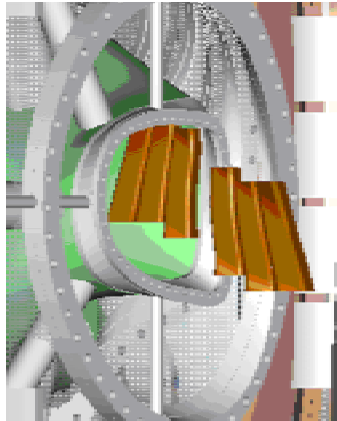
Personnel access

Personnel access requirements for different stages of fabrication and operation were considered, including:

- During manufacture – measure, inspect, assemble, and install components

- During field period subassembly – weld/inspect ports; leak check and repair welds; install trim coils, magnetic diagnostics, and PFCs

- During final assembly of vessel – connect vessel segments; clean, leak check, and inspect; complete installation of in-vessel components

- After final assembly of vessel – maintenance and reconfiguration of internal components

Port access is limited because of the modular coils, PF coils, TF coils, and structure supporting the modular coils. The three large ports through which the neutral beams are injected have a clear opening of 33 inches tall by 23 inches wide and are adequate for personnel access into the vacuum vessel. Although in the initial configuration only one of the three ports would have neutral beams installed, it is anticipated that ultimately two or perhaps all three would have equipment installed that would block ready access to the vessel interior. For this reason, the port extensions at these locations are now fitted with a large rectangular port covers that can be removed even with two neutral beam injectors installed at the same location. This port is illustrated in Figure 13.

Figure 13 Removable Port Cover for Personnel Access

Removable port cover for personnel access
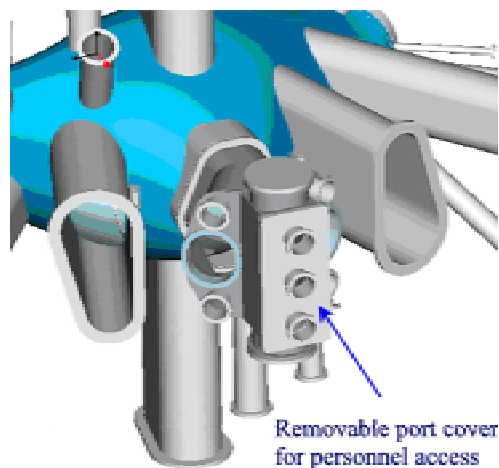
Alternate routes for personnel access are available through the ports adjacent to the neutral beam ports. These ports have been enlarged during conceptual design to have a tear drop shape with an 18 inch clear diameter at one end tapering to a 12 inch diameter at the other end. This adds six more ports that would provide adequate openings for personnel.

2.2.2   In-Vessel Components

Baseline Configuration

The baseline PFC configuration provides a limited system adequate for initial operation, through the Ohmic heating phase of the program. A set of simple fixed limiter tiles will be attached to either side of the vessel assembly flanges to provide poloidal limiters at those three locations. The tiles bolt to the flanges via graphite (Grafoil^R) gaskets. This design permits conduction cooling to the vessel coolant tracing while allowing thermal growth. The limiter locations and design concept are illustrated in Figure 14 and Figure 15.

Figure 14 Poloidal Limiter Configuration for Initial Operation
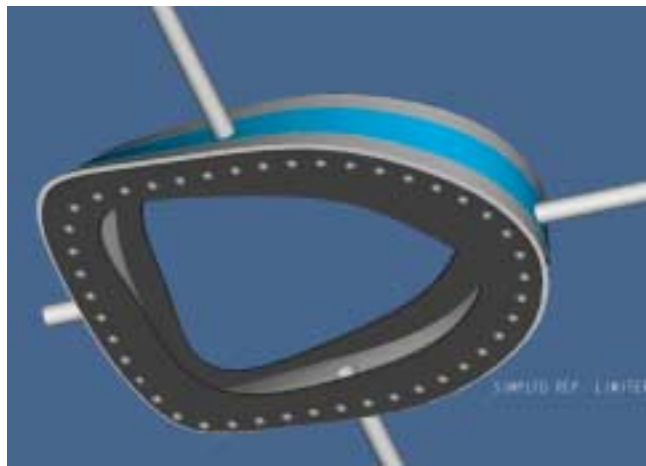
Figure 15 Cross-Section of Limiter Concept at VV Field Joints
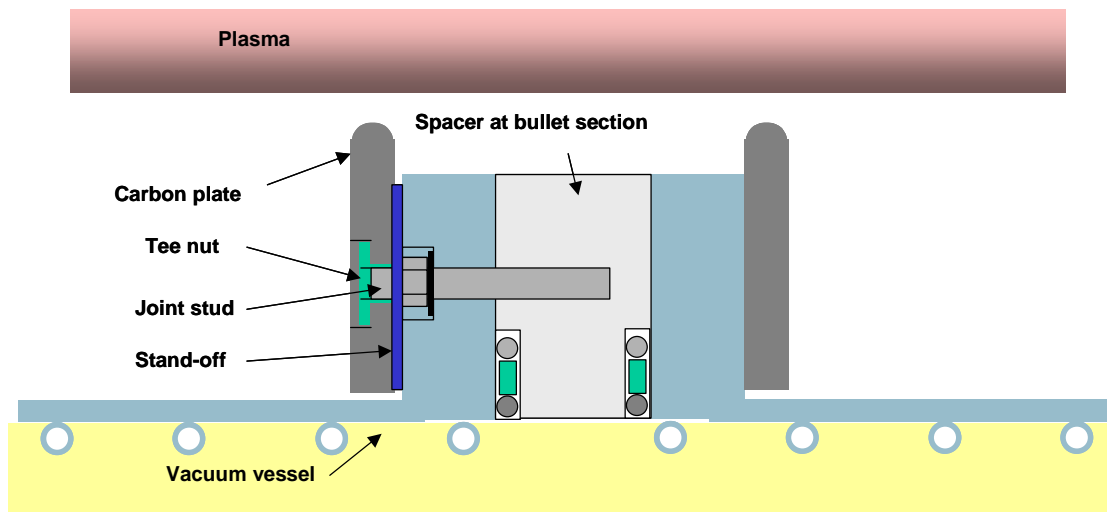
Upgrade Configuration

The design is required to accommodate substantial upgrades to the PFCs to meet the requirements for the later stages of the research program, from the Initial Auxiliary Heating Phase onward. To demonstrate that such upgrades are feasible and able to meet requirements, a flexible, re-configurable design concept has been developed. It is a robust concept that can be adapted in its geometrical details and implemented in stages to meet the needs of the research program as it evolves and the detailed requirements are clarified.

The upgrade concept is a contoured liner, shown in Figure 16, constructed of molded carbon fiber composite (CFC) panels mounted on a frame of poloidal rings. When the full complement of panels is installed, they will shield the entire interior surface of the vessel. It is compatible with staged implementation, such that the support structure and the panels can be installed during later operation. Having an independently supported, bake-able liner avoids the need to design the vacuum vessel and the in-vessel components mounted on the vessel for baking at 350ºC and reduces the heat loads to the cold mass during bakeout. The liner is baked at 350ºC while maintaining the vessel at 150ºC. Radiation heat loads to the vacuum vessel and in-vessel components are reduced by thermal shields mounted on the backside of the panels. During normal operation, the liner will have a lower pre-shot temperature in the range of 20ºC to 150ºC. The molded panels form a continuous shell around the plasma with penetrations for diagnostics, heating, and personnel access. This shell serves many functions. It provides a high heat flux surface in the regions of sharp curvature where the heat flux from the plasma is expected to be highest. It can act as a belt limiter on the inboard midplane. On the lower half of the shell, it will absorb the power deposited by the beam ions that are promptly lost from the plasma. On the outboard side, the shell serves as armor to protect the vacuum vessel and in-vessel components from heat loads due to neutral beam shine-through. The shell also protects in-vessel components mounted on the vessel, e.g., trim coils and magnetic diagnostics, from heat loads from the plasma.

Figure 16 Internal Liner with Full Complement of Panels

Panel mounting rib, (one of 18)

Typical panel (20 types, 90 total)
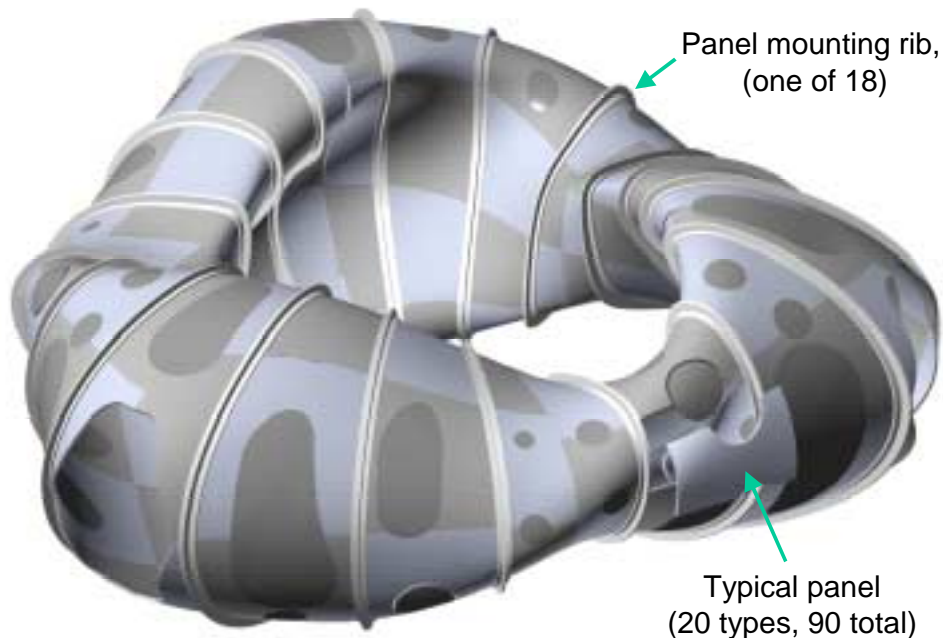
The continuous shell allows great flexibility in plasma shaping because any surface that the plasma impinges on can act as a limiter and be resistant to damage from plasma heat loads. The properties of the CFC panels can be tailored to the local heat loads if necessary. More expensive panels with high thermal conductivity can be used in limited regions of higher heat loads. Less expensive panels with modest thermal conductivity will be sufficient for most regions.

The panels are attached to 18 Inconel ribs, which are traced to provide heating for the carbon liner during bakeout and cooling between shots. They also serve as thermal isolation members that maintain alignment of the PFC liner during thermal cycling. Figure 17 shows the general arrangement of the panel ribs, and Figure 18 illustrates the attachment concept for the panels to the ribs. Bake-out of the PFC panels is provided by circulating helium gas at up to 19 atmospheres through the tracing on the mounting ribs. The tracing also serves to remove the heat deposited in the PFCs during normal operation.   In the present design, the plasma-facing surface is located approximately 7 cm from the vacuum vessel surface.

Figure 17 General Arrangement of Panel Ribs
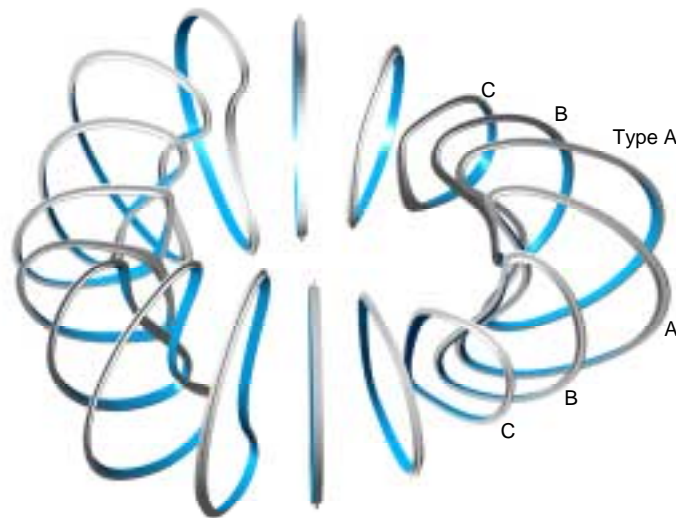
Figure 18 Panel-to-Rib Attachment Concept
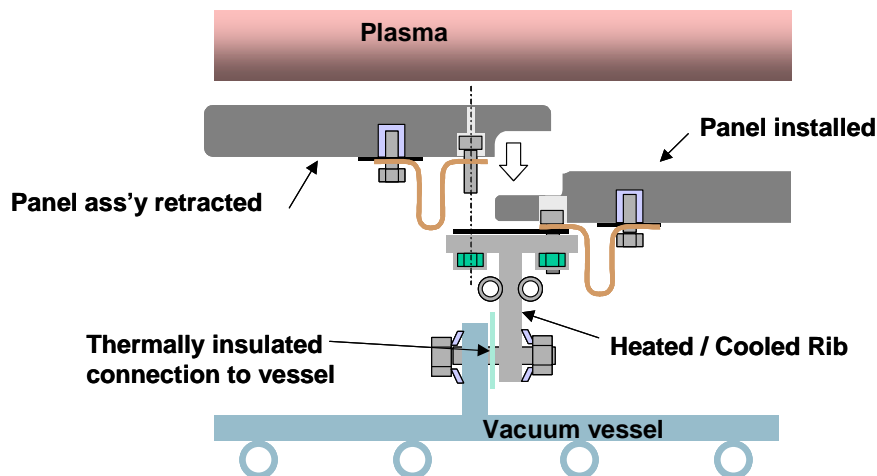
2.3   Design Basis

The design basis for the vacuum vessel includes design criteria, analysis, and vendor input from manufacturing studies conducted by multiple industrial vendors as part of the conceptual design process.

The design basis for the PFCs includes previous experience, analysis, and vendor input for the molded CFC panels. Because of the close thermal and mechanical interfaces between the VV and PFCs, they have been analyzed in an integrated fashion, including both the initial ohmic operating phases through all the upgrades to the full complement of plasma heating and full coverage of panels.

Design criteria

The vacuum vessel will be designed according to the NCSX Structural Design Criteria, which is based on the ASME Code, Section VIII, Division 2. The code provides a conservative but prudent approach to design stresses, fatigue, buckling, welding, and inspection of vessels. While the vessel will be designed to be in compliance with the ASME Code, the vessel will not be code-stamped.

Plasma facing components will also be designed to ASME code type stress limits, although the material properties for carbon fiber reinforced composites (CFC) are not included in the code. The basic material properties for the vessel and PFC materials are listed in Table 5.

Table 5 Material Properties for the VV and PFCs

Material	Inconel 625 [1]	Carbon Fiber Composite Stackpole 2D 0/90 Material[2]
Yield strength	55 ksi @ 70 F 45.7 ksi @ 750 F	15 ksi (flexural strength)
Ultimate Tensile Strength	110 ksi	8 ksi (in-plane)
Young's modulus	30 E-6 @ 70 F 27 E-6 @ 750 F	4.3 E6 psi
Fatigue strength, 100,000 cycles	73 ksi base material 39 ksi weld material	70% S_{ult}
Poisson's ratio	0.28 - 0.30, temp dependent	0.29 (in-plane)

Stress in vessel from pressure, disruption loads

The primary loads on the vessel include atmospheric pressure, gravity, disruption loads, port mounted equipment, internal components, and seismic loads. The most significant loads are the pressure and disruption loads, and these have been investigated in some detail[3].

The SPARK code was used to determine the forces on the vessel from a plasma disruption. One field period of the vessel with port extensions and port covers was modeled as a shell. Two disruption cases were considered; the first

[1] J. Mayhall, "Inconel properties and failure criteria for the ORNL/TFTR RF Antenna Faraday Shield Analysis", DM-XCS-14690-003, May, 1988

[2] F. Dahlgren "NCSX First Wall FEA Stationary Disruption Analysis", NCSX ENGR. MTG., 13 March 2002

[3] A. Brooks, "Vacuum Vessel and First Wall Disruption Analyses", February 2002

corresponded to the full current, full beta scenario with 175 kA in the plasma and 2 T combined toroidal field from the modular coils and TF coils. The second corresponded to the high current, zero beta scenario with 350 kA in the plasma and a 1.8 T toroidal field. The plasma was modeled as a single filament of current at the magnetic center. An inductive solution was obtained, analogous to the plasma vanishing instantaneously. The resulting current distribution for the 350 kA, 1.8 T case is shown in Figure 19. As shown in the figure, the current is concentrated on the inboard region of the vessel in the "trough" and follows a circuitous pattern around the ports on the top and outboard regions. The decay time constant for the net toroidal (and poloidal) current was 5.3 ms.

Figure 19 Induced Current Pattern From a 350kA Plasma Disruption
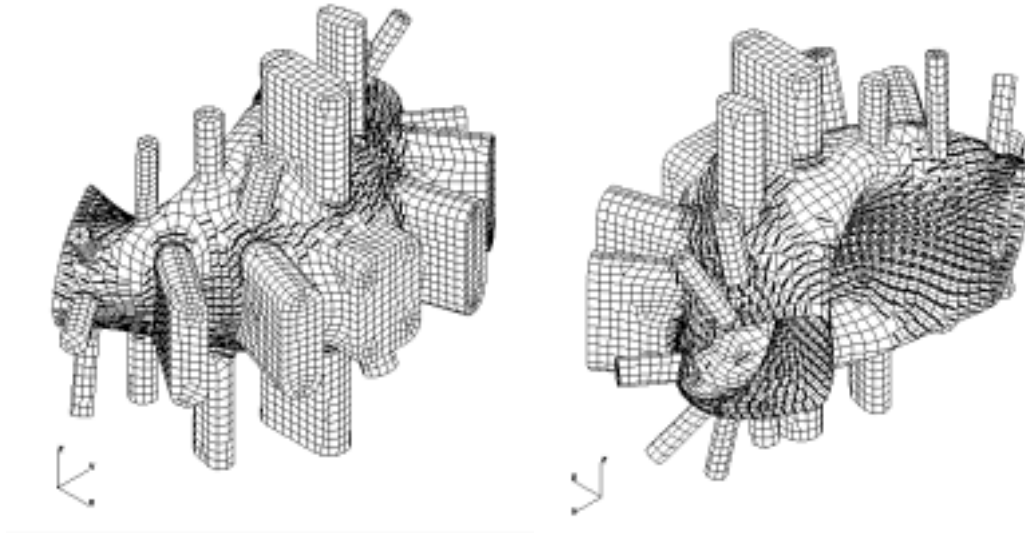
The forces were computed in two parts, the first being the force due to the self fields of the induced currents, and the second being the force due to the interaction of the induced currents with the background field from the coils. As expected, the self-forces from the 350 kA disruption were approximately 4 times higher than those from the 175 kA disruption. However, the background field contribution was proportionately higher for the 175 kA case, causing a higher net centering force. Table 6 summarizes the forces for the vessel disruption cases.

Table 6 Net Forces on One VV Field Period

Disruption scenario	Sum of forces on single field period, -60 to +6-0 degrees, x direction, (lbs)	
175 kA, 2T	Self force	2,518
	Force from coils	-9,329
	Net force	-6,810
350 kA, 1.8T	Self force	10,397
	Force from coils	-13,746
	Net force	-3,349

The forces were applied to a NASTRAN model of one field period of the vessel with cyclic symmetric boundary conditions. Three load cases were considered; pressure only, pressure plus loads from the 175 kA disruption, and pressure plus loads from the 350 kA disruption. Figure 20 and Figure 21 illustrate the maximum displacements. Figure 22 illustrates a typical stress distributions from these three cases. Table 7 summarizes the results of these load cases. As indicated in the table, the stresses are well below the allowable stress for Inconel 625. Further analysis must be undertaken considering the dynamic load conditions, but these stresses are not expected to be significantly higher than the statically calculated stresses. It should also be noted that the disruption loads were calculated with instantaneous plasma decay, so they represent limit loads, not actual loads. Even with this conservative assumption, the stresses area acceptable.

Figure 20 Displacements Under 1 Atmosphere Pressure Load
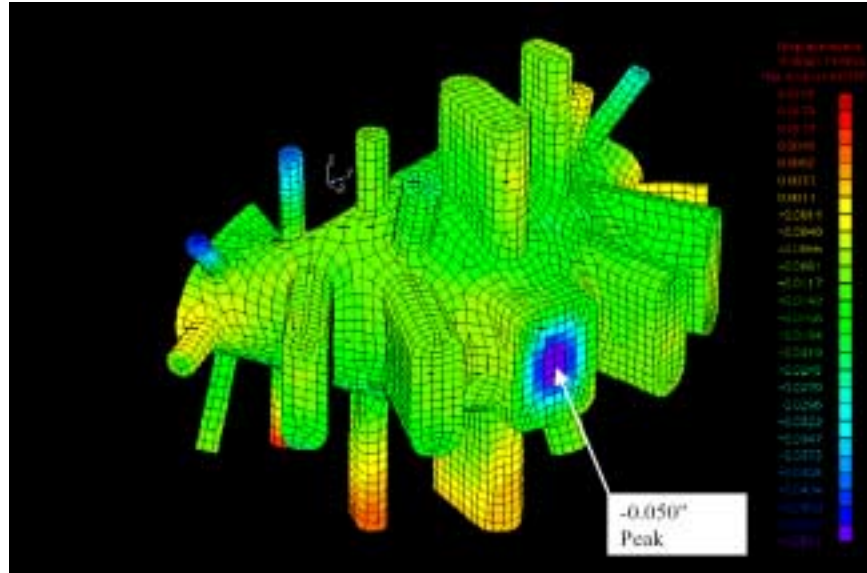
Figure 21 Toroidal Displacements (350kA Disruption, 1 at.)
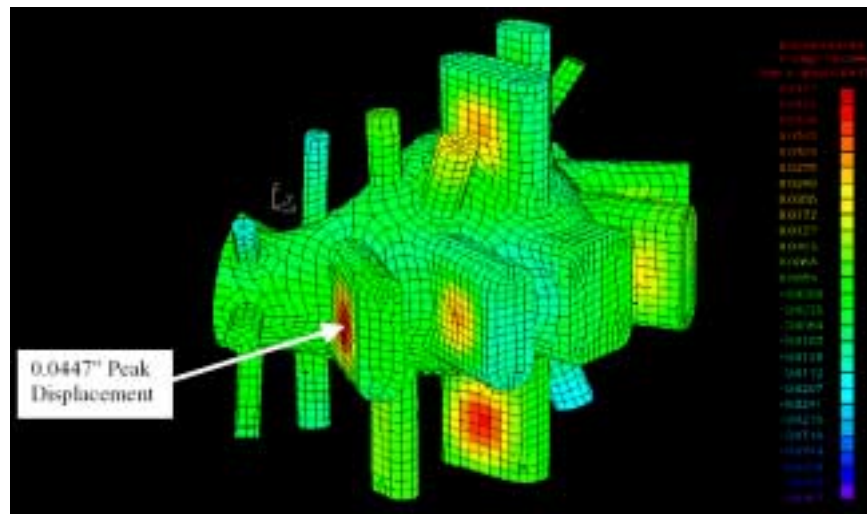
Figure 22 Minor Principle Stresses (350kA Disruption, 1 atm.)
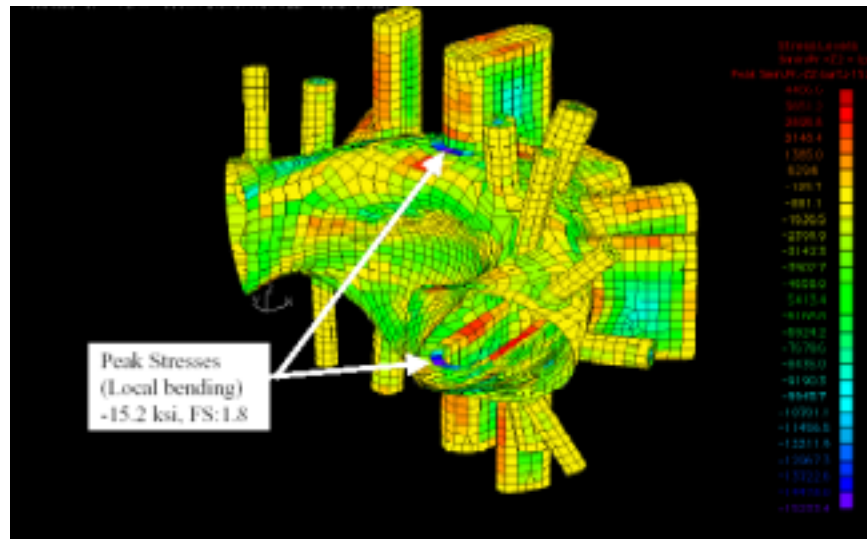
Table 7 Peak VV Stresses and Displacements

Peak Displacements:	Radial	Toroidal	Vertical
Press only	-0.050"	0.045"	-0.028"
Press. + 175 kA disruption load	-0.049"	0.047"	-0.019"
Press. + 350 kA disruption load	-0.047"	0.045"	-0.020"
Peak stresses:	Major or minor Principal stress	Tresca stress	Allowable stress, Sm
Press only	-11,648 psi	7,320 psi	
Press. + 175 kA disruption load	-13,932 psi	7,598 psi	27.5 ksi (ASME-Gr#1
Press. + 350 kA disruption load	-15,233 psi	7,522 psi	625 Inconel ASTM-B-443)

Buckling loads were also a concern for the vessel, and an elastic buckling calculation was performed. The analysis assumed a 0.25 inch shell, to conservatively account for any thinning that may occur during forming operations. The analysis indicated the first eigenvalue for buckling under a uniform pressure load of 1 atmosphere was 6.7. This is equivalent to the factor of safety for buckling on the 1 atmosphere load. The deformed shape is illustrated in Figure 23.

Figure 23 Shape Deformation From Buckling Analysis
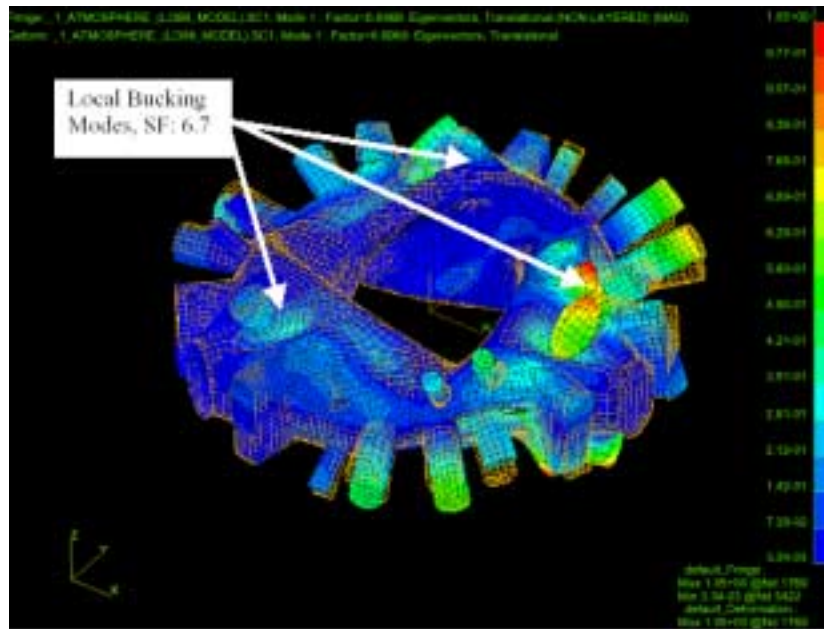
Vessel Vessel and Plasma Facing Component Thermal Analysis

The vacuum vessel temperature is controlled by passing pressurized helium gas through trace lines covering the external surfaces of the shell and ports. Several operating cases must be considered, including bakeout of the vessel without first wall panels, bakeout with the first wall panels, normal operation without first wall panels, and normal operation with first wall panels. The vessel must be heated for bakeout without the first wall panels, and cooled during bakeout of the first wall panels. Conversely, the vessel must be cooled to maintain its temperature during normal operation without the first wall panels, and must be heated to maintain its temperature during normal operation with the panels present. These various thermal loading cases are summarized in Table 8. The required repetition rate for all modes of operation is 15 minutes between pulses.

A series of analyses were performed to verify the thermal performance of the NCSX vessel and PFCs, specifically, to establish the design basis for cooling and heating requirements and coolant supply header design.

- Calculations were performed to determine the heat losses from the vessel as a function of insulation thickness.

- Vessel temperature and cool-down times were determined, based on the operation rep rates, vessel thickness, coolant flow rates, and coolant line spacing.

- Coolant parameters were determined for vessel bakeout and operation. These included pressure drops, flow rates, and temperature change, based on the tracing diameter, length, and number of passages.

Initial operation with limited PFC coverage of vessel

During early operation, and early stages of PFC implementation, portions of the vacuum vessel surface area may not be protected by CFC panels. Figure 24 shows the temperature of the vessel as a function of repetition rate, assuming the full complement of 12 MW of heating was used. The analysis assumes helium gas at 19 atmospheres pressure, a passage ID of 0.81 cm, and an inlet velocity of 17 m/s. A 100C coolant temperature was assumed. The pre-shot temperature ratcheted up less than 15C above the coolant temperature and stabilized after only 7 pulses.

Table 8 VV and PFC Operational Parameters

Operating state:	PFCs - surface min (C)	max (C)	PFC - ribs min (C)	max (C)	Vessel min (C)	max (C)	VV extensions min (C)	max (C)	Mod Coils/shell min (K)	max (K)
Standby	20	100	20	100	20	100	20	100	77	85
Pre-operating	20	100	20	100	20	100	20	100	77	85
Equilibrated operation		< 1200	20	100	20	100	20	100	77	85
Bakeout	150	350	150	350	150	150	150	150	77	100

Typical operating modes for analysis:

		PFCs - surface	PFC - ribs	Vessel	VV extensions	Mod Coils/shell
Typical standby:	case 1	100	100	20	20	77
Pre-op / conditioning:	case 2	100	100	100	100	77
Operation:						
- no PFCs, 3 MW, .3 s	case 3a	n/a	n/a	20	20	77
- no PFCs, 6 MW, .3 s	case 3b	n/a	n/a	100	100	77
- 12 MW, 1.2s, partial PFCs	case 3c	n/a + < 1200	n/a + < 350	TBD	TBD	77
- 12 MW, 1.2s with PFCs	case 3d	< 1200	< 350	100	100	77
Bakeout:	case 4	350	350	150	150	100

Figure 24 Thermal Ratcheting of VV Temperature

12 MW operation
Tracing on 20 cm (~8") spacing
0.95 cm Inconel vessel
1.2 sec ESW pulse length
10 minutes between pulses
100 C coolant temperature
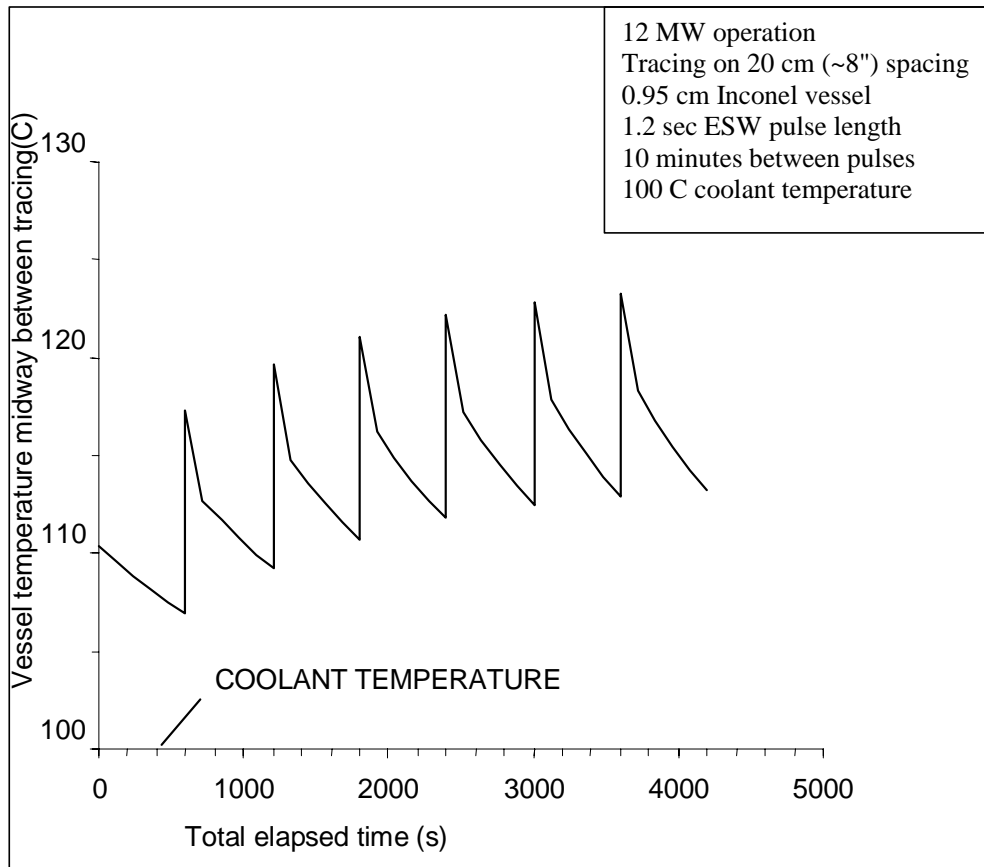
In this configuration there is little effect on cool down time using other cooling media or varying the coolant parameters. This is because the spacing of the tubing and the diffusivity of the material in this geometry, rather than the heat transfer coefficient, limit the time constant. If the material was more conductive or if the spacing decreased dramatically, then the opposite would become true.

Vessel Tracing Thermo-Hydraulic Analysis

The vessel is assumed to have a minimum of 2.5 cm of thermal insulation on its external surface and around all the ports, with 15 cm average fill between the shell and vessel wall to thermally isolate the modular coils. Using an efficiency allowance of 75% results in a loss of 12 kW from the liner to the cryostat (100K) during bakeout at 150 C.

A tradeoff study indicates that 24 kW, double the calculated minimum, may be supplied through the liner tracing using the following parameters:

- Helium at 19 atmospheres and inlet temperature of 166 C.

- 3/8 inch OD, 0.32 inch ID tubing (0.81 cm ID)

- Helium inlet velocity 33 m/s

- Total mass flow to liner 1054 kg/hr (2320 lbs/hr)

- 78 parallel tracing circuits (26 per period)

- Tracing length per circuit is assumed to be 5.3.m

The resulting pressure drop is only 0.2 atmospheres, so the length of tracing circuits will not be a concern. However, every effort will be made to keep the runs approximately equal in length. Analysis for 10 minute cool down times between shots indicate that the heating lines with the factor of two safety factor have 8 times the cooling capacity required. As noted earlier, this does not significantly reduce cooling time, as the liner is conduction limited.

Thermal load on vessel from full PFC system during bakeout

Baking the PFCs to 350 C, while maintaining the vessel at 100 C results in high heat loads to the vessel coolant system unless radiation heat shields are used. Table 9 shows the dependence of the heat loss to the vessel on the number of shields. Since the vessel tracing is designed for 24 kW, it should be able to handle the heat load with no changes, provided that three heat shields are utilized under the PFC tiles.

Table 9 Heat Loss to VV From PFCs

Number of shields	Heat loss (kW)
0	121
1	49
2	31
3	22

PFC panel cooling

Since heat shielding is required to limit the vessel thermal loading during 350 C bakeout operation, the PFCs do not have a radiation cooling path to the vessel and must be cooled by conduction to another heat sink. This resulted in the rib design that is thermally isolated from the vessel but is traced to remove PFC heat. This is shown schematically in Figure 25. It assumes that there is a helium cooled tracing mounted on each side of the liner mounting rib. The rib must be thermally isolated to best of effort to assure that the load goes into the rib coolant

circuit, not the vacuum vessel. This is accomplished by minimizing the contact area using thin sections and shoulder bolts to prevent clamp up of surfaces. This also permits thermal growth during heating cycles.

Figure 25 Panel Mounting Schematic
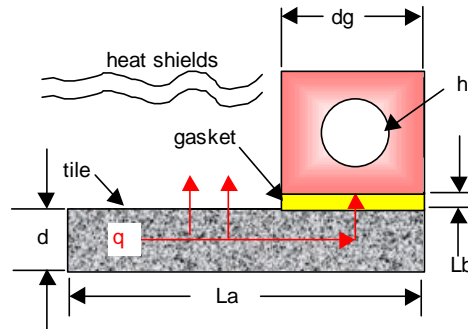
The resulting heat transfer is shown in Figure 26. Thermal ratcheting is almost eliminated, with the vessel leveling off at about 20 C above its initial temperature.

Figure 26 Thermal Response of Shielded Tiles
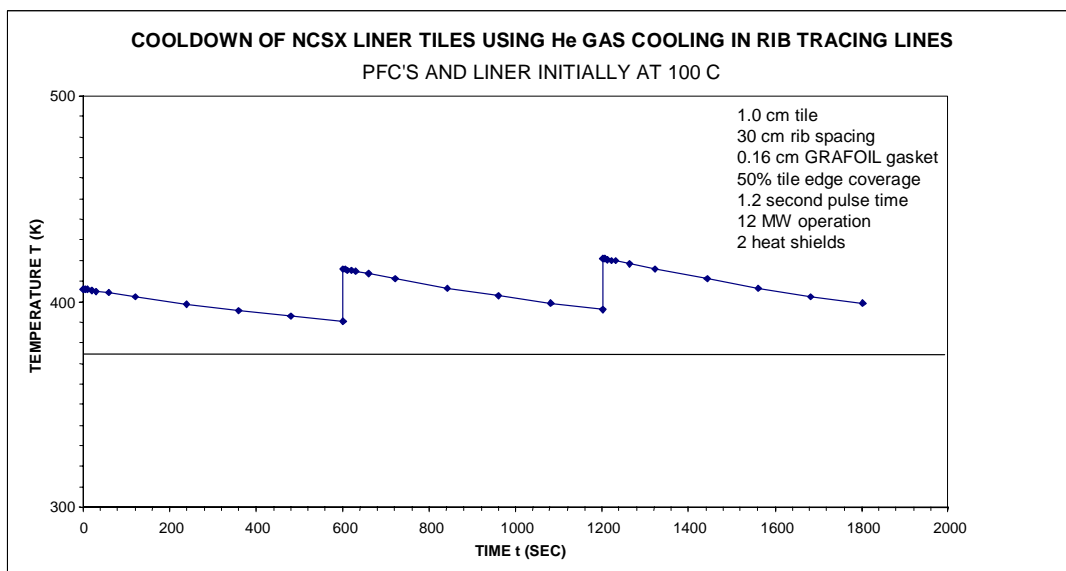
Limiter and NB Tile Geometry

The graphite liner panels can potentially be the same design for all the PFC components used in the vessel; provided the maximum temperatures predicted during one plus seconds of operation do not exceed the 1200 C maximum usually permitted. Limiters could operate up into the 1500 W/cm^2 range. By using graphite gaskets or omitting them and varying the number of heat shields between the liner and the vessel, it is possible to customize thermal performance, that is, permit tiles to float up in temperature and utilize radiative cooling or on the other hand tightly couple them to the ribs and use conductive cooling to the tracing. Figure 27 illustrates permissible heat flux as a function of pulse length.

Figure 27 Maximum Heat Flux v. Heating Pulse Length
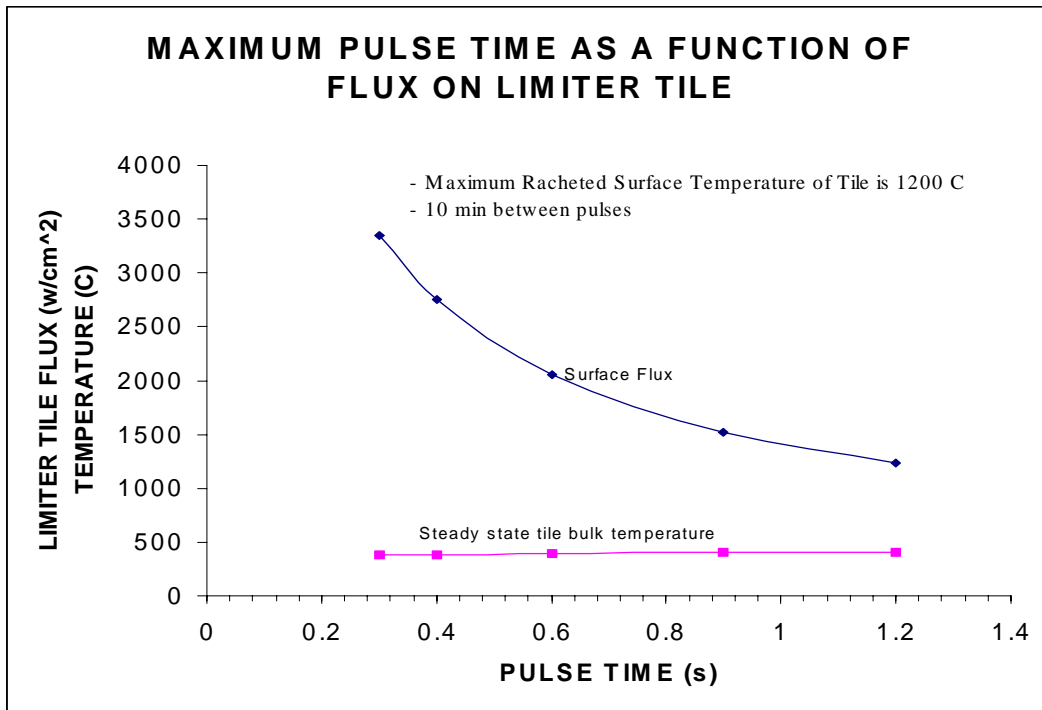
PFC Support Rib Thermo-Hydraulics

The PFC support ribs must be assembled into the vessel in two pieces in order to fit through the large access ports. There also needs to be a tracing on both sides of the ribs to permit close coupling to each of the two panels mounting to the ribs. The ribs are installed on 20 degree radial centers, making 18 ribs total. A helium supply system similar to the vessel tracing system will be used, but it will be operated at the elevated temperature. There is one helium header to each period, entering the bottom vertical port and exiting the top vertical port. The heating system parameters for 350 C bakeout are provided in Table 10.

Table 10 PFC Thermo-Hydraulic Parameters

Total heat required	24 kW
Number of tracing circuits	72
Average length of circuit	3.5 m
ID of tracing	1.09 cm (½ " OD)
Helium inlet velocity	27 m/s
Helium inlet temperature	367 C
Helium supply	19 atmospheres
Supply header OD	5 cm (2 inch)
Total helium mass flow	945 kg/hr (2080 lbs/hr)
Pressure drop	0.047 atmospheres

Plasma Facing Component Structural Analysis

The initial plasma facing components will consist only of the fixed poloidal limiters at the 3 vacuum vessel assembly joints, and these have no structural implications. However, the upgrade system that must be accommodated consists of a full, stand alone shell structure consisting of ribs and CFC panels that could be loaded

by plasma disruptions. A SPARK analysis was performed on a CFC shell to obtain the loading conditions[4]. The calculation did not consider the presence of the vacuum vessel and is conservative from that standpoint. The same plasma disruption cases were considered for the first wall as were considered for the vessel, namely a 175 kA, 2T scenario and a 350 kA, 1.8 T scenario. Table 11 summarizes the net forces on the first wall from these two cases.

Table 11 Net Forces on One Liner Field Period

Disruption scenario	Force on single field period, -60 to +6-0 degrees, x direction, (lbs)	
175 kA, 2T	Self force	3.033
	Force from coils	-9,285
	Net force	-6,252
350 kA, 1.8T	Self force	12,635
	Force from coils	-13,858
	Net force	-1,223

The structural response of the first wall from these forces was calculated using ANSYS, and the stress distribution is illustrated in Figure 28. The general stresses are relatively low, below the 3000 psi allowable for the material. The peak stresses are slightly high around the ports, but the analysis does not include any reinforcement due to the rib structure or molded reinforcements that could be included around discontinuities such as the port openings. Table 12 summarizes the stresses and deflections for the two loading conditions. As with the vessel analysis, it should be noted that an instantaneous plasma disruption was assumed and the loading is conservative.

Figure 28 Tresca Stresses From 350kA Disruption

---
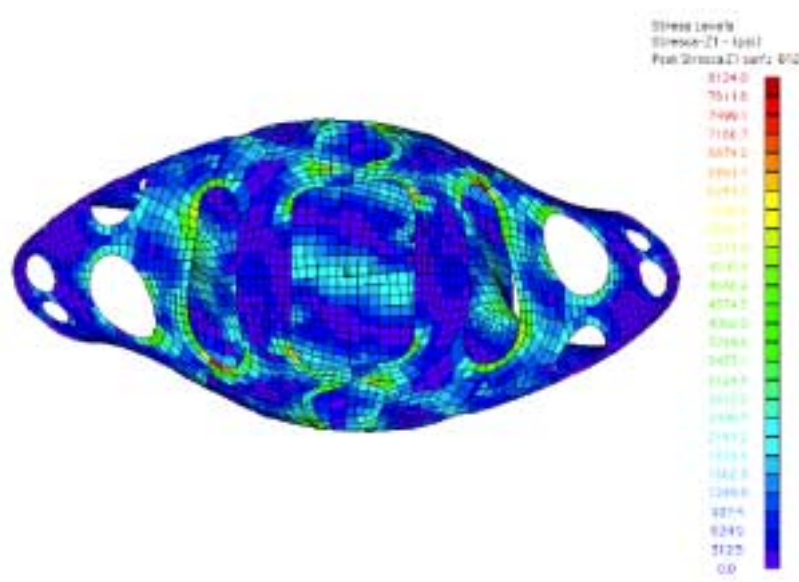
[4] A. Brooks, "Vacuum Vessel and First Wall Disruption Analyses", February 2002

Table 12 Summary of Stresses in Disruption Analysis of Liner

	175 kA disruption	350 kA disruption
Max force	829 lbs	1819 lbs
Max displacement	0.08 inches	0.24 inches
(E = 2E+6 psi)		
Max stress	5096 psi (MinPr- Z1)	8124 psi (Tresca -Z1)

Vacuum Vessel and PFC Vendor Input and Manufacturing studies

In order to obtain feedback from potential fabricators concerning the feasibility, methods, and cost for fabricating the vacuum vessel, funded manufacturing studies of the NCSX vessel were performed by five capable suppliers. The studies were based on a set of CAD models and a draft procurement specification. The vendors proposed several methods for forming the vessel, including hot pressing, cold pressing, explosive forming, and casting. Several suggestions were made concerning details such as port reinforcement design, spacer design, assembly flange design, etc. All the vendors recommended some R&D, but all concluded that the vessel shape, tolerances, and other requirements were feasible.

Input was obtained from a potential vendor concerning the large PFC panels, which are not part of the baseline project but will be required as an upgrade during later phases of operation. The approximate size limitations and processing data were discussed. The panels are feasible using commercial pressing and infiltration processes.

2.4   Design Implementation

Component Procurement and Fabrication

The vacuum vessel will be procured via a fixed price subcontract, including the supply of all required labor and materials, machining, fabrication, and factory acceptance inspections and tests. The vessel will be delivered to the Princeton Plasma Physics Laboratory (PPPL) site as three complete field period subassemblies with separate (unattached) port extension assemblies. All of the labor for the final installation and assembly of the vessel will be supplied by PPPL.

Prior to contracting for the final vessel, two separate R&D contracts will be awarded to establish the feasibility of proposed fabrication processes and to guide the design team toward the optimum design for the selected process. Processes under consideration include press forming and welding, explosive forming and welding, and casting. The feasibility of the press forming and welding is not an issue, but some R&D is suggested to establish forming parameters for the Inconel in the 0.375 inch thickness, and for verifying the number of panels needed for a complete half period of the vessel. In addition, the welding of a port extension into the vessel torus from inside the vessel must be demonstrated to verify the welding equipment requirements, identify fixturing, and finalize the design details for the joint. The investment casting process has the potential to provide an accurate part with very little welding. Many of the features that would otherwise be attached by welding could be included as part of the basic casting, such as in-vessel component rib attachment features, port reinforcement features, field period assembly flanges, etc. However, vacuum vessels are not commonly cast, so the process must be verified for that application. Castings are typically treated to remove porosity by hot isostatic pressing (hipping), and this may be sufficient to produce a vacuum quality part.

Subsystem Assembly, Installation, and Testing

The vacuum vessel will be provided in three identical sections, corresponding to field periods of the magnetic configuration. A set of six modular coils will be assembled over one field period of the vessel. The vessel port extensions will then be welded in place. At this point the vessel will be leak checked and any repairs made to the port extension welds. The helium trace lines will be connected to the headers at the top and bottom of the large central port extensions. After these connections are leak checked, the thermal insulation will be applied around the torus and all the port extensions.

2.5   Reliability, Maintainability, and Safety

The reliability of the vacuum vessel is critical to the operation of NCSX. Once the vessel is installed, there is essentially no access to the outer surfaces for inspection or maintenance, and limited access to the interior surfaces of the vessel. To ensure adequate margin against failures, the vessel will be designed in accordance with the rules of the ASME Boiler and Pressure Vessel Code, Section VIII, Division II and fabricated in strict conformance with an approved manufacturing, inspection and test plan. Numerous quality checks will be performed during subsequent assembly and installation operations. A formal Failure Modes and Effects Criticality Analysis (FMECA) will be performed during the preliminary design phase of the project.

2.6   Cost and Schedule

The cost estimate for the PFCs and Vacuum Vessel is summarized in Table 13. This estimate was developed as a bottoms-up estimate, and includes significant input from manufacturers who participated in the manufacturing studies. The vacuum vessel (WBS 12) is the dominant cost element, with a cost of $4840K. The cost of the PFCs, which in the Fabrication Project, is limited to the poloidal limiters provided for ohmic operation, is $260K.

The contingency recommended for the vacuum vessel is 39%, due to the developmental nature of the system. The contingency recommended for the PFCs is 27%.

The schedule for implementing the Vacuum Vessel (WBS 12) and PFCs (WBS 11) may be seen in the **Project Master Schedule**, provided as part of the Conceptual Design Report**.** The vacuum vessel is close to the critical path. Title I design will start at the beginning of FY03. Title II design is scheduled to be finished early in FY04. Manufacturing R&D will be conducted in parallel with Title I and Title II design. The production contract will be awarded in mid-FY04. The first vacuum vessel segment will be shipped to PPPL in early FY05; the second in late FY05; and the third in mid FY06.

Design of the poloidal limiters for ohmic operation will not begin until mid FY06, with the procurement scheduled to be complete by the end of FY06.

Table 13 PFC and VV Cost Summary

Total Estimated Cost (K$)		111	116	11 Total	121	122	123	124	125	12 Total
Manufacturing Development	Labor/Other	15		15	173					173
	M&S				497					497
	Total	15		15	671					671
Design (Title I & II)	Labor/Other	79	31	110	354	57	39	37	21	508
	M&S									
	Total	79	31	110	354	57	39	37	21	508
Fabrication/Assembly (incl Title III)	Labor/Other	30	8	38	289	26	70	8	2	395
	M&S	92	5	97	3179	36	29	17	5	3266
	Total	122	13	135	3469	62	98	25	7	3661
Installation/test	Labor/Other									
	M&S									
	Total									
Grand Total		216	44	260	4494	118	137	63	28	4840

2.7 Risk Management

PFCs

The primary technical risks associated with the PFC system are 1) damage to the first wall or vessel from excessive heat flux and 2) excessive impurity influx to the plasma. These problems may arise due to lack of proper materials in the high heat flux regions and/or insufficient wall conditioning or bakeout temperatures to remove wall impurities. In stellarators, it is difficult to predict with certainty where the high heat flux regions will be, and these regions will move with different magnetic configurations. To mitigate these concerns, the PFC system has been designed to allow coverage of the entire interior surface of the vessel with CFC armor. Graphite and CFC tiles have been used successfully on most of the fusion experiments worldwide, and can tolerate extreme heat flux and thermal shock without failure. However, these materials must be baked at temperatures in excess of 300C. For that reason, the NCSX, the PFC system is supported from a rib structure inside the vacuum vessel that can be heated to 350C while the vessel is maintained at 150C. This is the approach used successfully on NSTX. It provides the high temperature necessary to condition the PFCs while maintaining the vessel at 150C to minimize engineering problems of the vessel, viewing windows, and diagnostics.

Vacuum vessel

The vacuum vessel has potential technical, cost and schedule risks. The technical risks can be listed, as well as the way in which each has been addressed:

Potential Technical Risk #1. The vessel will not permit a high quality vacuum (leaks, outgassing, etc.)

The first potential risk, that the vessel will not permit a high quality vacuum, is addressed in the design, the procurement specification, and the manufacturing, inspection, and test plan. The vessel will have the minimum number of welds consistent with the fabrication technique. The welds will be full penetration with a GTAW root pass and GTAW or GMAW filler passes, with no SMAW welding permitted. The vessel will be leak checked at the fabricator after multiple heating and cooling cycles. The interior surfaces will be polished and cleaned according to accepted vacuum equipment standards. The main assembly flanges between field periods will have double seals, with differential pumping between the seals, as will the large, irregular shaped ports. All the circular ports will have conflat seals. In addition to leak checking at the manufacturer, leak checking will occur after the port extensions are welded in place and prior to assembly of the three field periods.

Potential Technical Risk #2. The vessel will not have the correct shape

The second potential risk, that the vessel will not have the correct shape, is mitigated by the 3-D CAD technology and the use of modern 3-D measurement equipment such as laser trackers and portable coordinate measurement systems. The vessel can be continuously measured and corrections made during the fabrication process, and intermediate heat treatment will be provided to reduce residual stresses that could cause distortion during operation. All the fabrication processes will be demonstrated and optimized during the R&D phase of the vessel procurement, where full scale, partial prototypes will be fabricated and measured. A spacer is included between each field period subassembly that will be used to accommodate any misalignment between field period assembly flanges.

Potential Technical Risk #3. The coils will not fit over the vessel

The third potential risk, that the vessel will not fit inside the modular coils, is also mitigated by the 3-D CAD technology, the use of laser scanners and/or multilink measuring systems to verify geometry, and using accurate scale models of the vessel and coils during the design and development processes. A 1/12 scale model of the present design verifies that the coils and vacuum vessel can be assembled as planned.

Potential Technical Risk #4. The vessel will fail mechanically

The fourth potential risk, that the vessel will fail mechanically, is mitigated by analysis and conservative design criteria. Critical analysis, such as disruption load calculations, stress and deflection calculations and buckling analysis will be performed by independent groups using different codes and models. The disruption loads are relatively small compared to a tokamak of similar size, so these are not expected to cause significant problems. The stresses will be compared to the ASME code allowables, which provide a safety factor of 1.5 on yield for primary membrane stresses at the operating temperature.

Potential Technical Risk #5. The vessel will not have adequate thermal performance

The fifth potential risk, that the vessel will not have adequate thermal performance, is mitigated by using the same temperature control system successfully used for the NSTX vessel. The system is designed to provide twice the heating capability and eight times the cooling capability predicted by analysis. Multiple redundant paths ensure that minor blockages or minor leaks will not affect overall performance.

Potential Technical Risk #6. The vessel will introduce static or transient field errors

The sixth potential risk, that the vessel will introduce field errors, is mitigated by the choice of material and the strict adherence to stellarator symmetry. The material, Inconel 625, has a relatively high electrical resistivity, about 50% higher than 300 series stainless steel. This results in an electrical time constant of less than 10 ms for the most persistent induced current path. In addition, the relative magnetic permeability of the material, even after forming and welding is very low, less than 1.01, so field errors due to induced magnetism should be negligible. Finally, the port locations and geometry are stellarator symmetric, so any currents that are induced in the vessel should also be stellarator symmetric.

Potential Technical Risk #7. The vessel will not permit sufficient access for inspection, maintenance or reconfiguration of internal components

The final potential risk, that the vessel will not permit sufficient access for maintenance and reconfiguration of internal components, is mitigated by providing as many ports as possible that are large enough for manned access. The three neutral beam locations each have a 14 x 33 inch oblong port that is accessible even with the beams installed. On either side of the neutral beam port are tear-drop shaped ports with an 18 inch clear diameter at the large end tapering to 12 inches at the smaller end, providing a total of six more manned access ports. Finally, the large neutral beam port cover flanges can be removed in at least one location to provide a clear, diamond shaped opening of 23 x 33 inches.

The cost and schedule risks associated with the vacuum vessel could also be significant, but steps have been and are being taken to reduce those risks substantially. Manufacturing studies were carried out during the conceptual design process to obtain advice from manufacturing engineers on ways to make the design easier or less expensive to fabricate. Five different studies of the vessel were carried out, and several fabrication processes were considered, including hot pressing, cold pressing, explosive forming, and casting. Vendor input will be continued after the CDR with an extensive R&D program. This effort will be carried out concurrently with the vessel design process such that the results can be included in the final design. Two different vendors will fabricate partial prototypes of critical regions of the vessel. The forming, welding, machining, polishing, and inspection processes will all be

demonstrated and optimized. At the conclusion of the R&D phase, a fixed price contract will be awarded for the production vessel. The selection of two vendors for the R&D phase will result in at least two qualified vendors for the production articles, and provides an extra incentive to keep production costs (and bids) low.

3   MAGNET SYSTEMS

3.1   Design Requirements and Constraints

The magnet system includes all the coils required to provide the magnetic field for plasma shaping, position control, and inductive current drive. Ex-vessel coil are added for low poloidal mode number (m=2,3) field error correction. Additional coils may be added inside the vacuum vessel during the operational phase for higher order (m=5,6) field error correction. The coil sets and their primary functions are listed in Table 14, and the coil geometry is shown in Figure 29

Table 14 Magnet System Functions

Coil set	Function - Coil set provides:
Modular coils	Basic quasi-axisymmetric magnetic configuration
Poloidal field coils	Inductive current drive, plasma position control, plasma shaping
Toroidal field coils	Addition or subtraction of toroidal field for control of magnetic transform
Trim Coils	Control of magnetic flux surface quality

Figure 29 Modular, TF, and PF Coil Geometry
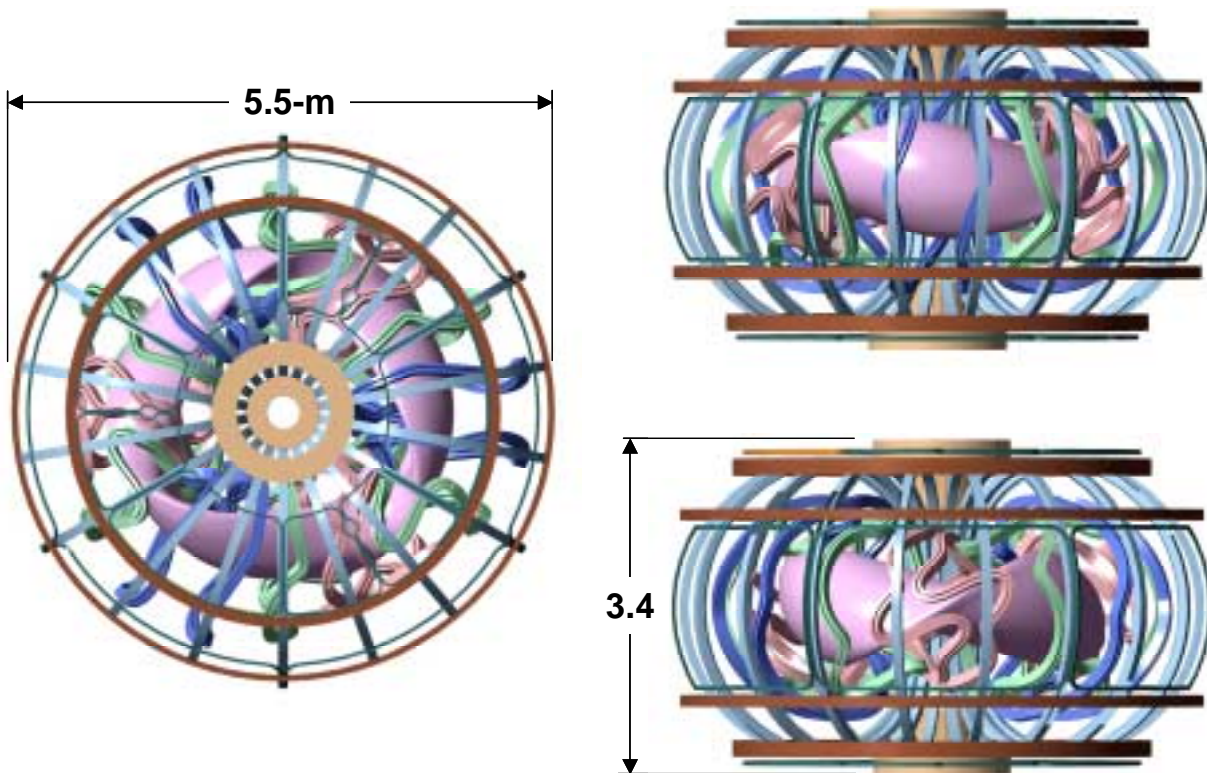
The basic requirements are listed in Table 15. These requirements are extracted from the general machine requirements described in the **General Requirements Document**, provided as part of the Conceptual Design Report. The overarching requirement is to provide windings that can accurately produce the desired magnetic field configuration. The coil configurations (number of coils , etc.) have been optimized to best meet a combination of physics and engineering constraints.

Table 15 Magnet System Requirements

General requirement	
	A set of modular (stellarator) coils, PF coils, and TF coils shall be provided to support the reference scenarios and meet flexibility, field error, and polarity requirements.
Performance	
	Operating scenarios:
	- Initial Ohmic Scenario: 1.5 T for .49 seconds, 164 kA Ip
	- 1.7T Ohmic Scenario: 1.7 T for 0.46 seconds , 175 kA Ip
	- 1.7T High Beta Scenario: 1.7 T for 0.46 seconds , 175 kA Ip
	- 2T High Beta Scenario: 2 T for .22 seconds, 205 kA Ip
	- 350kA Ohmic Scenario: 1.8 T for .46 seconds, 350 kA Ip
	15 minute rep rate between pulses
Flexibility	
	- Independent control of three modular coil circuits (grouped by coil shape)
	- Independent control of all PF coils
	- Variable background TF field
Accuracy	
	Islands from field errors shall be less than 10% of local plasma size
	+/- 1.5 mm assumed for installed winding accuracy
	·Coils must provide access for tangential NBI, RF, vacuum pumping, diagnostics, and personnel access
	·Limit conductor current to ~ 24 kA peak to match with existing TFTR power supplies

3.2   Design Description and Performance

3.2.1   Modular Coils

The modular coil set consists of three field periods with 6 coils per period, for a total of 18 coils. Due to symmetry, only three different coil shapes are needed to make up the complete coil set. The coils are connected electrically with 3 circuits in groups of 3, according to type. Each circuit is independently powered to provide maximum flexibility. The maximum toroidal field at 1.4-m produced by the modular coils varies up to 2 T, depending on the pulse length, but the nominal field produced is 1.7 T. The toroidal field on axis can be raised above 2-T by energizing the TF coils, which can add ±0.5-T to the field generated by the modular coils, or by operating the modular coils for a shorter pulse length. However, the standard scenarios do not require the total field to be higher than 2 T.

Figure 30 shows the general arrangement of the coil set. Like coils are shown in the same color. The coils are grouped in field periods of 6 coils each. The coils on either side of the v=0.5 symmetry plane (60º away from the v=0 symmetry plane) exhibit the largest toroidal excursion and are the most difficult to fabricate. Table 16 summarizes the main modular coil parameters.

Figure 30 Arrangement of Modular Coils
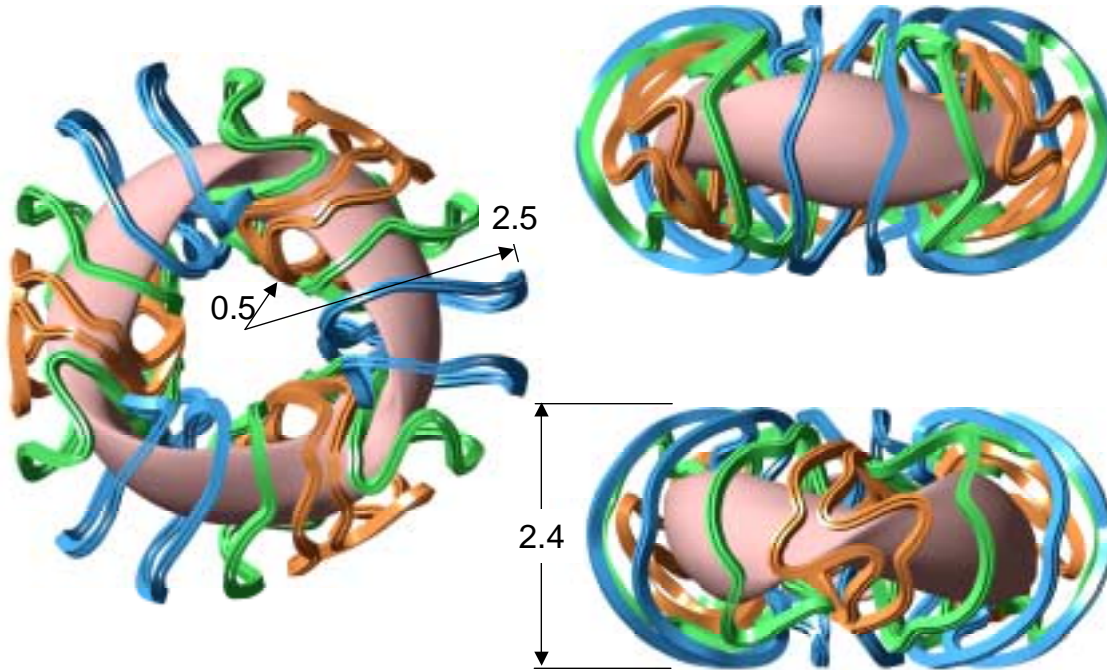
Table 16 Modular Coil Parameters

Parameter	Unit	Value	Remarks
Number of field periods		3	
Number of modular coils		18	
Number of turns per coil		36	
Maximum toroidal field at 1.4 m	T	2.0	
Winding length along winding center	m	6.6-7.4	
Winding cross-section	cm^2	2 x 48	Gross cross section of winding packs in single coil
Winding accuracy	mm	±1.5	Location of current center relative to theoretical center

The winding center for each modular coil is specified through a physics optimization process that emphasizes both plasma properties and geometric constraints, such as coil-to-coil spacing (a key factor determining the current density) and minimum bend radius. The design satisfies physics requirements, a minimum coil-to-coil spacing of 16 cm, a minimum bend radius of 10 cm, and is compatible with a feasible structure geometry. From this data, a cross-section is developed that is normal to the winding surface, except in regions where there are sharp bends or the coils are very close together. Twisting in these areas has been adjusted so as to avoid crimps and maximize the available conductor space. A study of the effect of finite-build coils on plasma reconstruction indicates that these small coil

adjustments do not significantly affect the magnetic field or plasma properties. The main coil geometry parameters are summarized in Table 17. As shown in the table, the coil-to-coil spacing, bend radii, length per turn, and distance to the plasma are similar but not the same for each coil.

Table 17 Modular Coil Spacing and Geometry Parameters

Coil Position (deg)	Coil Type	Length (m)	Min Radius of Curvature (cm)	Min Coil-to-Coil Distance (cm)	Min Coil-to-Vessel Distance (cm)	Min Coil-to-Plasma Distance (cm)	Current for 1.7-T scenario (kA)
-10	M1						
				16.1			
10	M1	7.4	11.0		9.4	20.4	694
				16.2			
30	M2	7.1	10.9		8.9	20.5	655
				16.1			
50	M3	6.6	10.8		11.7	21.0	551
				16.0			
70	M3						

The design concept uses flexible, copper cable conductor. The primary advantage of the flexible cable design is low cost, both to purchase the conductor and to wind it. The primary disadvantage is the loss of copper area compared to a solid conductor. A packing fraction of 75% can be assured, although 80% is theoretically possible. The design is based on a packing fraction of 78%. There is also an apparent increase in electrical length of the flexible conductor due to the twisted nature of the cable that adds about 12% to the overall resistance.

The conductor is purchased as a round cable that has been compacted into a rectangular cross-section. Turn-to-turn insulation is then applied. Even after compaction, the conductor is flexible and easy to wind. A picture of the conductor before and after compaction is provided in Figure 31. Once wound, the conductor is vacuum impregnated with epoxy. The epoxy fills the voids within the cable conductor so the winding pack becomes a monolithic copper-glass-epoxy composite.

Figure 31 Cable Conductor Compaction
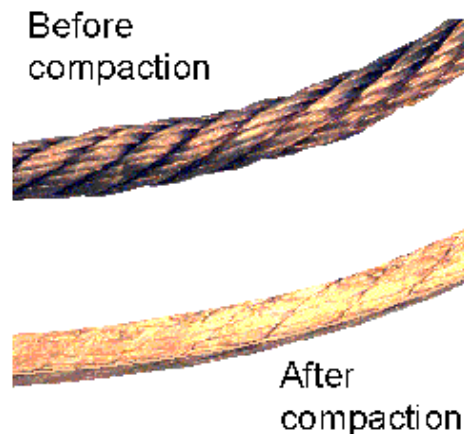
The cross-section dimensions of coil are 10-cm x 12-cm, as shown in Figure 32. Within this envelope is a 19-mm thick, tee-shaped member that supports two multi-turn winding packs. Each winding pack is a double-layer pancake with 9 turns per layer. A crossover between layers occurs at the top of the tee. The leads extend from the bottom of the winding pack in a coaxial arrangement. A thin chill plate is located on both sides of each winding pack to remove the joule heating in the coil between plasma discharges. The chill plate consists of a .040 inch thick sheet of copper that is cut into the flat developed shape of the winding and then formed to match the winding pack contour. The forming is simplified by cutting the long edge of the plate into multiple strips to avoid the necessity of stretching the copper. The chill plate on the outer side is cooled by running liquid nitrogen through a tube brazed to the outer surface, while the chill plate on the structure side of the winding is cooled with a tube on the edge away from the plasma. The nitrogen will enter the chill plate circuits near the bottom of each coil and exit near the top of each coil.

Figure 32 Modular Coil Cross-Section
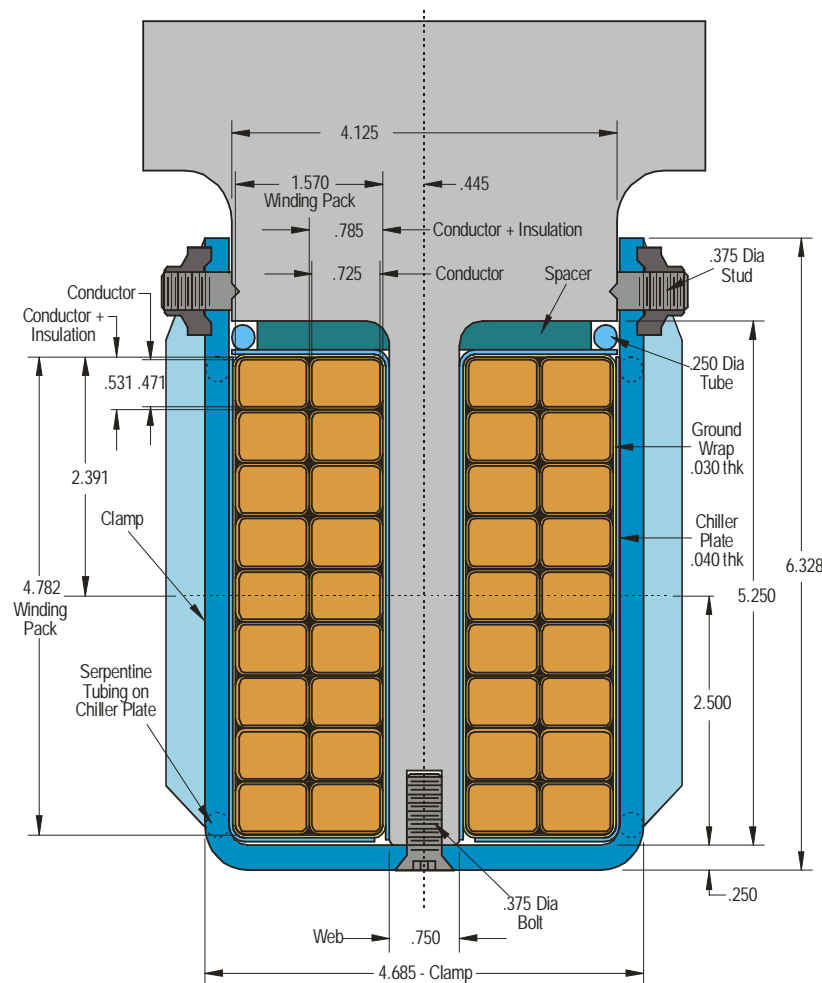
The winding packs are clamped in place by discrete u-shaped brackets that preload the winding packs against the structure. The predominant electromagnetic loads are towards the web structure. Outward loads do exist in tight bend areas, and the u-shaped brackets react the loads in these regions.

In order to avoid unwanted field errors, the position of the winding current center must be tightly controlled. The true position tolerance (TPT) for the winding current center is ±1.5mm. In order to achieve this tolerance, the

conductor will be wound on a precision surface on each side of the structural tee, which is part of the winding form. The winding stackup is illustrated in Figure 33. The figure shows potential positions of individual conductors that still provide acceptable tolerance of the current centroid. Errors in on winding pack can be partially or completely compensated by modifications to the adjacent winding.

Figure 33 Coil Winding Stackup

Winding form

Winding

theoretical geometry   **possible geometry**
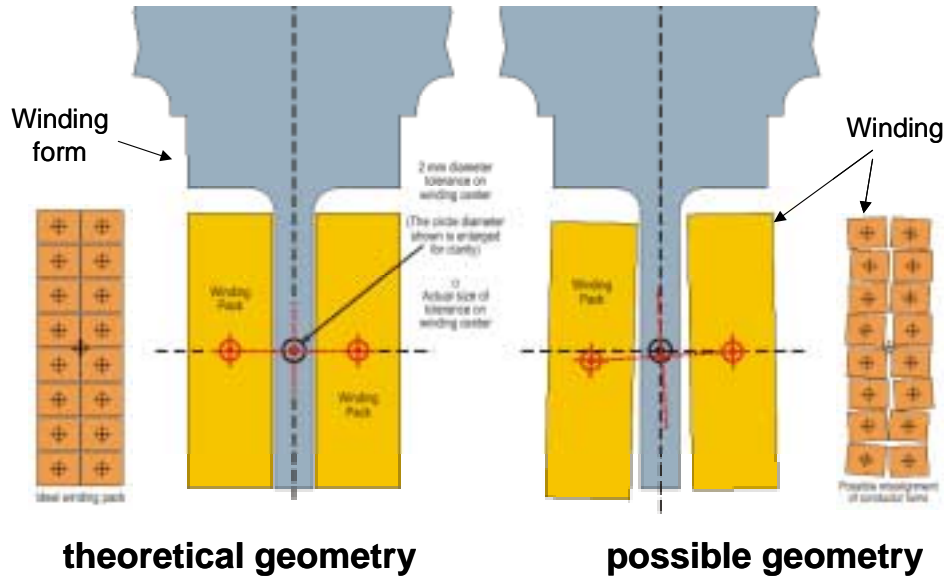
The conductor is insulated as shown in Figure 34, and wound in a double pancake on each side of the tee. The inner chill plates are installed first, followed by layers of glass cloth which later serves as ground wrap. The surface contour is measured with a portable coordinate measurement machine (CMM) to verify the geometry. The conductor is then clamped into position, starting at the shell side and moving toward the plasma side. The position of each turn is checked with the portable CMM and continuous adjustments are made with the clamps and shims to provide the best possible turn placement. Once the outer half of the double pancake is wound, the glass ground wrap is pulled around the winding followed by the outer chill plates. The final geometry is verified and the assembly is ready for vacuum pressure impregnation with epoxy.

Figure 34 Conductor Insulation Scheme
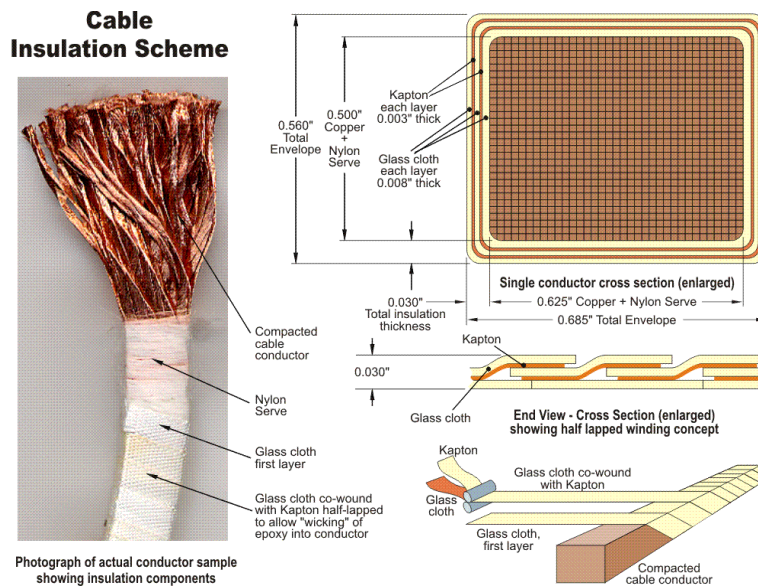
Several concepts are under consideration for the epoxy impregnation process, and these will be developed as part of the R&D activities during the preliminary design phase. After the epoxy is cured the support brackets are installed and adjusted.   The brackets are all identical and planar, and fit over cylindrical pockets milled into the side of the tee structure. A shim is used in the pocket to provide a planar surface to bolt to, and to make any needed adjustments in the width. The clamp is retained with the same studs that were welded in place and used for the winding clamps. An illustration of a completed modular coil in the winding form is shown in Figure 35.

Figure 35 Completed Modular Coil (M2)
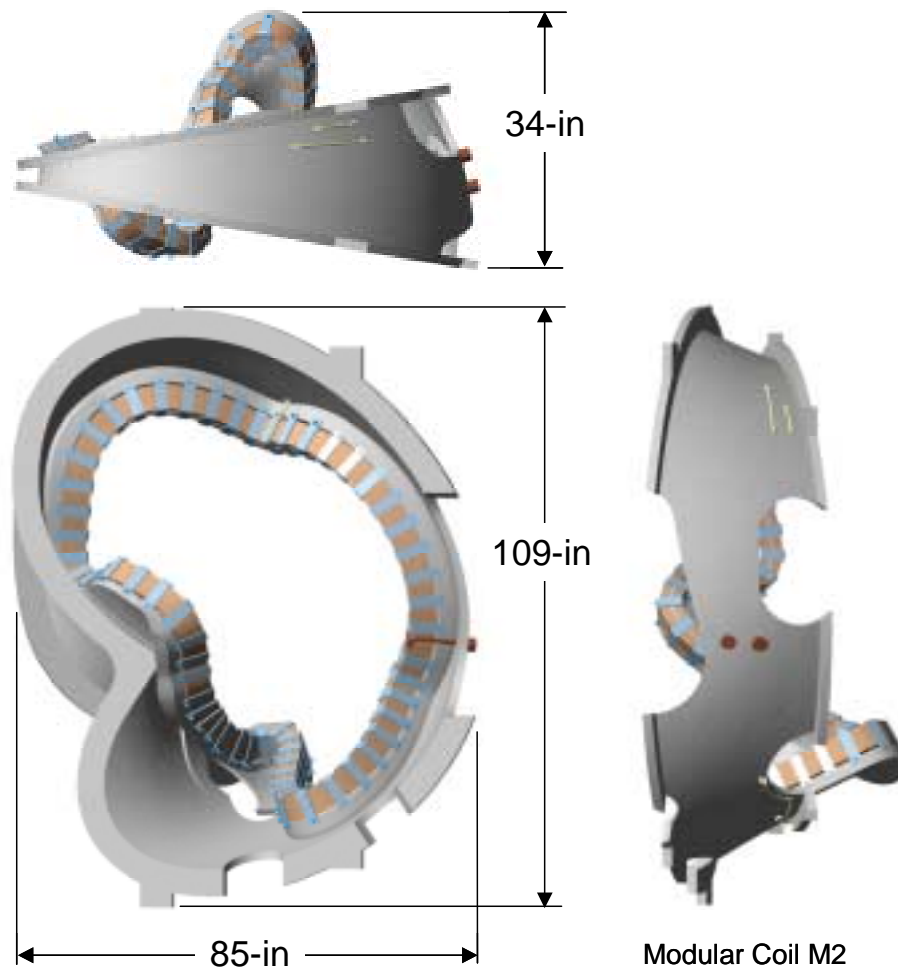
Tests of the behavior of some prototype conductor indicate that for tight bend radii, the cross section will "keystone". This will result in an apparent "swelling" of the winding pack locally. Two options are available for correcting this problem. The first is to locally deform the conductor with tooling to force it into the correct cross section. This may be difficult due to the complicated geometry. A second option is to simply allow for the extra stackup by allowing the envelope of the winding to increase locally. The winding form would be machined to allow for the extra size, and the judicious use of shims and roving would be used to fill gaps and arrange the turn spacing to preserve the current center.

The winding form is fabricated as a casting. Due to the complexity of the shape, the pattern geometry will likely be developed through several iterations by a pattern maker. In order to minimize machining, the as-cast part should be within 6-mm of the true shape anywhere in the section. After stress relieving in a fixture, the casting would be re-

measured and have all structural interface features as well as the winding cavity surfaces machined. Figure 36illustrates the major process steps.

Figure 36 Coil Fabrication Sequence
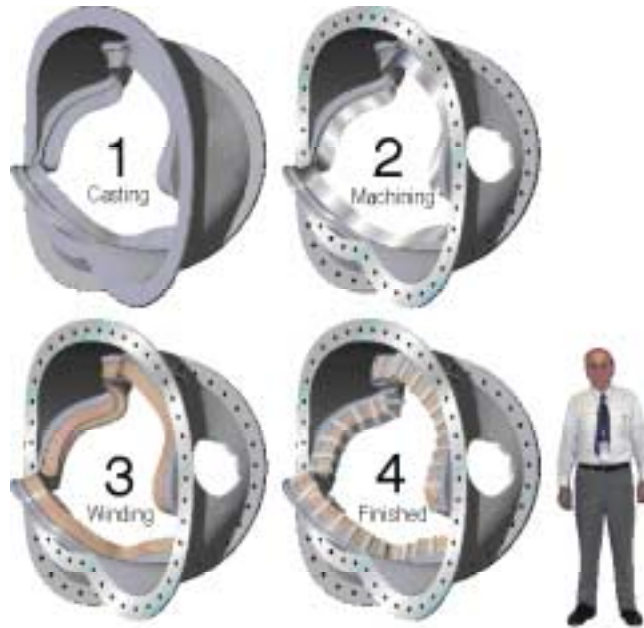
After the windings are installed in the coil forms, the coil forms are bolted together to form a monolithic shell structure. Insulating shims and bolts are provided at the v=0 symmetry planes to prevent circulation of toroidal currents. The completed shell structure is illustrated in Figure 37.

Figure 37 Completed Modular Coil Shell Structure

This is a robust structure mechanically and should also result in the best accuracy possible. The coils are wound directly into the fully machined winding cavities, which are referenced and machined to the assembly flanges. The accuracy of the winding cavity with respect to the flanges is expected to be very good, probably within .010 inches (.25mm). Nevertheless, the coils can still be shimmed at the interface flanges to recover tolerance if necessary. No other structure is needed for the modular coils, except the interfaces to the gravity supports.

The leads for the modular coils consist of commercial, "kickless" cables, which have been modified to operate at liquid nitrogen temperatures by substituting Teflon for the insulation. The cables consist of 6 conductors, 3 of each polarity alternating and twisted together and contained within a common jacket. They are cooled by conduction and by bleeding nitrogen gas through the interspace of the jacket.

3.2.2   Toroidal Field Coils

A set of toroidal field coils is included to provide flexibility in the magnetic configuration. Adding or subtracting toroidal field is an ideal "knob" for lowering and raising iota. There are 18 identical, equally spaced coils providing a 1/R field at the plasma. The TF coils are supported from the external coil support structure. The coils are located at radial locations coincident with the modular coil locations, both for symmetry and to avoid introducing additional obstructions to access. All of the coils are connected in a single circuit initially, but the capability will exist to connect like coils, e.g. coils in the same location relative to the modular coils within a field period, to be connected in separate circuits. Each coil consists of 12 turns in a single bundle, as shown in Figure 38.

Figure 38 TF Coil Geometry

The coils are wound from hollow copper conductor and insulated with glass-epoxy. They operate at 80K, cooled by liquid nitrogen, and are connected in series. The leads consist of coaxial conductor to minimize field errors. The nominal TF coil parameters, insulation builds, and details are described in Table 18.

Table 18 TF Coil Parameters

Parameter	Unit	Value
Number of TF coils		18
Number of turns per coil		12
Maximum toroidal field at 1.4 m (TF coils only)	T	±0.5
Maximum current per turn	kA	16
Winding length along winding center	m	9.5
Winding cross-section	cm^2	21
Double pancake length	m	51.942
Bundle height	mm	87.1
Bundle width	mm	100.0
Bundle area	mm2	8701
Conductor height	mm	27
Conductor width	mm	22.5
Corner radius	mm	2.5
Cooling hole diameter	mm	13.5
Conductor area	mm2	459
Weight/coil,	kg	409
Max current in reference scenario	kA	14.28
Maximum copper current density	kA/cm^2	3.1

3.2.3   Poloidal Field Coils

A set of poloidal field coils is provided for inductive current drive and plasma shape and position control. The basic coil geometry is shown in Figure 39. The coil set consists of two inner solenoid pairs (PF-1 and PF-2), two mid-coil pairs (PF-3 and PF-4) and two outer coil pairs (PF-4 and PF-5). All the coil pairs are symmetric about the horizontal midplane. The coils are of conventional construction, wound from hollow copper conductor and insulated with glass-epoxy. The PF coils operate at the same temperature as the TF coils - nominally 80K, cooled by liquid nitrogen.

The PF coil parameters are listed in Table 19. As shown in the table, the conductor size and maximum current per turn are almost identical for all the coils, including the TF coils. This provides common tooling for manufacture and should help to reduce costs.

The two OH solenoid coils, PF1 and PF2, are connected in series and assembled over a common structural core, as shown in Figure 40. An epoxy glass cylinder is molded to the outside of these coils to provide a bucking cylinder for the TF coils. Upper and lower PF coils in a given pair are connected in series, and the PF1 and PF2 coils are also in series. Thus, there are five independent electrical circuits. The PF coils, when independently driven, provide flexibility for plasma shaping and position control. With an OH (nullapole) distribution in the PF coils, the coil set can provide 1.15-Wb (double swung). This capability is adequate, even for the maximum plasma current of 350-kA.

Figure 39 PF Coil Geometry

Dimensions in cm
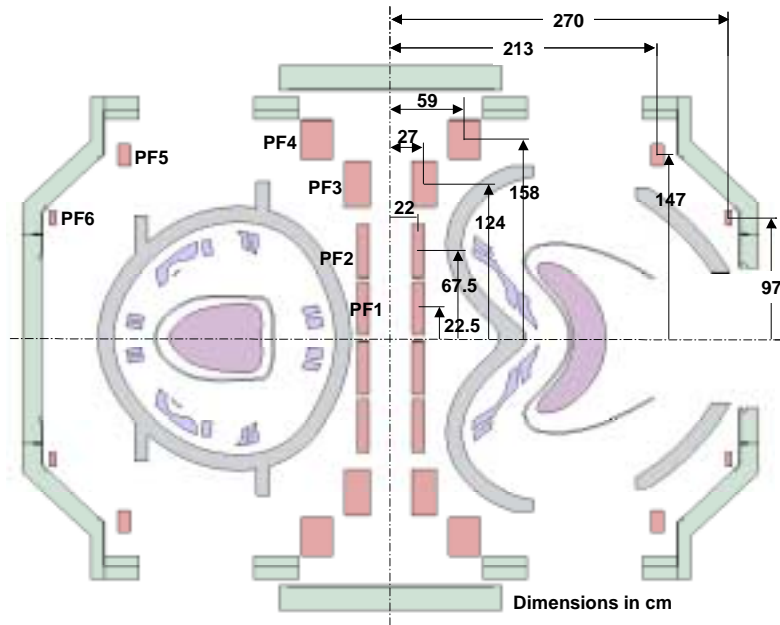
Table 19 PF Coil Parameters

Parameter	Units	PF-1	PF-2	PF-3	PF-4	PF-5	PF-6
Max total current	MA-turns	1.34	1.63	2.35	1.9	0.19	0.09
Radius	m	0.22	0.22	0.27	0.59	2.13	2.7
Installed height, Z	m	0.23	0.68	1.24	1.58	1.47	0.97
bundle dr	mm	101.4	101.4	200.6	250.2	101.4	51.9
bundle dz	mm	402.4	403.0	402.4	288.3	174.2	117.1
gross current density	A/mm^2	32.83	39.88	29.12	26.35	10.75	14.82
total turns	#	56	68	112	100	24	8
turns high	#	14	17	14	10	6	4
turns wide	#	4	4	8	10	4	2
current per turn	A	23929	23971	20982	19000	7917	11250
packing fraction		0.75	0.75	0.75	0.75	0.75	0.75
length per turn	m	1.38	1.38	1.7	3.71	13.38	16.96
total length of copper, per coil	m	77.4	94.0	190.0	370.7	321.2	135.7
turn height	mm	27	22	27	27	27	27
turn width	mm	22.5	22.5	22.5	22.5	22.5	22.5
coolant hole width	mm	13.5	13.5	13.5	13.5	13.5	13.5
copper corner radii	mm	2.5	2.5	2.5	2.5	2.5	2.5
conductor area	mm^2	459	346.5	459	459	459	459

Figure 40 OH Solenoid (PF1/2) Assembly
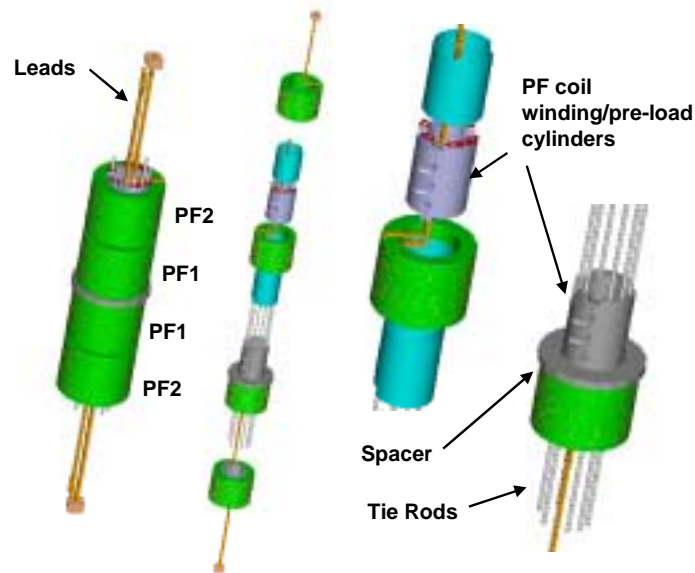
3.2.4   External and Internal Trim coils

Two types of correction coils are envisioned for NCSX. The first is a set of windowpane coils, referred to as external trim, or field error correction coils. These are provided on the top, bottom and outside perimeter of the coil support structure primarily to reduce n/m= ½ and 2/3 resonant errors that may result from manufacturing or assembly errors in the modular coil geometry. These coils will be installed during the initial assembly of the machine because it is much more cost effective than retrofitting them later. However, the power supplies will be provided later, after the current requirements are determined.

Figure 41 illustrates this set of coils. The coil parameters are listed in Table 20. These coils are wound from conventional, hollow copper conductor and vacuum pressure impregnated with epoxy. They are supported by the External Coil Support Structure, and operate at liquid nitrogen temperatures. Each coil must be independently powered to provide the flexibility needed for correcting field errors.

Figure 41 External Trim Coils
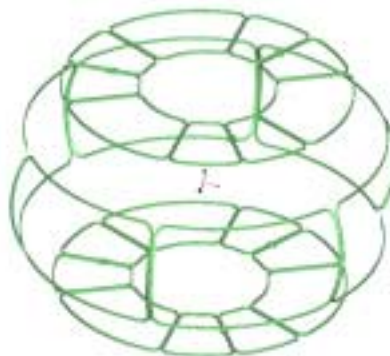
Table 20 External Trim Coil Parameters

Parameter	Units	Top and Bottom Coils	Outer perimeter Coils
Max total current	MA-turns	1.34	1.63
Coil size	m x m	2.2 x 1.6 wide	1.7 x.2.7 wide
bundle dr	mm	21.8	21.8
bundle dz	mm	43.6	43.6
gross current density	A/mm^2	84.3	84.3
total turns	#	8	8
turns high	#	4	4
turns wide	#	2	2
current per turn	A	10000	10000
packing fraction		0.75	0.75
length per turn	m	8.5	5.1
total length of copper, per coil	m	67.9	40.9
turn height	mm	9	9
turn width	mm	9	9
Net conductor area	mm^2	60	60

The second set of trim coils are referred to as internal trim coils. These are not included in the baseline configuration, but may be provided as a future upgrade during the operation of NCSX to control m=5 and m=6 resonant field perturbations. To demonstrate that such an upgrade can be accommodated, a preliminary design concept has been developed.

The internal trim coils are configured in a saddle geometry as shown in Figure 42, and are located inside the vacuum vessel on the inboard and outboard regions of the v=0 (bean-shaped) plasma cross-section. This location is based on a study to determine where the coupling with the plasma was best. The m=5 coils are on a surface that is offset 63 mm from the plasma on the inboard and 143 mm from the plasma on the outboard side. The m=6 coils are in a layer offset 15 mm farther out from the plasma.

Figure 42 Internal Trim Coil Concept
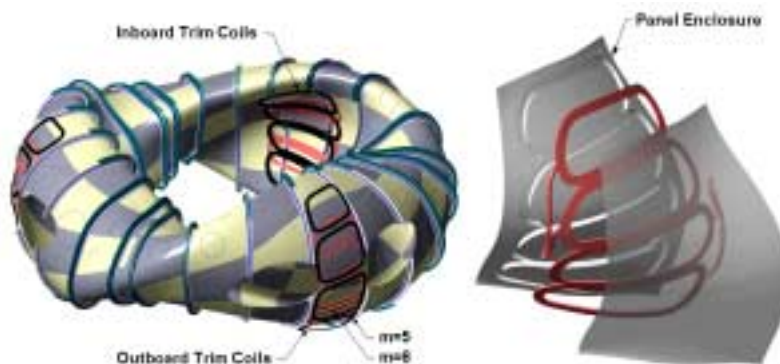
The windings are presently sized for 10 kA-turns per coil, but recent calculations have shown that only a few hundred A-turns may suffice for field correction. To provide 10 kA-turns, five turns are envisaged in a 5 cm x 1 cm winding pack. Since the coils are located in the vacuum vessel, they must be vacuum tight (canned). High temperature electrical insulation will be required. The present concept for the coils is to provide a formed and embossed stainless steel panel into which the four saddle coils would be wound, with a second panel seam welded over the coils to provide the vacuum closure. Special tooling will be required to provide an accurate, contoured shape. The completed panels can be fully supported by the vacuum vessel on the inboard side, but must be cantilevered from the top and bottom on the outboard side.

There are six panels (3 periods, each with an inboard panel and an outboard panel) for the m=5 resonance and six for the m=6 resonance. Coaxial leads from each panel will be routed to the outside through continuous conduit. There, the coils in each group will be connected in series and then to associated power supplies.

3.3   Design Basis

The magnet system design is based on design criteria, analysis, and discussions with potential vendors via manufacturing studies. Results of limited R&D on the cable conductor has been very encouraging.

Design criteria

The coils will be designed according to the NCSX Structural Design Criteria, which is based on the ASME Code, Section VIII, Division 2. The code provides a conservative but prudent approach to design stresses, fatigue, buckling, welding, and inspection of components.

The primary element for analysis is the modular coil set. The material properties are not known with certainty, since design decisions for all the materials have not been made. However, the assumed properties, based on what has been demonstrated by testing, are listed in Table 21. The copper epoxy mixture for the cable conductor has not been tested at 77K yet, but at room temperature the compression modulus seems to be dictated by the epoxy, not by a rule of mixtures. Full testing of sample windings, including thermal cycling is planned for preliminary design.

Table 21 Material Properties for Modular Coils and Structure

Material	Cast shell material Modified 317 at 4 K[5]	Copper / epoxy winding pack @ RT
Yield strength	122 - 138 ksi	19 - 24 ksi (compression)
Ultimate Tensile Strength	141 - 207 ksi	22 - 27 ksi (compression)
Allowable stress, Sm	47 ksi	12 ksi[6] (compression)
Young's modulus	25 - 28 x 10^6 psi	1.2 – 1.7 x 10^6 psi
Total Elongation	22 – 55 %	TBD
Poisson's ratio	.28 - .30, temp dependent	0.29 (in-plane)

Analysis

The design has been analyzed for field errors, forces, stresses and thermal response.

---

[5] J. Chrzanowski, "NCSX Preliminary Modular Coil Procurement Specification", PPPL, November 2002

[6] Results are very preliminary. R&D planned during preliminary design to better characterize copper-glass-epoxy composite.

Field errors

The first analysis concerns field errors. For design purposes, the center of the current within any coil winding is specified to be within 1.5 mm of its theoretical position, except in regions around leads and crossovers. In these regions the conductor steps from layer to layer or from pancake to pancake, introducing local field errors within the windings. These errors have been analyzed in detail [7]. Three design rules are used to minimize these errors:

- Arrange the joggles from layer to layer within a winding pack such that the pattern of turn to turn joggles on one pie form an X shape with the pattern of joggles on the adjacent pie.

- Make sure the lateral cross over from pie to pie occurs in opposite directions on the two winding packs within a coil. This reverses the field errors from the lateral current paths and cancels them to first order.

- Minimize the errors at the lead entrance by immediately tying the leads together into a coaxial arrangement.

Figure 43 illustrates a candidate lead arrangement for the modular coils.

Figure 43 Candidate Lead Arrangement for Modular Coils
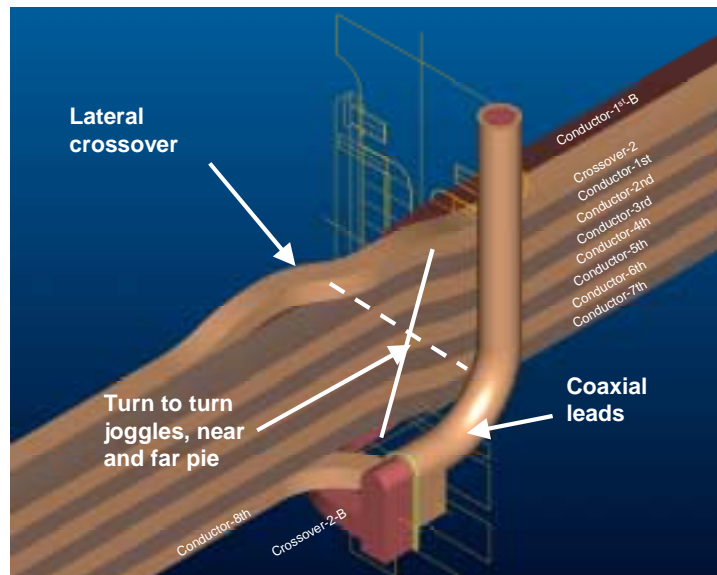
In addition to the errors from the coil geometry perturbations around leads and crossovers, the field errors associated with fabrication and assembly tolerances have also been studied in detail[8]. Assessing the impact of coil fabrication and assembly errors a priori requires examining a large number of potential coil perturbations. A large number of possible perturbations to the coil geometries were chosen for detailed evaluation.

A perturbation field for each is calculated by subtracting the field from the unperturbed coils from the field from the perturbed coils. The reference plasma configuration was used to provide as the background field to show the effect of the coil perturbations using both analytic expressions for island size and field line tracing. The use of a perturbation field applied to a reference plasma configuration - as apposed to using the full field from the perturbed coil set by itself - was chosen to separate the influence of coil tolerances from islands inherent in the free boundary plasma configuration of the unperturbed coils. It also allowed for accurate benchmarking of analytic results with field line tracing for both symmetric and symmetry breaking field errors.

---

[7] A. Brooks, A. V. Georgiyevskiy, W.U.Reiersen, V.A.Rudakov, "Current Feeds And Connection Part Perturbation Study On Magnetic Configuration Of NCSX Stellarator, (M45 coils c01r00), April 2002

[8] A. Brooks, "NCSX Coil Tolerance Study, Impact on Plasma Surface Quality", April 2002, PPPL

The worst case found was for the modular coils with an n=2 assembly perturbation in vertical positioning (18.7% m=2 island). In general, most of the large islands induced were symmetry breaking m=2 islands. An m=2 "out of plane" distortion (i.e., toroidal deformations) of individual modular coils also produce large m=2 islands (15.7% for mod1, 12.6% for mod2 and 11.6% for mod3). TF coils were less sensitive, presumably due to their being further from plasma and carrying less current. The worst case showed a 2.7% island. The PF coils were all less than 4% for the cases considered.

Two cases that lead to large m=2 islands were used to demonstrate the capability of the field error correction coils to suppress the islands without producing severe distortion of the boundary. Figure 44 shows the nearly symmetric islands produced by an m=2 distortion of Modular Coil 1. Adding the correction coils that target these visible islands and also target the other low order resonances correction shown in the right hand side of the figure. The largest current required of the correction coils is 64 kA-turns, but the design current is 80 kA-turns to provide additional margin.

Figure 44 n/m=1/2 Island Suppression With External Trim Coils
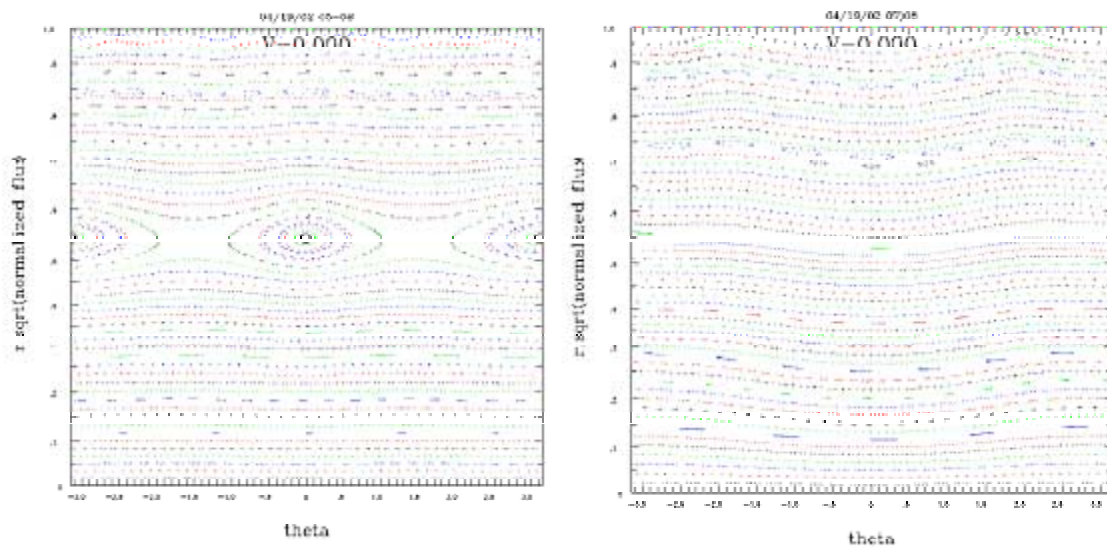
EM Forces on Coils

The fields and forces on all the coils have been calculated for each of the various operating scenarios[9][10][11]. Table 22 summarizes the load cases that were considered and the time snapshot for the currents where the currents are either at their maximum positive or negative values. The worst case for forces in the modular coils appears to be the 2T high beta at the zero beta point in the discharge.

---

[9] H.M. Fan, "EM Analysis of NCSX Coils", PPPL, February 2001

[10] D. E. Williamson, "Fields and forces from multi-turn model of modular coil", April 2002

[11] D. E. Williamson, "Field and force comparison for modular coils", April 2002

Table 22 Load Cases Analyzed for Fields and Forces On the Coils

		M1	M2	M3	PF1	PF2	PF3	PF4	PF5	PF6	TF	Plasma
350 kA ohmic scenario												
1) 1.8T low iota		20068	20763	15815	-18374	-22502	-2590	-2598	-5644	-1995	1869	0
2) 350kA		16201	14648	11590	19142	23443	6977	769	-1882	8606	16076	–350000
2T High beta scenario												
3) Low iota vacuum		22228	22998	17518	16675	20422	5168	5025	-5625	748	2071	0
4) 2T zero beta		22697	21265	18432	17622	21582	15691	9302	1651	1699	2420	-205071
5) 2T high beta		22685	21392	18008	539	660	16127	13996	4676	-296	2729	–204989
1.7 T High Beta Scenario												
6) High iota vacuum		22139	20102	17621	3067	3756	13556	15091	-5867	-1677	-4770	0

Green fields represent maximum and minimum coil currents

Two sets of analyses were performed, one with the ANSYS code and the other with the MAGFOR code. Plots of fields at the surface of the modular coils for the 2T case at 0 seconds are illustrated in Figure 45. These calculations were completely independent, using different models, and the peak field was within about 9%. The MAGFOR model (4.9T) had a finer mesh and more integration points than the ANSYS code (4.5T), so some difference was expected.

Figure 45 Peak Fields at Surface of Modular Coils
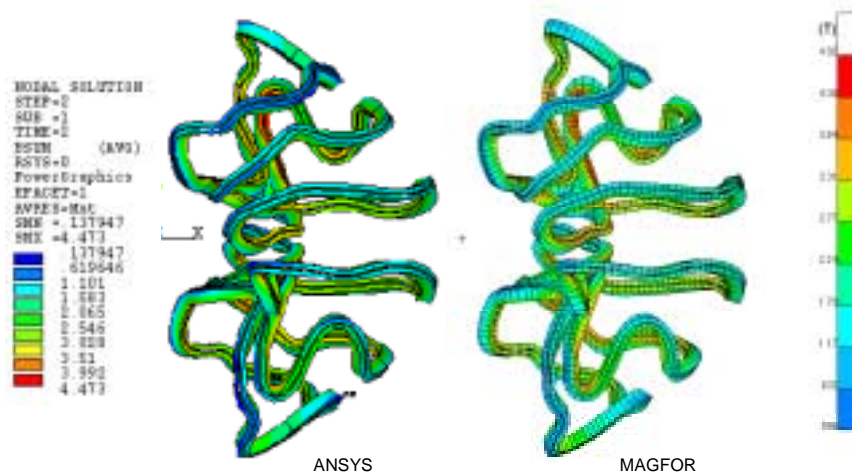
The forces in the modular coils for the same 2T case at 0 seconds are shown in Figure 46. The forces calculated by ANSYS and MAGFOR are almost identical.

Figure 46 Forces on the Modular Coils
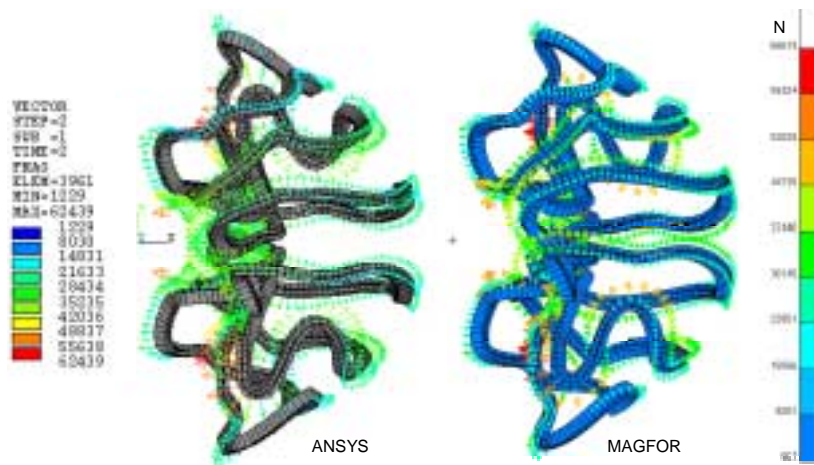
In order to better understand the forces on the modular coils, they were resolved into local coordinates in the radial and lateral direction relative to the winding form structure. The lateral forces are in the direction normal to the surface of the supporting "web" structure and the radial forces are those directed outward against the shell. Figure 47 plots these force components as a function of coil perimeter for the M2 coil. As shown in the figure, the largest lateral force is about 5500 lbs per linear inch, but this is countered nearby with a similar force on the other side of the web from the other winding.

What is also illustrated in the figure is the very local problem of the winding pack force being away from the web. This occurs primarily in regions of sharp lateral curvature, and is due to the local peak fields. For the condition shown, there is a local force of about 7200 lbs acting over a distance of about 10 inches. The force will be reacted partially by the coil clamps and partially by the winding acting as a beam in this region. For the present spacing of clamps, at least two clamps will act to restrain this region.

Figure 47 Running Loads on Coil M2 Resolved into Lateral and Radial Components
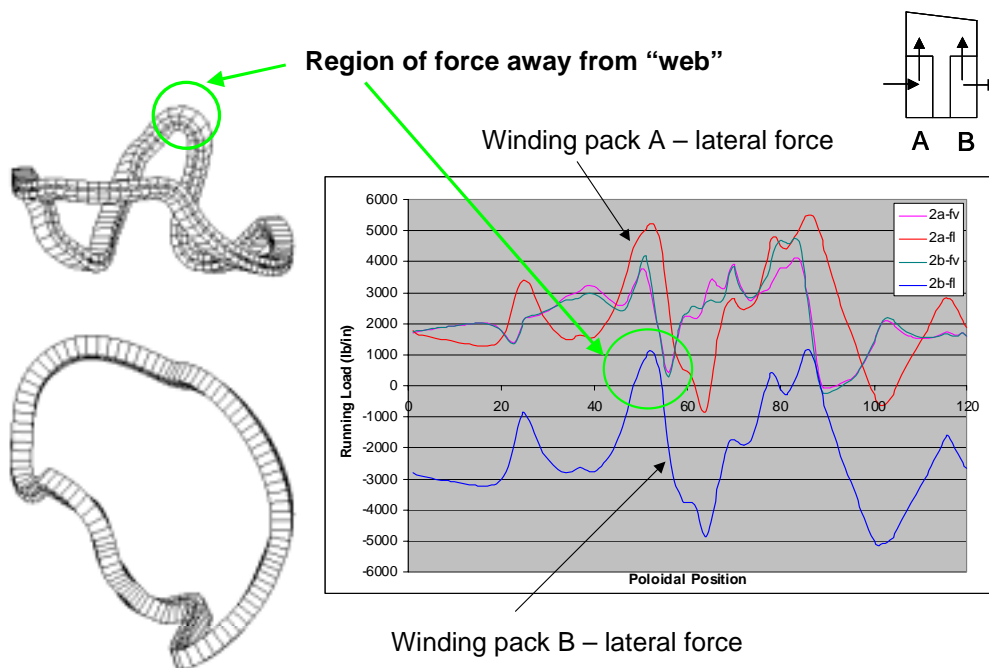
The force distributions for all the PF coils and TF coils for a typical case are illustrated in Figure 48 and Figure 49. As shown in these figures, the loading on the TF and PF coils is somewhat complicated due to the interaction with the modular coils. For example, the TF coils on one half of a field period experience a net vertical force upwards, and the corresponding TF coil on the other half of a field period experiences a net vertical force downward.

Figure 48 Typical Force Distribution (N/element) for PF Coils for Case 2
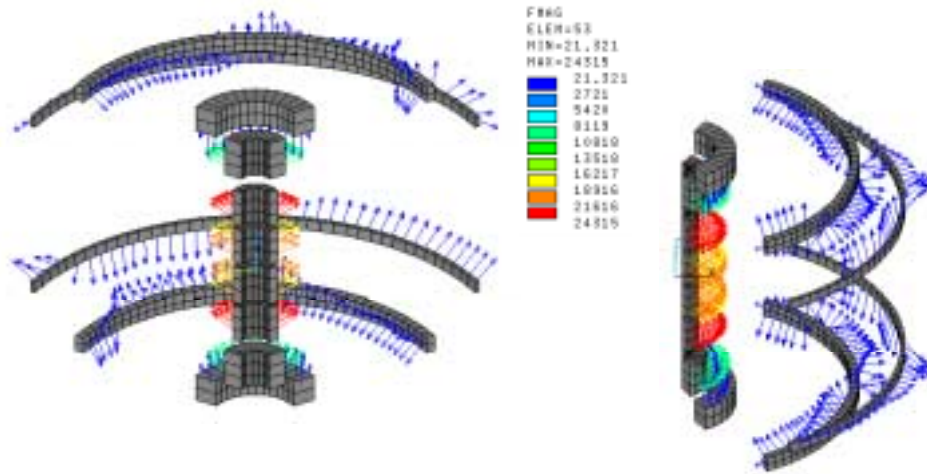
Figure 49 Typical Force Distribution (N/element) for TF Coils for Case 2
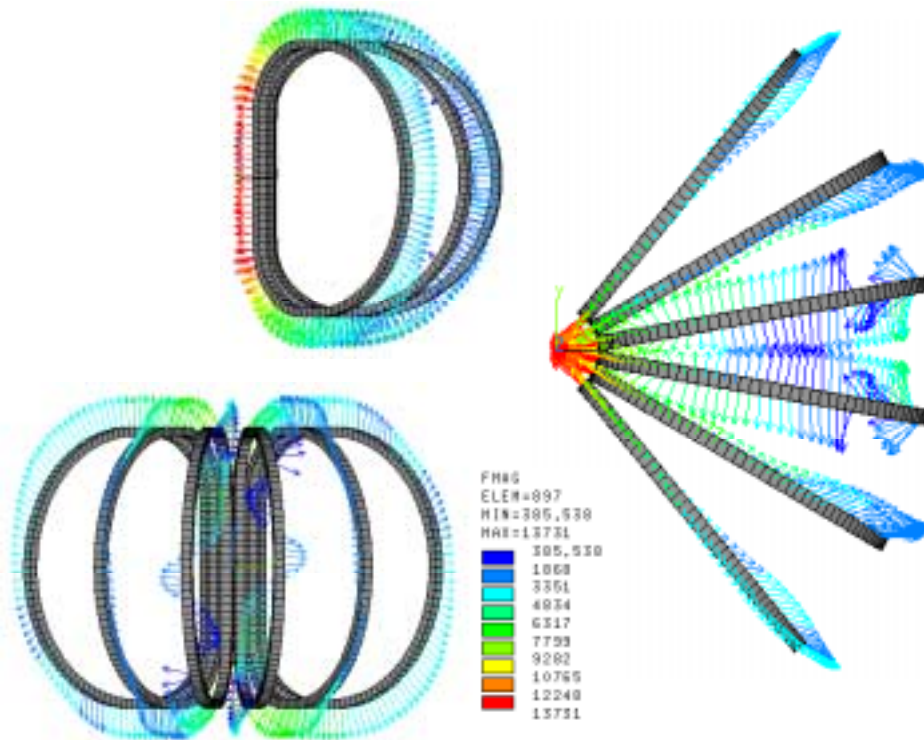
The net forces on each coil were also calculated for all the cases listed in Table 23 and Table 24. Coil identification keys are provided alongside each table.

Table 23 Maximum Net Forces on Modular Coils

	Fr (N)	case	Fφ (N)	case	Fz (N)	case
MC9-up	-294805	2	1407585	4	-167444	4
MC10-up	-416190	3	-1416809	5	163592	6
MC11-up	-276838	3	1149933	3	-159663	3
MC12-up	-652477	3	-1112232	3	-201193	3
MC13-up	220499	6	627097	4	-191696	4
MC14-up	125682	6	-337223	4	-168948	4
MC9-lw	-294805	2	-1407588	4	167451	4
MC10-lw	-416187	3	1416804	5	-163610	6
MC11-lw	-276839	3	-1149933	3	159665	3
MC12-lw	-652478	3	1112233	3	201195	3
MC13-lw	220500	6	-627097	4	191697	4
MC14-lw	125683	6	337223	4	168948	4
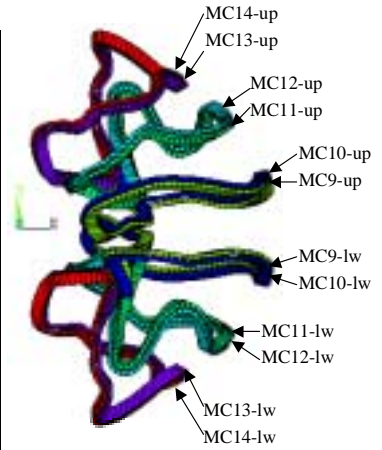
Table 24 Maximum Net Forces on TF and PF Coils

	Fr (N)	case	Fφ (N)	case	Fz (N)	case
TF1-up	-456324	2	-25650	2	6150	2
TF2-up	-335765	2	-114882	2	-62540	2
TF3-up	-294382	2	-36564	2	-32945	2
TF1-lw	-456349	2	25572	2	-5942	2
TF2-lw	-335747	2	114790	2	62707	2
TF3-lw	-294373	2	36476	2	33099	2
PF1-up	700230	4	0	1	31589	1
PF2-up	920541	4	0	1	-93392	1
PF3-up	2268173	5	0	1	285290	5
PF4-up	1263530	6	0	1	-335687	5
PF5-up	36400	6	0	1	-18913	1
PF6-up	10776	2	0	1	1828	2
PF1-lw	700230	4	0	1	-31589	1
PF2-lw	920541	4	0	1	93392	1
PF3-lw	2268173	5	0	1	-285290	5
PF4-lw	1263530	6	0	1	335687	5
PF5-lw	36400	6	0	1	18913	1
PF6-lw	10776	2	0	1	-1828	2
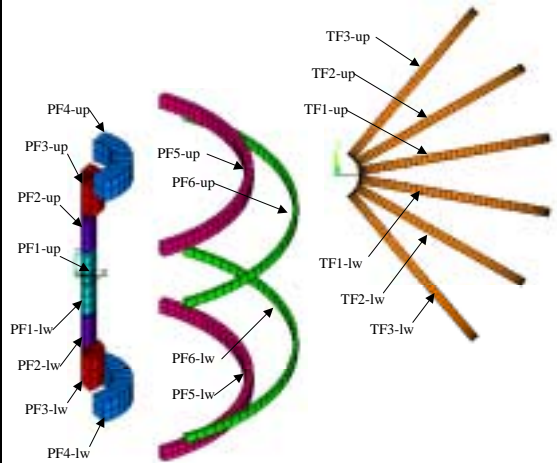
Stress Analysis Under EM Loads

The modular coils are structurally supported by the integral shell structure, and its analysis is reported here. The TF and PF coils are supported from the external coil support structure. The modular coil shell structure and coils were modeled and connected with multi-point constraints. The primary load case for the analysis was the low iota vacuum phase of the 2T High Beta scenario (Case 3). Figure 50 shows the model, which consisted of the full 360-degree assembly of the shell, coil windings, and spacer between the windings and shell. The properties used assumed that the shell is made of stainless steel for the shell, the coil windings consist of a homogeneous copper/epoxy mixture, and the spacers are made of G-10. The properties are listed in Table 25

Table 25 Material Properties Used For Modular Coils

Component	Material	Modulus of elasticity (MPa)	Poisson's ratio	Comment
Tee/shell casting	Cast stainless steel	206,000	.29	Similar to 317 cast alloy
Modular coil windings	Copper epoxy mixture	65,500 6550	.30	Two stiffnesses tried, 50% and 5% solid Cu
Spacer	Epoxy glass laminate	206,000	.30	Conservative if assumed to be stiff

Figure 50 FEA Model of Modular Coil Winding and Shell

Constraint equations between tee nodes and shell elements
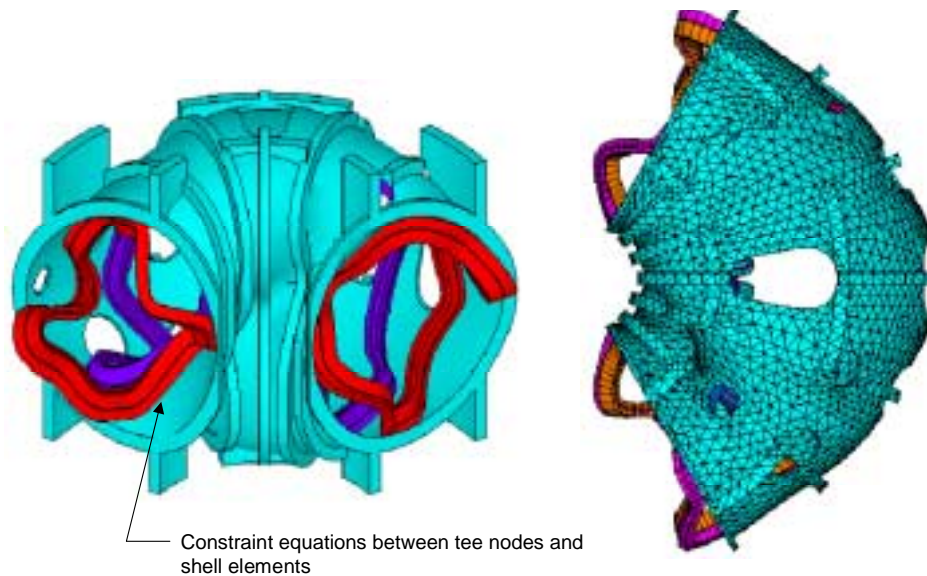
Two cases were run assuming different copper stiffnesses; [1] the modulus of the winding pack was assumed to be 50% of the modulus of copper and [2] 5% of the modulus of copper. Tests conducted on epoxy-impregnated samples of the compacted cable conductor indicated the actual modulus is about 10% of copper, which is toward the soft side of the analysis. This tends to put more load into the shell structure, and reduces the load carried (and stress) in the windings.

The model was constrained only at the toroidal stiffeners on the bottom side of the shell, so the vertical deflection is not stellarator symmetric. As shown in Figure 51, the vertical and total deflections are nearly the same, indicating that most of the deflection is in the vertical direction. The stress picture is summarized in Table 26. The stress picture in the shell is relatively benign, as indicated in Figure 52, with a localized area of high stress in the inner folds of the shell structure of 13 ksi, which is far less than the allowable of 47 ksi. There are also some locally high stresses in the tee structure upon which the coil is wound (Figure 53), which are not well resolved due to the coarseness of the model, although they appear to be well within allowable limits. The higher stress regions in the shell and tee can be eliminated by making these components thicker in the regions of high stress. Peak stresses in the winding due to EM loads are below 7 ksi, which is below the anticipated allowable of 12 ksi. Testing is planned as part of the R&D program in FY03 to provide a firmer basis for determining material properties and allowable stresses.

Table 26 Summary of Modular Coils Stress Analysis

Winding Pack Modulus (MPa)	Shell (ksi)	Coil (ksi)	Tee (ksi)	Spacer (ksi)
65500	12.7	7.2	20.2	1.8
6550	13.0	2.6	32.1	2.2

Figure 51 Vertical and Total Displacement Contours
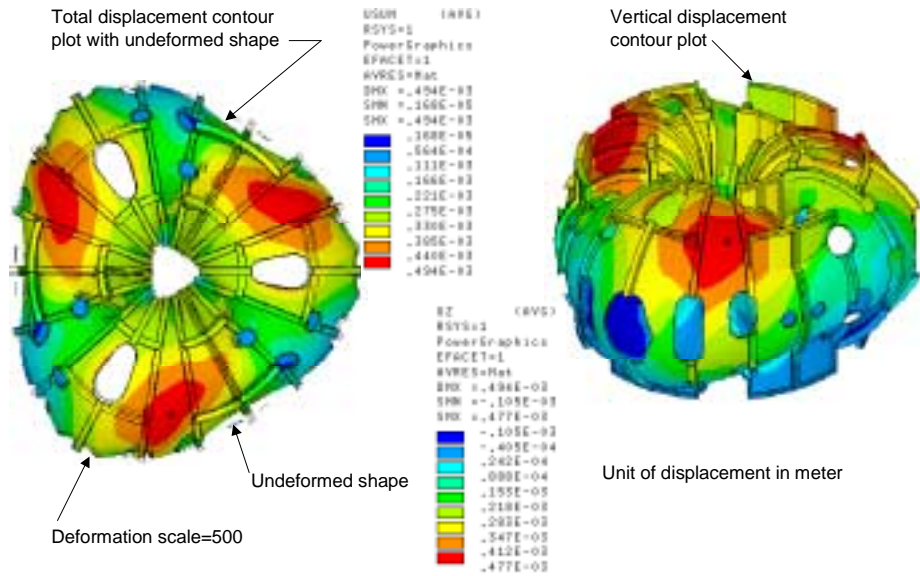
Figure 52 Von Mises Stress Distribution in Shell (50% Modulus)
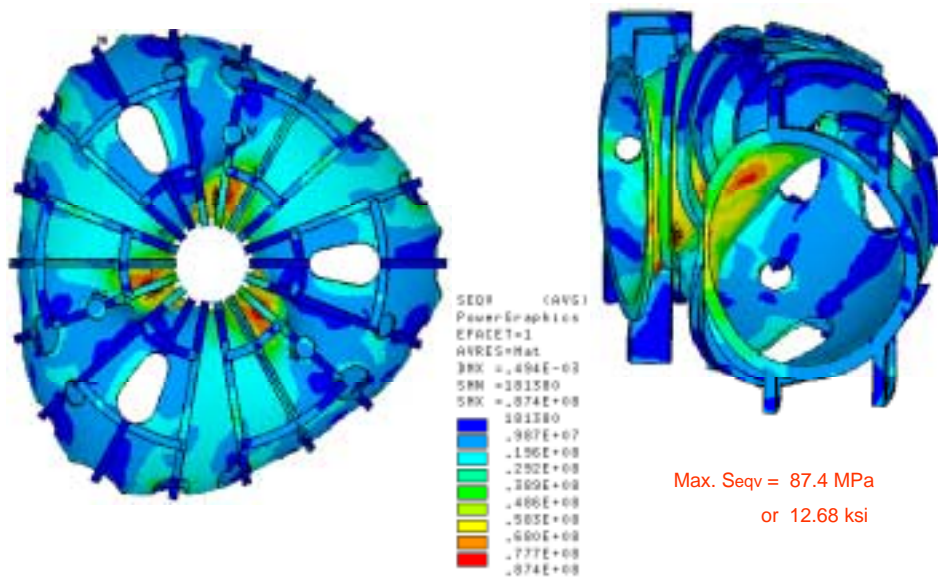
Figure 53 Von Mises Stress Distribution in Tee (50% Modulus)

Max. S_{eqv} = 139 MPa
or 20.16 ksi
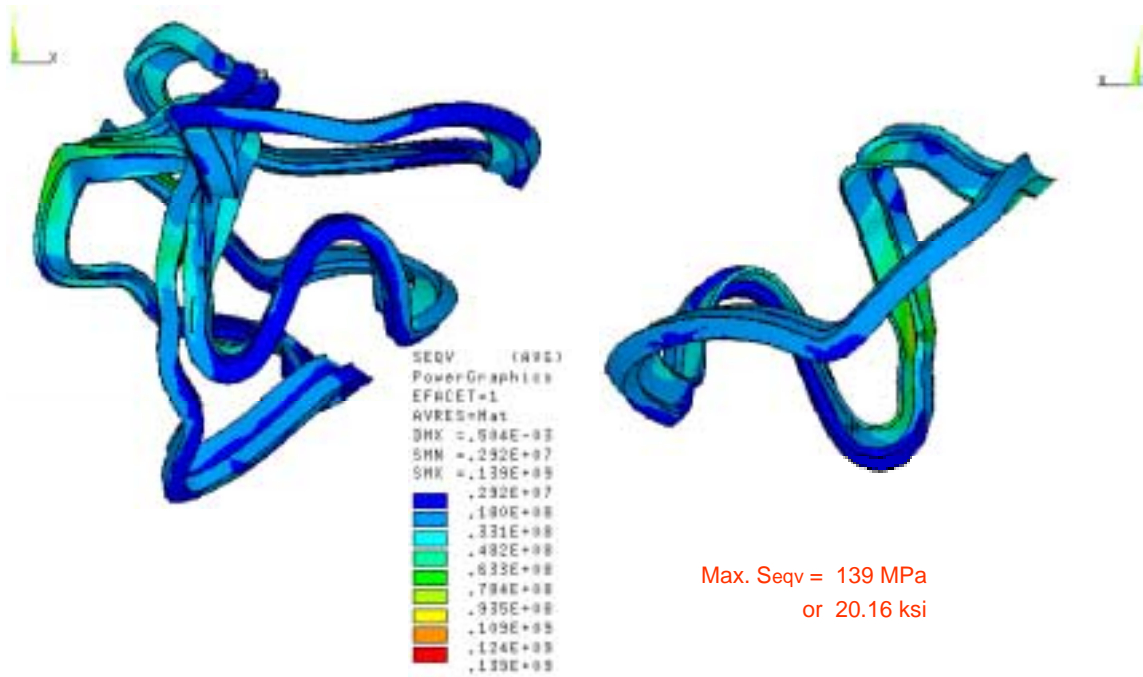
Figure 54 Von Mises Stress Distribution in Windings (50% Modulus)

Max. S_{eqv} = 50.4 MPa
or   7.31 ksi
Note: the Young's modulus
had been made by a factor
of 1/2 from copper
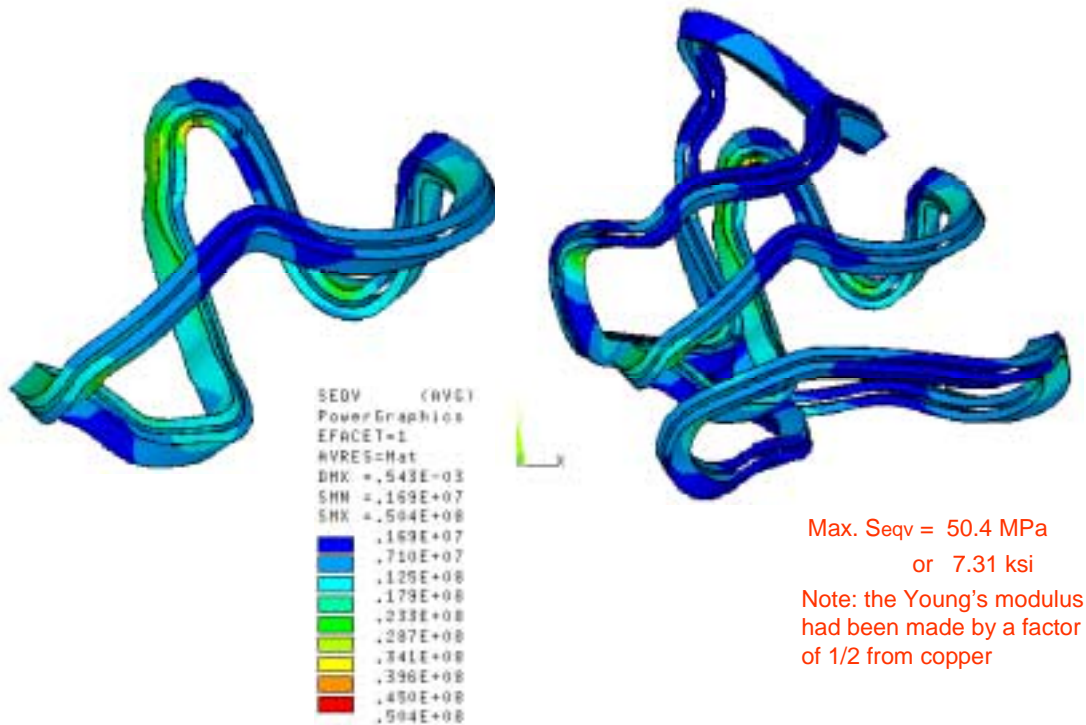
Modular coil thermal stresses

In addition to the stresses arising from electromagnetic (EM) loads, there are thermal stresses due to the sudden increase in winding temperature relative to the structure during a pulse. The maximum temperature rise expected is 40K, but a higher allowable temperature rise would provide more headroom on pulse length and / or field capability. A simple non-linear analysis was performed by modeling a single tee structure, fixed at the shell boundary, a single winding pack, and the spacer. The properties of the materials were similar to those shown in Table 21, but the coefficient of expansion for the tee structure was set to zero. The modulus of the winding was assumed to be 10% of the modulus of copper. The model temperature was then raised 100 F, corresponding to a relative thermal strain between the winding pack and the structure of 9.4 E-5 in/in. Contact elements were used between the tee and the winding to allow the winding to pull away from the structure laterally or slide. The resulting stress and deflection is illustrated in Figure 55, . The stress is very nearly equal to the product of the total strain and the modulus of the winding, indicating most of the strain is in the winding pack. There are some discontinuities, however, and the winding does pull away from the web structure in very local areas, and the total deflection is less than 0.03 inches.

Figure 55 Simple Model of Winding and Structure to Assess Thermal Stress
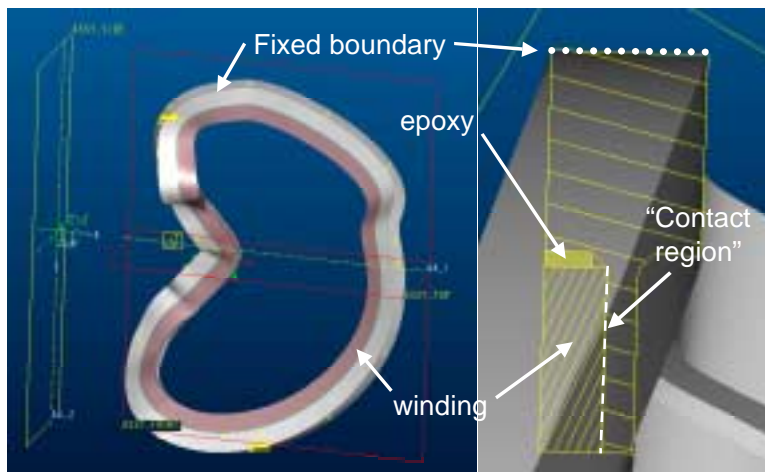
Figure 56 Thermal stress distribution in winding pack and structure
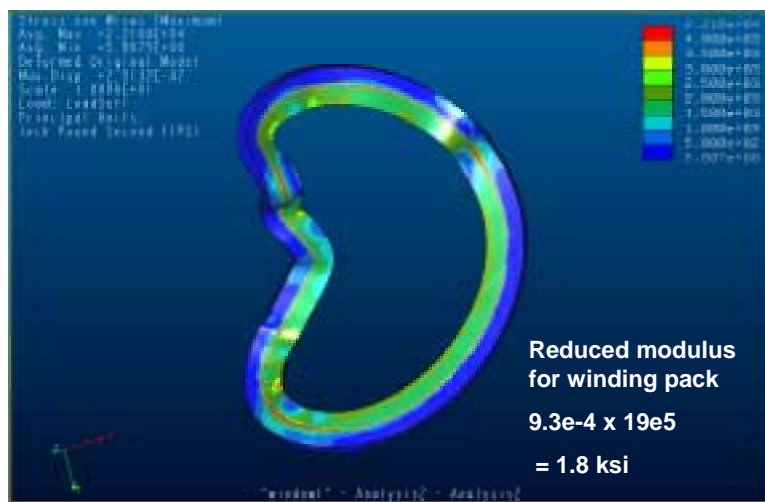
Figure 57 Local Gap Due to Abrupt Temperature Rise
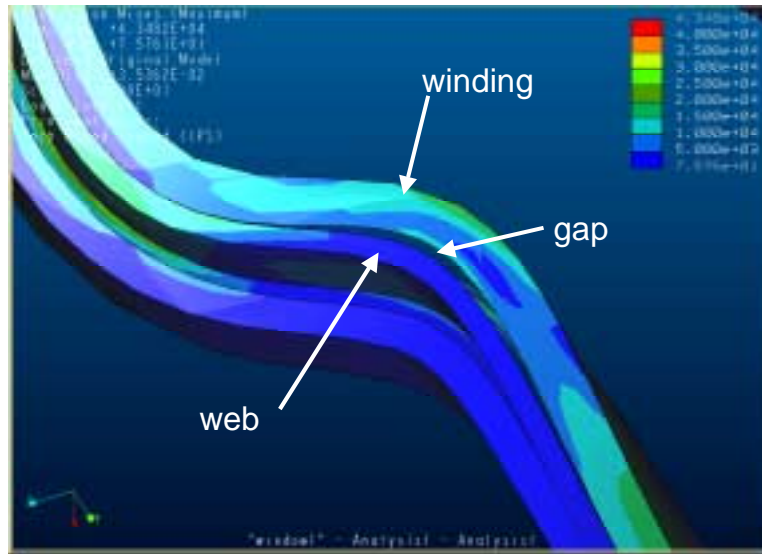
Thermal analysis of modular coils

The temperature rise in an adiabatic copper coil is governed by the current density, equivalent square wave time (ESW), and initial temperature. The allowable temperature rise is set by a combination of acceptable cool-down times and thermal stress considerations. A limit of 40 K has been imposed pending more detailed analysis and testing.

Of the standard operating scenarios, the worst case is the initial ohmic operation at 1.7T, which has a current density of 12 kA/cm^2 in the copper and an ESW of almost 1.4 s. For an assumed starting temperature of 85 K, the temperature rises to 125 K during the shot, which corresponds to the 40 K temperature rise imposed as an initial limit. Lower current density would of course translate into longer flattop times and/or higher toroidal field capability.

Three independent analyses of the coil cooling were performed to determine liquid nitrogen flow characteristics, cool-down times and ratcheting. All the analyses indicate that cool-down within 15-minutes can be accomplished with thermal conduction to chill plates, which are edge cooled with liquid-nitrogen.

The primary issue with the modular coils is the conduction of the heat through the winding insulation (0.06 inches) and along the copper plate to the cooling tubes. Early analysis indicated and later analysis confirmed that a chill plate must be in contact each pie of the winding, so it is not possible to cool the whole winding with a single chill plate on one side of the winding pack and meet the 15 minute cool-down requirement. To illustrate this, Figure 58 shows several cooling schemes and the temperature distribution after cool-down for 15 minutes based on a 2-D finite element analysis.

The center septum design has the best response but heat entering the web structure is not removed. Edge cooled chill plates on both sides work nearly as well, and avoid the structural discontinuity of a cooled septum splitting the winding pack. Cooling from one side does not work.

Figure 58 Cool-Down Analysis for 3 Different Configurations
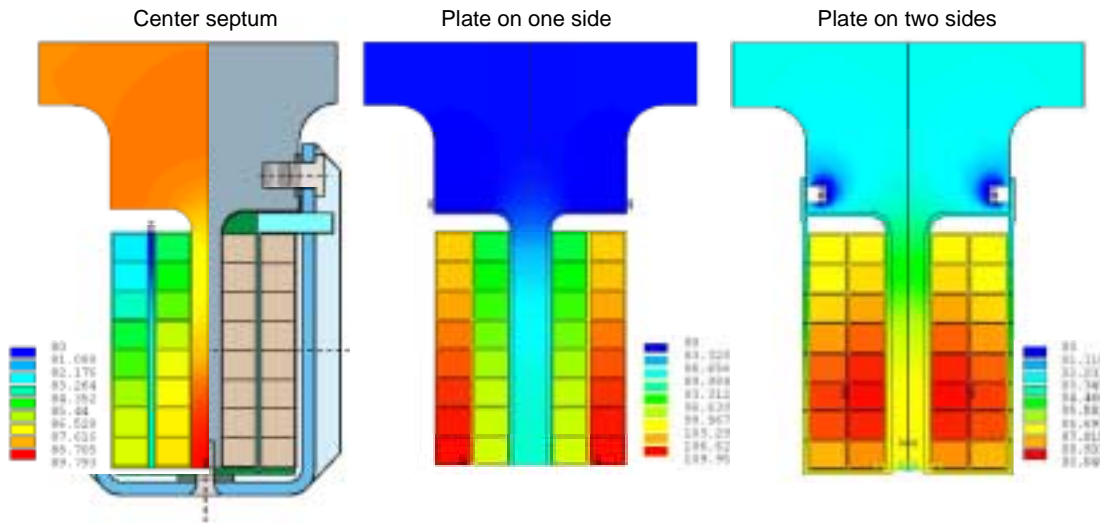
Coil thermo-hydraulic analysis

A thermo-hydraulic analysis was performed for all three coil systems (PF, TF, and Modular)[12]. The present design calls for forced flow LN2 cooling of all coil systems with a prescribed inlet temperature of 80 K at 200 psi. The prescribed equivalent square wave (ESW) used was 1.2-3.5 sec. at the maximum rated current for each coil system. The duty cycle (cool-down period) was specified as 15 minutes (900 sec.). A summary of the results is shown in Table 27. The total LN2 flow requirements for the main coil systems will be 46 GPM. The cool-down of the M1 modular coil is illustrated in Figure 59. The modular coil stops ratcheting after about 4 pulses. The TF and PF coils use internally cooled solid copper conductor, and a pressure drop of only 2 psi is sufficient to cool the coils back to the initial conditions after every shot with not ratcheting. As shown in the table, there is a negligible temperature rise in these coils.

Table 27 Thermo-Hydraulic Analysis of Coils

	ESW	I (kA)	Δ T peak (deg.K)	T max (deg.K)	ΔP (psi)	flow/coil (GPM)	(total flow) (GPM)
M1	1.2	24.0	36.1	117.4	10	0.88	5.2
M2	1.2	24.0	36.2	117.2	10	0.90	5.4
M3	1.2	24.0	36.4	116.5	10	0.94	5.6
PF1	1.5	30.0	7.9	84.9	2	0.92	1.9
PF2	1.5	38.0	12.4	89.4	2	1.14	2.3
PF3	1.1	10.0	0.3	77.3	2	0.68	1.4
PF4	1.6	10.0	0.7	77.7	2	0.68[1]	2.8
PF5	2.5	8.6	0.7	77.7	2	0.75[1]	3.0
PF6	1.5	16.8	2.2	79.2	2	0.82	1.7
TF1	3.2	18.0	5.6	82.4	2	0.95	5.7
TF2	3.2	18.0	5.6	82.4	2	0.95	5.7
TF3	3.2	18.0	5.6	82.4	2	0.95	5.7
							46.4

---

[12] F. Dahlgren, "NCSX Coil Thermo-Hydraulic Analysis", April 4, 2002, PPPL

Figure 59 Modular Coil Cool-Down

Vendor input and Manufacturing studies

In order to obtain feedback from potential fabricators concerning the feasibility, methods, and cost for fabricating the modular coils, four small contracts were awarded to qualified vendors to provide manufacturing studies of the coil winding and coil winding form manufacture. The studies were based on a set of CAD models and a draft procurement specification. The vendors made comments on the design, the specification, and the CAD models. Several suggestions were made concerning the winding form details, such as clamp machining, winding path machining, pre-assembly operations, etc. Additional suggestions were made for the winding; some in considerable detail, concerning items such as the chill plate design, winding order and lead arrangement, and vacuum impregnation method. As was the case with the vacuum vessel study, all the vendors recommended significant R&D, but all said the coil shape, tolerances, and other requirements were difficult but feasible.

R&D studies to date

Some limited R&D has been performed to investigate the behavior of the cable conductor.

Cable fabrication and characteristics: The first step was to procure 1000 feet of conductor, which consists of 12,240 strands of 36 AWG wire, compacted to a 0.5 x 0.625 inch rectangular bundle. This corresponds to a packing fraction of almost 78%. The cable dimensions are within +/- 0.01 inches of the nominal cross section.

Cable handling: The cable was tested with respect to general handling characteristics typical of winding processes. The cable is extremely flexible, but repeated bending and manipulation cause it to "unpack". The bend radius that can be made comfortably is about 3 inches, after which the conductor locks up and requires more force. At this point, the cable also shows significant keystoning, which must be addressed in the cable build. If the cable is wound on a 3.2 inch diameter mandrel[13], the difference in width from inside to outside diameters is 0.15 when the conductor was bent the hard way and about 0.9 inches when bent the easy way around the mandrel.

---

[13] J. Chrzanowski, "Copper Cable Keystone Tests", PPPL, November 2001

Cable resistance measurements: The cable resistance was measured and found to be, on average, about 12% higher than one would expect for a straight copper conductor of the same area as contained in 12,240 strands of 36 AWG wire[14]. This is believed to be due primarily to the twist in the cables before they are compacted and the fact that the wire may have been on the low side of the 36-gage specification (nominal diameter of a single wire = 0.005 inches).

Epoxy fill measurements: Experiments at Auburn University[15] confirmed that epoxy does flow into the interstices between wires within a 3 x 3 bundle of insulated conductors. The conductors were insulated with glass and kapton tape.

Cable strength and stiffness measurements: Two tests were conducted on strength of epoxy-impregnated cable. The first was a punch shear test designed to shear the center conductor out of the 9-conductor bundle. The results with and without the Kapton insulation indicated a shear stress limit of between 1 and 4 ksi (7.4 and 27 MPa) respectively. The failure occurred at the Kapton surface.

The second test was a simple axial compression loading of several 0.5-inch long specimens from one of the Auburn 9 conductor bundles. The samples failed between 154 and 188 MPa (22 – 27 ksi). Yielding occurred between 132 and 166 MPa (19 – 24 ksi). The apparent modulus of elasticity was between 8 and 12 GPa (1200and 1700 ksi). This is significantly softer than a rule of mixtures would have predicted, and is only 10 % of the value of solid copper. The implications are very positive, since it implies much lower thermal stresses than would otherwise have been expected.

3.4   Design Implementation

3.4.1   Component Procurement and Fabrication

Modular coils   Procurement and fabrication of the modular coils will follow a multi-step process. The first step is to award R&D contracts to procure two cast-and-machined coil forms, one each from two different vendors. Upon the successful completion of the prototype coil forms, the production forms will be ordered via evaluated fixed price contracts. R&D is also planned at PPPL in several key areas:

- Keystoning evaluation: Keystoning of the cable at the tight bend areas will be quantified so compensation can be built into the castings and insulation details.

- Vacuum-Pressure Impregnation (VPI): As previously mentioned, the cable-wound coils will require vacuum-pressure impregnation with epoxy to form a monolithic structure. This is a critical process, affecting both the mechanical characteristics and electrical reliability of the coils, in addition to being a pacing schedule process. Consequently, a series of 6-12 trial windings will be made and vacuum-pressure impregnated. Carbon steel I-beams will be shaped to serve as mock-ups of the castings. The cable will be wound in place, a vacuum impregnation shell of glass/epoxy will be spray-cast over the winding and sealed, and the winding will be vacuum-pressure impregnated. Each winding will be cut apart and carefully evaluated for completeness of impregnation. Test specimens will be subject to electrical and mechanical tests.

- The prototype coil castings will then be used to wind at least one prototype modular coil at PPPL.

This series of R&D steps will help develop the processes and tooling required for the production coils, which will also be wound and vacuum pressure impregnated with epoxy at PPPL. The logic is to retain as much control as possible over schedule and processes, and avoid as much as possible the integrating contractor costs. In addition, this logic permits an accelerated schedule, since it avoids the typically 3 month cycle required to advertise, vendor preparation of bid responses, bid evaluations, and contract placement. Since the flexible cable is very easy to wind, the specialized equipment that would normally be necessary to wind a solid conductor is not needed, nor are the associated talents of a conventional coil fabrication vendor. The conductor for the coils will be procured on a fixed price subcontract.

---

[14] S. Knowlton, Private communication, Jan-April 2002

[15] S. Knowlton, Private communication, Jan-April 2002

TF and PF coils The TF and PF coils are relatively simple, conventional, wound coils using hollow copper conductor and vacuum pressure impregnated with epoxy. One or more fixed price contracts will be awarded, based on a best value analysis of the submitted bids. The contract(s) will be structured similar to that successfully used by the NSTX project. The vendors will be given a specification and a basic set of drawings that specify important features such as tolerances, transitions, crossovers, and lead details.

The vendor will be responsible for developing the manufacturing detail drawings and a Manufacturing/Inspection Test Plan. These documents are subject to review and approval by the NCSX prior to release for fabrication.

Coil-to-Bus Leads All the coils have nearly the same peak operating current, so all the coil leads can be essentially the same. These will consist of slightly modified, commercial "kickless" cable, whose insulation has been replaced with reinforced Teflon to operate safely at liquid nitrogen temperatures. The cables will be purchased as assemblies in the correct length, via fixed price contract.

Local I&C The local I&C consists only of temperature and strain sensors, which will be procured via a fixed price subcontract.

3.4.2   Subsystem Assembly, Installation, and Testing

Modular coils The modular coils will be assembled first into field periods in the D-site pre-assembly area, and the field periods will then be installed on the support frame in the NCSX test cell at C-site.

PF and TF coils The TF coils will be assembled in the same sequence as the modular coils, first as part of the field period subassembly in the D-site pre-assembly area, then the field periods will be installed in the NCSX test cell at C-site. The lower PF coils will be pre-positioned below the field period assemblies and raised into position, while the upper PF coil assemblies will be lowered into position, after the three field period subassemblies are brought together.

Coil-to-Bus Leads   The lead pairs for the modular and TF coils will be installed on the field period subassemblies, while the leads for the PF coils must be installed after the field periods have been brought together in the test cell. As previously mentioned, these leads will be fabricated from commercially available "kickless" cable.

Local I&C The strain and temperature sensors will be installed on the modular and TF coil windings just prior to or during the field period subassembly operation. The PF coils sensors can be installed at any time after receipt of the PF coils but prior to the cryostat installation. PPPL technicians will install these sensors.

3.5   Reliability, Maintainability, and Safety

A formal Failure Mode, Effects, and Criticality Analysis will be performed for the magnet systems during the preliminary design phase. Nevertheless, several design features have been included to enhance the reliability of the coil systems or to simplify inspection and repair of obvious trouble spots.

- The first feature is to provide a coil fault detection system that would prevent operation of the coils outside their design envelope. The system would guard against control errors and shorted buswork.

- Other features intended to improve reliability or maintainability are specific to individual coil types. For example:

    - The modular coil windings are composite structures of copper and epoxy, which could degrade if subjected to large deflections during operation. To prevent overloads that could damage the windings, they are continuously supported against magnetic loads by the stainless steel winding form. Clamps are provided to keep the winding in close contact with the structure.

- The crossovers and leads are located in a relatively straight section of each winding to simplify the crossover geometry and minimize the local forces on this critical area.

- The leads are collected into a coaxial arrangement immediately adjacent to the winding pack to reduce forces further. This arrangement also mechanically connects the two exiting ends of the winding to reduce the possibility of shear failure between the exiting conductor and the winding pack. The coaxial leads are brought all the way outside the shell as hard conductor before transitioning to the flexible coaxial cables that connect the coils to the buswork system.

- The cooling is redundant since there are two chill plate systems for each winding pack. Failure of one chill plate circuit can be compensated for by slightly longer cool-down times.

- A continuous cooling tube is brazed to the chill plates, and routed through the shell structure at the near the bottom of the coil and the top of the coil where it is connected to small supply and return manifolds respectively. These manifolds are then connected to the primary LN2 distribution system inside the cryostat.

- All the connections are intended to be accessible and with only minor disassembly of external components. This also allows each circuit to be individually tested in the event of a leak.

- The PF and TF coils are of conventional construction and operate at relatively low current density. This results in benign thermal cycles and stress levels. The coil structure provides almost continuous support for these windings as well to further reduce cyclic deflections.

- Finally, all the coils will use the same flexible, coaxial cable for the leads, which minimizes loads on the coil terminals and standardizes the lead design and analysis.

3.6   Cost and Schedule

3.6.1   Modular Coils (WBS 17)

The cost estimate for the modular coil set is summarized in Table 28 and totals $16928K. This estimate was developed as a bottoms-up estimate, and includes significant input from potential vendors. The cost is split approximately equally between the coil winding, to be done at PPPL, and the coil winding forms. The winding costs are based on a detailed schedule-based estimate of R&D, tooling, winding, and vacuum impregnation costs, based on previous experience winding coils at PPPL. The cost of the cast-and-machined coil forms is based on vendor estimates from four vendors who participated in the manufacturing studies. These estimates included both R&D and production unit costs. As with the vacuum vessel, there was a wide variation of costs that reflects both the method of manufacture and the level of cost uncertainty that exists. The contingency recommended for the modular coils is 40%, due to the developmental nature of the system.

The schedule for implementing the Modular Coils (WBS 17) may be seen in the **Project Master Schedule**, provided as part of the Conceptual Design Report. The modular coils lie right on the critical path. Title I and Title II design for the modular coil winding forms will be completed in FY03, along with the Manufacturing R&D. The production contract is scheduled to be awarded early in FY04. The first modular coil winding form is scheduled to be delivered early in FY05. The last will be delivered at the end of the first quarter in FY06.

Tiltle I and II for the coil windings will be conducted in parallel with the design of the winding forms. In-house R&D will extend from early in FY03 into early FY04. Winding the modular coils will start early in FY05 and be completed in mid FY06.

Table 28 Modular Coil (WBS 17) Costs

Total Estimated Cost (K$)						17 Total
		171	172	173	174	
Manufacturing Development	Labor/Other	1777	174			1951
	M&S	489	1491			1979
	Total	2266	1664			3930
Design (Title I & II)	Labor/Other	882	312	47	24	1265
	M&S					
	Total	882	312	47	24	1265
Fabrication/Assembly (incl Title III)	Labor/Other	4086	402	25	5	4518
	M&S	2004	5147	60	5	7215
	Total	6090	5549	85	9	11734
Installation/test	Labor/Other					
	M&S					
	Total					
Grand Total		9237	7525	132	33	16928

3.6.2   TF (WBS 13) and PF (WBS 14)

The costs for the TF and PF coils were developed as a bottoms up estimate using recent experience on the NSTX coil sets. The costs are summarized in Table 29. Cost savings have been realized by using the same, standard, conductor in all the coils except PF2. This allows the same forming tooling to be used for virtually all the coils.

The TF Coils (WBS 13) cost $1496K. The PF Coils (WBS 14) cost slightly more, $1847K. The recommended contingencies are 24% for the TF and 21% for the PF.

The schedule for implementing the TF Coils (WBS 13) and PF Coils (WBS 14) may be seen in the **Project Master Schedule**, provided as part of the Conceptual Design Report**.**   Title I design begins in mid FY03. Title II design is scheduled to be finished by mid FY04. Production contracts will be awarded shortly thereafter. Production articles should be delivered in mid FY05. TF coils are needed in time to be assembled with the first field period. The lower PF coils need to be placed on the floor of the Test Cell prior to installation of the first field period in the Test Cell.

Table 29 TF (WBS 13) and PF (WBS 14) Costs

Total Estimated Cost (K$)					13 Total								14 Total
		131	132	133		141	142	143	144	145	146	147	
Manufacturing Development	Labor/Other												
	M&S												
	Total												
Design (Title I & II)	Labor/Other	129	45	23	197	163	61	61	61	61	74	18	500
	M&S												
	Total	129	45	23	197	163	61	61	61	61	74	18	500
Fabrication/Assembly (incl Title III)	Labor/Other	116	4		120	125	39	39	39	39			280
	M&S	1112	60	8	1179	239	194	242	201	147	39	5	1067
	Total	1227	65	8	1300	364	233	281	240	185	39	5	1346
Installation/test	Labor/Other												
	M&S												
	Total												
Grand Total		1357	110	30	1496	527	294	342	301	247	112	23	1847

3.6.3   Trim Coils (WBS 18)

Trim coil costs were estimated assuming small conductor and simple winding forms. There are only two shapes for these coils, one shape for the top and bottom coils and the other for the outer perimeter coils. The costs are based on engineering judgment and recent experience with the NSTX coil windings. Standard sized conductor is used to help keep the cost down. The cost estimate for the Trim Coils (WBS 18) is $278K. The recommended contingency is 40%, due primarily to uncertainties in performance requirements at this early stage of design.

The schedule for implementing the Trim Coils (WBS 18) may be seen in the **Project Master Schedule**, provided as part of the Conceptual Design Report**.**   Design (Title I and II) will take place in the second half of FY05. The coils will be delivered by mid FY06. The upper and lower external trim coils and three of the outer trim coils will be installed on each field period in the TFTR Test Cell. The other three outer trim coils, because they span the assembly joint, will be installed after the field periods are joined, in the NCSX Test Cell.

Table 30 Trim Coil (WBS 18) Costs

Total Estimated Cost (K$)		
		18 Total
Manufacturing Development	Labor/Other	
	M&S	
	Total	
Design (Title I & II)	Labor/Other	57
	M&S	
	Total	57
Fabrication/Assembly (incl Title III)	Labor/Other	145
	M&S	76
	Total	222
Installation/test	Labor/Other	
	M&S	
	Total	
Grand Total		278

3.7   Risk Management

Modular Coils

The modular coils have potential technical, cost and schedule risks. The technical risks can be listed, as well as the way in which each has been addressed:

Potential Technical Risk #1. The coils do not have the correct geometry and tolerance

The first potential risk, that the coils will not have the specified geometry and accuracy, is addressed in the design, R&D, the fabrication process, assembly process, and operation.

Design: The coils are designed around a cast and machined winding form that is very accurate, with the winding surfaces and mounting features integrated into a single unit. The coils are wound directly onto this form and vacuum pressure impregnated with epoxy. The casting is massive (just like the frame of a high precision machine tool) and deflections due to the winding and assembly process should be negligible. Since the windings are not removed from the winding form, the distortions that would normally occur during this operation are avoided.

In addition to the basic design concept, the coil leads and bus interfaces are designed for minimum field errors.

R&D Significant R&D is planned to begin immediately with the start of preliminary design to demonstrate and test all operations connected with the modular coil fabrication. This includes procurement of two cast and machined winding forms, winding up to 12 partial coil packs and at least one full prototype coil, and performing thermal, and fatigue tests on critical features. This will all occur with sufficient time to incorporate any changes to the design suggested by the R&D.

Fabrication The coil forms are dimensionally stabilized prior to machining to an accuracy of +/- 0.25 mm anywhere on the winding surface. The forms can be readily and independently inspected by NCSX personnel with conventional laser tracker or multi-link coordinate measuring systems to confirm compliance with specifications.

Once acceptable coil forms are delivered, the coils will be wound at PPPL with total control over all processes by NCSX personnel. PPPL has experienced personnel and a demonstrated capability for winding and epoxy - impregnating coils for a variety of magnet systems. The use of the modern 3-D measurement equipment mentioned above will allow the conductor placement to be continuously measured and corrections made throughout the winding process. Once the coils are completed, additional measurements of the as-built geometry can be entered into codes and the relative placement of each coil can be optimized, if necessary, for best control of error fields.

Assembly Continuous measurements will be made during the assembly process to ensure that the coils are aligned correctly. Each coil will be located to a global reference frame that is continuously updated for the best fit to the coil array.

Potential Technical Risk #2. The coils will not fit over the vessel

The second potential risk, that the modular coils will not fit over the vessel, is also mitigated by the 3-D CAD technology, the use of laser scanners and/or multi-link measuring systems to verify geometry, and by using accurate scale models of the vessel and coils during the design and development processes. A 1/12 scale model of the present design verifies that the coils and vacuum vessel can be assembled as planned.

Potential Technical Risk #3. The coils will fail mechanically

The third potential risk, that the modular coils will fail mechanically, is mitigated by analysis, conservative design criteria, and by an active coil protection system. Independent groups using different codes and models will perform critical analysis, such as electromagnetic load calculations, stress and deflection calculations, and thermal stress analysis. The stresses will be compared to the ASME code allowables as specified in the NCSX Structural Design Criteria, which provide a safety factor of 1.5 on yield for primary membrane stresses at the operating temperature. The materials chosen for the cast coil form have been demonstrated to have extremely high tensile strength, which adds additional margin. The winding is continuously supported in the cast form, so the winding and coil forms will have approximately the same strain. Since the coil modulus of elasticity is much lower than the steel (~ 1/20), the winding should have very low stresses. The only caveat to this point is the thermal stress, where the coil form restraint adds stress to the winding. Again, the low stiffness mitigates this problem significantly. Nevertheless, R&D testing will be performed to determine thermal stress limits during the preliminary design phase.

In addition to designing and analyzing expected loading conditions, the coils will be evaluated for and protected from fault conditions by an active coil protection system. A coil fault detection system would prevent operation of the coils outside their design envelope. The system would be programmed to monitor the signals from voltage, strain, temperature, and possibly magnetic field sensors on or around the various coil windings and structures as the coils were being energized. If any of the sensor signals were out-of-bounds for the specific current scenario being run, the fault system would crowbar all the power supplies. The system would guard against control errors and physical faults such as shorted buswork.

Potential Technical Risk #4 The coils will fail electrically

The fourth potential risk, that the coils will fail electrically, is mitigated by a redundant insulation system and non-conducting coolant. The insulation will consist of half-lapped Kapton tape in addition to the glass tape. The fiberglass/epoxy matrix is adequate by itself, but just in case there are small dry areas between turns the Kapton will provide more than adequate insulation strength.

Potential Technical Risk #5 The modular coil cooling will be inadequate

The fifth potential risk, that the coils will not cool down in the specified time, will be mitigated by providing two chill plates for each winding and cooling from both ends of the chill plates. Multiple cooling circuits also provide redundancy.

Potential Technical Risk # 6 The coil structure will introduce static or transient field errors

The sixth potential risk, that the modular coil structure will introduce field errors, is mitigated by including insulating breaks at three places in the shell structure and by strict adherence to stellarator symmetry.

Potential Technical Risk #7 The cable conductor will not behave as planned

The final potential technical risk is that the compacted cable conductor will not behave as planned. This problem is mitigated by design and R&D. The design approach, as explained in detail above, is to full support the windings against electromagnetic forces, nearly eliminating the cyclic bending strain in the conductor that would normally occur in a free standing coil. Extensive R&D is planned and already underway to build a small racetrack-shaped coil that can be electrically and thermally cycled. The winding, vacuum impregnation, and restraint conditions would be matched as closely as possible to the planned design.

Cost and schedule risks

The cost and schedule risks associated with the modular coils could also be significant, but steps have been and are being taken to reduce those risks substantially. Manufacturing studies were carried out during the conceptual design process to obtain advice from manufacturing engineers on ways to make the design easier or less expensive to fabricate. Four different studies of the modular coils were carried out, and various methods for winding, vacuum impregnation, casting and machining were investigated. Vendor input will be continued after the CDR with an extensive R&D program. This effort will be carried out concurrently with the modular coil design process such that the results can be included in the final design. Two different vendors will fabricate full-scale cast and machined coil forms. At the conclusion of the R&D phase, one or more fixed price contracts will be awarded for the production castings. The selection of two vendors for the R&D phase will result in at least two qualified vendors for the production articles, and provides an extra incentive to keep production costs (and bids) low.

This approach also mitigates the schedule risk by starting the R&D process as soon as possible and incorporating any needed design changes as they are uncovered. Two qualified vendors will be available at the end of the R&D process, so schedule pressures could be relieved by adding more capacity. It should be noted that the present schedule for procurement of the winding forms is completely consistent with vendor input, and no specific schedule issue is apparent. The coils will be wound in-house at PPPL, which affords more control over the schedule and resource allocation than would be possible with an outside vendor. Slight in-process changes could be made without ponderous approval cycles.

PF, TF, Trim coils

The other coil sets do not have any specific technical, schedule, or cost risks that have been identified. The coils are all of conventional design and fabrication processes are well known and established. The operating current densities, temperature rise, forces, etc. are conservative. They are well supported and with features for adjusting alignment individually. None of these coil sets is on the critical path.

4   CRYOSTAT AND MACHINE SUPPORT STRUCTURE

4.1   Design Requirements and Constraints

4.1.1   Cryostat

The cryostat provides the thermal insulation for the cold coil set and structure, and must seal the coil space from the outside air to prevent condensation on the cold surfaces. The cryostat must also provide a means for circulating dry nitrogen inside the cold volume to cool down and maintain the temperature of the interior structures.

The primary constraints on the cryostat are that it be installed near the end of the overall assembly operation, be easy to remove and replace, and be easy to reconfigure for new diagnostic access requirements.

4.1.2   Machine Support Structure

The machine structure provides the gravity support for the device and the integrated support for the TF and PF coils. The base structure must also minimize the heat leak to the cold structure from the floor, must accommodate the radial thermal contraction of the cold mass, and must provide the sliding mechanism and rails to allow the three field periods to be brought together simultaneously during final assembly (or to be retracted for major modifications or repair). The primary constraints are that it operates at cryogenic temperatures, be non-magnetic, and not interfere with diagnostic or heating access.

4.2   Design Description and Performance

4.2.1   Cryostat

The baseline concept consists of a simple frame and panel design covered with urethane insulation and is illustrated in Figure 60 and Figure 61. The frame consists of molded fiberglass modules mounted along the outer perimeter, top and bottom of the external coil support structure. The frames have openings corresponding to the openings in the structure between the TF and PF coils. Fiberglass panels are attached to the frame modules to form a surface for the urethane.

Figure 60 Cryostat Assembly

S17e150-005.asm

S17e150-006.asm

Period
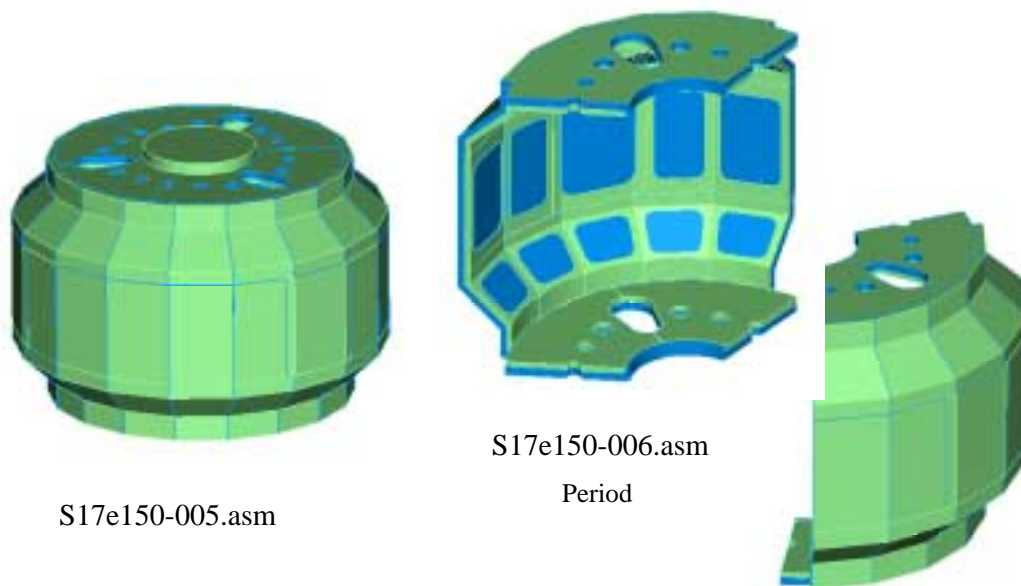
Figure 61 Exploded View of Cryostat
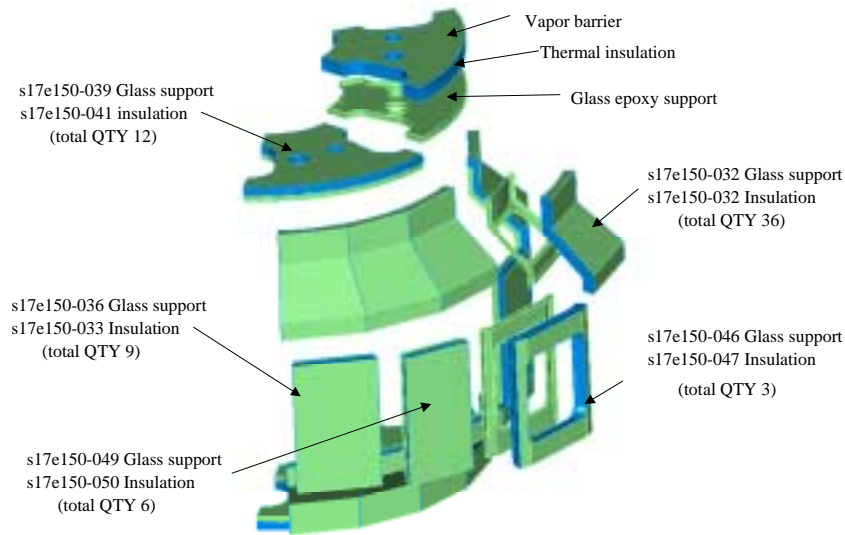
Fiberglass dams are positioned around each vacuum vessel port, coil lead, or utility penetration. A flexible silicone rubber boot is used to provide a seal, as illustrated in Figure 62. Urethane is then sprayed on the fiberglass panels using a commercial process typically used for large stationary cryogenic tanks. The exterior surface of the urethane is then sprayed with a butyl rubber coating for an additional gas seal and to provide a durable surface. For access to interior components, a few removable panels (including the top and bottom central openings) would be provided, but in general, the urethane would simply be removed and a hole cut in the panel where access is desired. The hole would be repaired by patching the panel and re-foaming. This process is analogous to accessing plumbing by cutting holes in a sheet rock wall.

The urethane insulation is approximately 6 inches thick, which provides good thermal isolation for the cold components (~ 2 kW heat leak), but is probably not sufficient to prevent condensation on the outside of the cryostat. For this reason, heaters and blowers will be used to control the outside surface temperature and prevent condensation. Flexible insulation must also be stuffed around the penetrations outside the boots.

Figure 62 Cryostat Boot Schematic
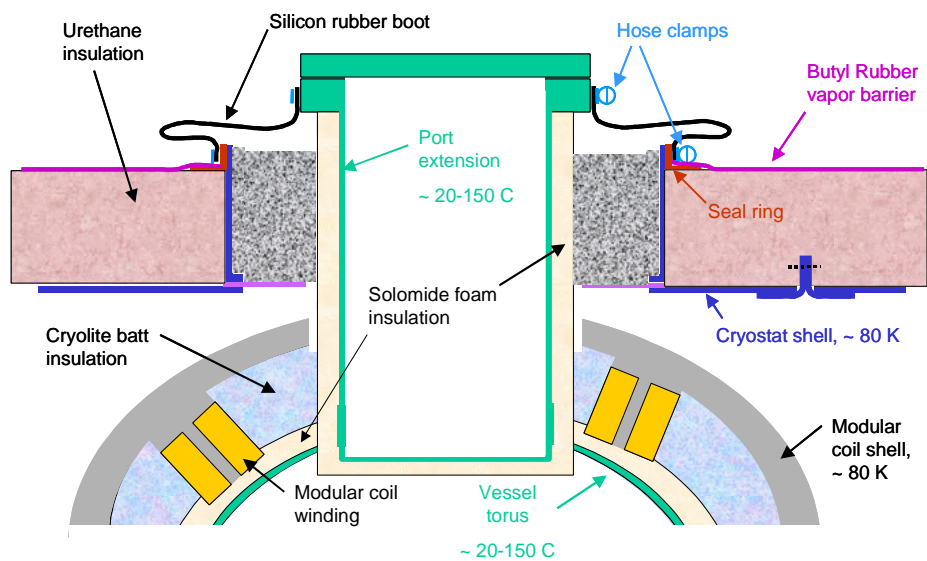
4.2.2   Machine Support Structure

 The machine support structure consists of the base assembly and external coil support structure. These components provide mounting points for all the other components and support the gravity and seismic loads on the device.

Base Assembly

The base assembly is illustrated in Figure 63. A frame is mounted to the floor with three pairs of rails oriented parallel to radial axes through each of the field periods. Retractable carriage assemblies are mounted to the rails to provide a means of assembling the machine in three field periods. The columns are mounted to the carriage assemblies and are tied together in the radial direction for stability. The tops of the columns connect to the underside of the external coil support structure.

Figure 63 Machine Base Assembly
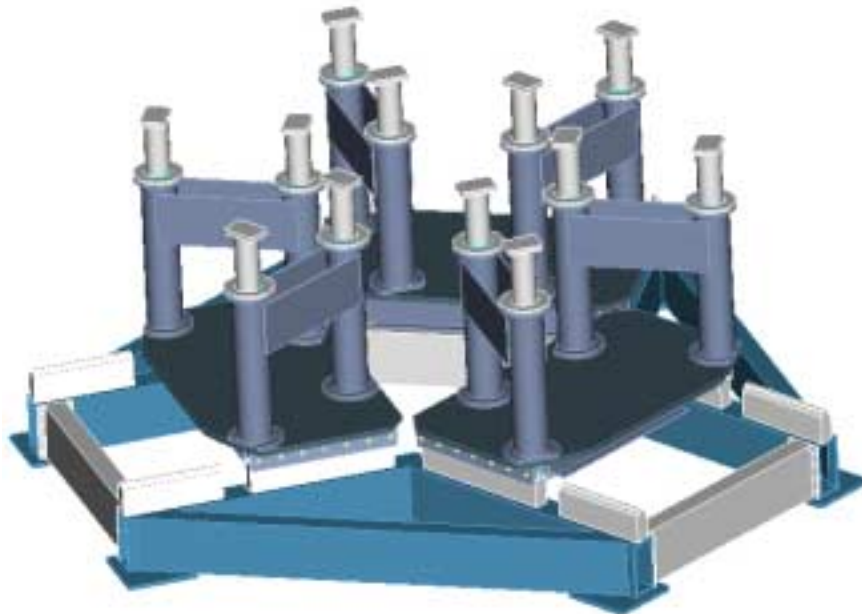
The columns will consist of three concentric tubes. The outer tube is attached to the rail carriage and the innermost tube is attached to the cold mass. These tubes are both in compression. Between these tubes is a thinner tube in tension, which provides a long conduction path for reducing heat leakage to the machine. The long tube is mounted such that it can pivot to provide about 0.15 inch compliance in the radial direction to accommodate the thermal contraction of the cold mass. The lateral direction will be constrained with snubbers to resist seismic loads. The concept for insulation between the tubes has not been decided, but the best thermal solution is to evacuate the interspace between the tubes.

Coil Support Structure

The coil support structure provides an integrated shell structure for accurately locating and supporting the TF and PF coils, the modular coil assembly, and the external trim coils. This structure is illustrated in Figure 64. The structure consists of segmented upper and lower shelf assemblies, outboard TF support brackets, upper and lower crown structures, and an integrated bucking structure and solenoid assembly.

Figure 64 Coil Support Structure
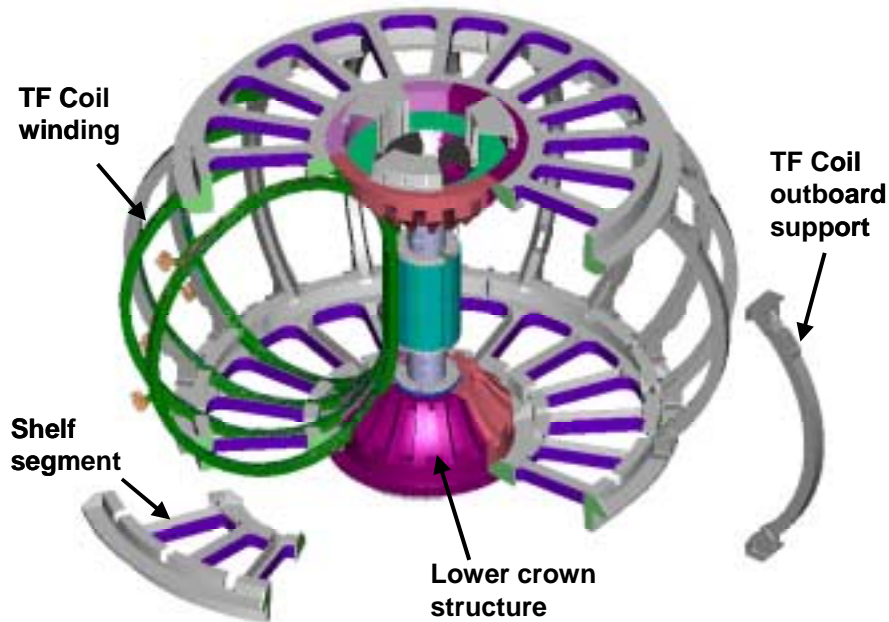
The shelf assemblies consist of 6 identical cast and machined frames bolted together across insulated joints. The joint locations are arranged to correspond with the v=0 and v=1/2 symmetry planes, such that the upper and lower shelf assemblies can be installed as part of the field period sub-assembly. The frames have pockets that receive the horizontal legs of the TF coils to provide lateral support for out-of-plane loads. The lower segments have machined pads where the lower shelf attaches to the machine base assembly. The upper and lower external trim coils are also mounted to these frames.

The modular coil assembly connects the upper and lower shelf assemblies through toroidal stiffener supports, as shown in Figure 65. These supports transfer any net reaction from overturning loads on the TF coils to the modular coil shell, as well as any local vertical loads from the TF. Individual TF coils do have vertical loads due to interaction with the modular coils, but there is no net vertical loading on the TF coil set. These supports are cast into the modular coil 1 and 3 shell segments, and spacers are used to fill the gap between the shell and the shelf assemblies. The spacers on either side of the v=1/2 plane are removed to bolt or unbolt the three field assembly joints on the shell.

Figure 65 Interface Between Coil Support Structure and Modular Coil Assembly
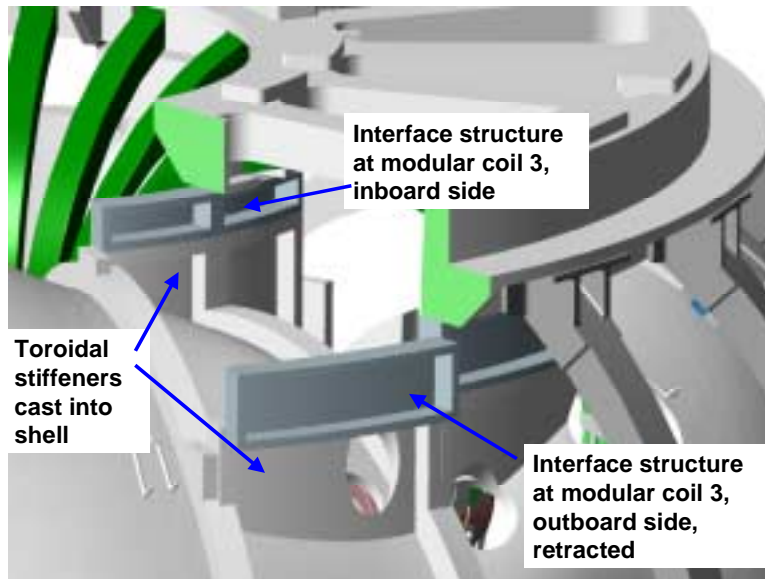
The upper and lower crowns are connected to the upper and lower shelf assemblies respectively. The centerstack assembly is attached to the upper and lower crowns. The TF coil support legs also connect the upper and lower shelf assemblies.

The centerstack assembly consists of the PF1 and PF2 coils, segmented cylinders, spacer assemblies, bucking structure, and tie rods. The PF1 and PF2 coils are wound on segmented cylindrical forms , then stacked together across spacers. The two PF1 coils are separated by a hard spacer, and the PF2 coils are separated from the PF1 coils by a spring loaded spacer that provides the necessary restraint while accommodating thermal expansion of the coil packs. To react the centering force of the TF coils, segmented bucking plates are attached to the outside of the centerstack. An alternate design with a machined glass epoxy cylinder is also being considered. The centerstack structural components are illustrated in Figure 66.

Figure 66 Centerstack Assembly
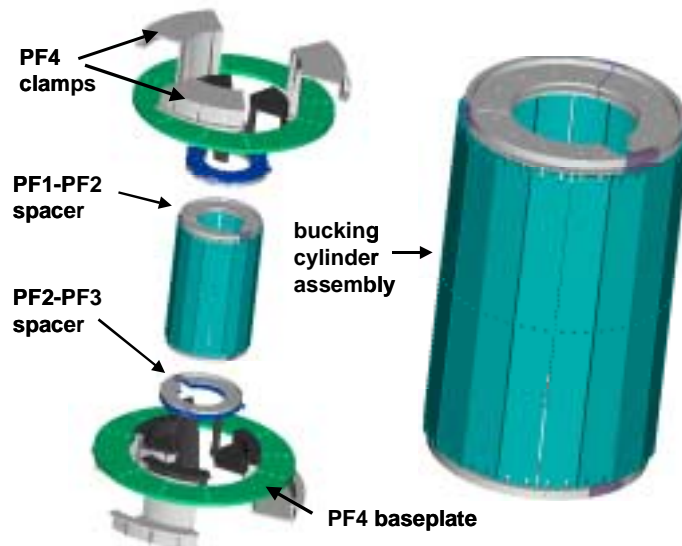
The crown assemblies consist of 3 cast and machined elements that are bolted together across insulating breaks to form a structural ring. They are slotted to support out-of-plane loads on the TF coils in the upper and lower inboard curved regions. The TF coils do not have a constant tension D-shape due to the constraints imposed by the PF coil geometry, so the crown structures may also be required to restrain some of the centering forces. The TF coil windings and structure will be pre-assembled and pillow shims installed in the crown structures to make sure the TF centering force is shared correctly between the bucking cylinder and the crowns.

The PF ring coils are attached to the shelf structures and the outboard TF leg supports with brackets that can be adjusted to accurately align the coils with respect to the modular coils and TF coils. Since large ring coils are often out-of-round, these brackets will also serve to bring the coils into an acceptably round shape.

4.3   Design Basis

The design basis for the machine structure and cryostat includes the design criteria and the associated thermal and structural analysis.

Design criteria

The machine structure will be designed according to the NCSX Structural Design Criteria, which is based on the ASME Code, Section VIII, Division 2. The code provides a conservative but prudent approach to design stresses, fatigue, buckling, and welding of structures.

The cryostat will also be designed to the NCSX Structural Design Criteria to the extent that it applies, but the loading is minimal.

Analysis

The primary loads on the machine base structure are the gravity and seismic loads from the cold structure. The approximate weight of the cold mass is 100 tons. The weights of individual components are summarized in Table 31. A thorough analysis of the base has not yet been performed, but the column size is consistent with the total vertical force assuming only 3 of the 12 columns take the entire vertical load. In addition, the bending strength appears adequate for a lateral force of 0.2g, assuming only 4 columns act to take the load. The sliding rails are locked after assembly, providing a rigid base structure.

The heat leak through the columns will depend on the final design choices, but for a vacuum insulated triple tube design, the heat leak could be as low as 100 W. If a single column design with simple external insulation were used, the heat leak would be on the order of 500 W. Either of these choices would be acceptable.

The coil support structure analysis is not yet complete. The structure is well suited to reinforcement if necessary by simple thickness changes to the cast elements.

Table 31 Component Weights

Component / Assembly	Weight each (lbs)	No.	Total weight (lbs)
Vacuum vessel w/o flanges	24,000	1	24,000
Vacuum vessel cover flanges		1	0
PFC assembly	3000		3,000
Subtotal, internals			27,000
Modular coil 1	5963	6	35,800
Modular coil 2	5490	6	32,900
Modular coil 3	5567	6	33,400
TF coil	1120	18	20,200
PF1,PF2 assembly	5100	1	5100
PF3	1680	2	3400
PF4	3855	2	7700
PF5	4226	2	8500
PF6	1808	2	3600
Error field correction coils	300	1 set	300
Crown structure	4788	2	9600
Misc central structure	3855	1 set	3900
Top and bottom shelf structure	2020	12	24200
TF coils support legs	383	18	6900
Subtotal, cold structures			195300
Base structure	32100	1	32100
Cryostat	6900	1	6900
Misc piping, etc.	1000	1	1000
Total weight of NCSX Core			262,000

4.4   Design Implementation

4.4.1   Component Procurement and Fabrication

Cryostat The cryostat is procured in three major packages. The first is for the molded frame elements. The intent is to award the entire assembly to one vendor on an evaluated fixed price basis. The vendor would be responsible for fabrication of the molds and panels, trimming and machining, and pre-assembly and fit check. The assembly would be built to a performance specification with geometric and functional requirements, but the vendor would propose the exact method of fabrication. The boots would be procured from a second vendor, also on an evaluated fixed price basis. The process would be similar, using a performance specification and functional requirements. The urethane insulation for the exterior of the cryostat would be awarded to a qualified contractor, who would apply the insulation in place to the completed cryostat assembly.

Base assembly The base assembly is relatively simple, stainless steel welded construction from standard pipe and plate. The intent is to award the entire assembly to one vendor on an evaluated fixed price basis. The vendor would be responsible for fabrication, machining, procurement of slides and rails, and pre-assembly and fit check of all the pieces. The assembly would be build-to-print.

Coil support structure The coil support structure consists of two types of components. The first type includes the shelf segments, crown segments and outboard TF coil supports, which are all cast and machined elements that must be bolted together into a precision assembly. This assembly could be split among several vendors, for example

casting and machining vendors. However, a better choice may be to award a contract to a single vendor who would supply a pre-assembled and fit-checked unit that included all the components, insulation, shims, bolts, etc. The contract would be awarded on an evaluated fixed price basis and would be build-to-print.

The second set of components in the coil support structure consist of the spacers, clamps, bucking plate assembly, etc. that are smaller and ideally integrated with the PF1/PF2 centerstack assembly. The intent here would be to include these components as part of the centerstack assembly procurement, which would be on an evaluated fixed price basis and build-to-print.

4.4.2   Subsystem Assembly, Installation, and Testing

Cryostat The cryostat is the last component assembled in the test cell. (It is possible that some of the panels could be pre-installed as part of the field period subassembly, but this may make subsequent operations more difficult.) First, the molded frame sections are bolted together in sections and attached to standoffs on the shelf structures. The flat panels in the port openings are then installed along with the conformal dams around each port extension (Fig. 2.1.3-3. The inter-spaces between the dams and the port extensions are packed with batting insulation and the silicon rubber boots are installed between seal rings on the dams and the outside of each port extension flange. The urethane insulation is then applied, followed by the butyl rubber vapor barrier. A fabric or thin sheet metal covering may be included as mechanical protection and a fire retardant, but the choice will not be made until preliminary design. Finally, the cryostat is leak checked to confirm there will be no ingress of air the cold mass.

Machine base assembly The machine base will be pre-assembled by the fabricating vendor. It will be the first component installed in the test cell. The primary steps will be to attach the base frame to the floor with adjustable anchors and grout in place, followed by assembly of the rails, carriages, and columns.

Coil support structure The coil support structure will be assembled as part of the field period subassembly operations in the D-site pre-assembly area. Two sub-assemblies, each with one sixth of the TF coils, shelf segments, and crown structures will be pre-assembled. Pillow shims will be provided between the TF coils and the crown structure to insure good fit for centering loads. The two subassemblies will then be rotated over the completed modular coil/vessel field period subassembly, one from each end. The connection is then made between the external coil structure and the modular coil shell, using the toroidal stiffener spacers. Since these spacers lie between flat, parallel, and horizontal planes, they can be shimmed to mitigate tolerance buildup and provide the exact relative position of the TF coils and modular coils.

Once the field period subassemblies have been completed, they are placed on the machine base structure. The carriages in the base structure are simultaneously moved inward to avoid interference between the interlocking modular coils, and the field period connections are made. After the field periods are joined, the centerstack assembly, the PF3 coils, and crown structures are installed and secured with the tie rods.

4.5   Reliability, Maintainability, and Safety

A formal Failure Mode, Effects, and Criticality Analysis will not be performed for the cryostat and machine structure until the preliminary design phase. Nevertheless, several design features have been included to enhance the reliability and maintainability of these components.

Cryostat The cryostat can maintain thermal isolation as long as the vapor seal function remains intact. Since this seal is applied as a coating, it can be easily repaired by patching any leaks or trouble spots. In addition, if access is required inside the cryostat for maintenance, it can be disassembled locally, re-assembled, re-insulated and re-sealed with little impact on adjacent areas. The boots that seal the ports are also readily accessible.

Machine base structure The machine base is not expected to have any reliability, maintenance, or safety issues, but all are mitigated by designing the system with a large margin on load capacity of the components.

Coil support structure The coil support structure must stay in alignment with the modular coils, which is accomplished by tying the two structures together at robust interfaces. The coil support structure can also be re-aligned by removing the interface spacers and shimming.

4.6　Cost and Schedule

The cost estimate for the cryostat and machine structure is summarized in Table 32. This estimate was developed as a bottoms-up estimate, and includes input from potential vendors. Most of the cost is in the cryostat frame and the coil support system, and these estimates were consistent with vendor input.

The Cryostat (WBS 15) cost $510K. The Machine Structure (WBS 16) costs more, $2245K. The recommended contingencies are 25% for the Cryostat and 32% for the Machine Structure.

Table 32 Cryostat (WBS 15) and Machine Structure (WBS 16) Costs

Total Estimated Cost (K$)		151	152	153	154	155	15 Total	161	162	163	16 Total
Manufacturing Development	Labor/Other										
	M&S										
	Total										
Design (Title I & II)	Labor/Other	88	12	44	24	22	190	96	379	18	493
	M&S										
	Total	88	12	44	24	22	190	96	379	18	493
Fabrication/Assembly (incl Title III)	Labor/Other	23	14	11	5		53	45	156	5	206
	M&S	138	28	67	34	2	268	296	1245	5	1546
	Total	160	41	78	39	2	321	342	1401	10	1752
Installation/test	Labor/Other										
	M&S										
	Total										
Grand Total		248	54	121	63	24	510	437	1780	28	2245

The schedule for implementing the Cryostat (WBS 15) and Machine Structure (WBS 16) may be seen in the **Project Master Schedule**, provided as part of the Conceptual Design Report. The coil support structure is assembled as part of the field period assembly in the TFTR test cell. Title I design will begin at the start of FY04. Title II design will be completed late in FY04. Procured components should all be delivered late in FY05.

The machine base structure needs to be in place before final assembly in the NCSX Test Cell can begin. Title I design is schedule to begin in mid FY05 and be completed early in FY05. Procured components should all be delivered late in FY05.

The cryostat is not installed until all the field periods have been assembled in the NCSX Test Cell. The exception is the cryostat base, which is installed after the machine base structure is installed and before final assembly begins. Title I design will begin in mid FY03. However, Title II design will not be completed until the end of FY04 because of the many interface details that need to be worked out. Procured components will all be delivered early in FY06.

4.7　Risk Management

The primary element of risk for both the cryostat and machine structure is cost growth. The main drivers for cost growth are changes to the design concept during preliminary design as a result of changes to the requirements, unfeasible fabrication, or lack of functional performance.

These have been addressed for the cryostat by adopting a simple concept that can be readily modified without affecting other components of the machine. If the heat leak is found to be too high after a more thorough analysis, the thickness of the insulation is increased with very little cost impact. If the structure is too weak, the section depth of the molded panels is modified with very little impact. The concept itself has been discussed with potential vendors and appears entirely feasible to fabricate in its present form. Contact with vendors will be expanded during preliminary design to ensure a feasible and cost effective design.

The machine structure risk is addressed in a similar way. The coil support structure is very robust to changes in coil loads because it is based on a "cast-and-machined" fabrication whose cost is relatively insensitive to section depth. Tolerances and accuracy for this type of structure have been demonstrated for other devices, so there should be no fundamental problem with alignment or other functions. On the machine base structure, there is adequate space for the carriages so slide dimensions and capacity are not an issue. The whole assembly is bolted together, so it can be disassembled and re-assembled without impairing its accuracy (as opposed to welded structures). Finally, there is no new technology to develop for this concept, so no development should be required.